11-1-2012 12:00 AM

TRPM2 in the Central Nervous System: Physiological Role and Critical Regulatory Pathways

Jillian C. Belrose
The University of Western Ontario

Supervisor
Dr. John MacDonald
The University of Western Ontario Joint Supervisor
Dr. Michael Jackson
The University of Western Ontario

Graduate Program in Anatomy and Cell Biology
A thesis submitted in partial fulfillment of the requirements for the degree in Doctor of Philosophy

TRPM2 IN THE CENTRAL NERVOUS SYSTEM: PHYSIOLOGICAL ROLE AND CRITICAL REGULATORY PATHWAYS

(Spine title: TRPM2 in the Central Nervous System)

(Thesis format: Integrated-Article)

by

Jillian Corinne Belrose

Graduate Program in Anatomy and Cell Biology

A thesis submitted in partial fulfillment
of the requirements for the degree of
Doctor of Philosophy

The School of Graduate and Postdoctoral Studies
The University of Western Ontario
London, Ontario, Canada

THE UNIVERSITY OF WESTERN ONTARIO

SCHOOL OF GRADUATE AND POSTDOCTORAL STUDIES

CERTIFICATE OF EXAMINATION

Supervisor

Dr. John MacDonald

Co-Supervisor

Dr. Michael Jackson

Supervisory Committee

Dr. Arthur Brown

Dr. Jane Rylett

Dr. Marco Prado

Examiners

Dr. Susanne Schmid

Dr. Walter Rushlow

Dr. David Litchfield

Dr. Jerry Warsh

The thesis by

Jillian Corinne Belrose

entitled:

TRPM2 in the CNS: Physiological Role and Critical Regulatory Pathways

is accepted in partial fulfilment of the
requirements for the degree of
Doctor of Philosophy

Date_____

Chair of the Thesis Examination Board

ABSTRACT

TRPM2 is a non-selective cation channel which is permeable to calcium. Although expression is highest in the brain, the physiological role for TRPM2 in neurons is unknown. Furthermore, our understanding of the pathways regulating TRPM2 channel function requires further investigation. In this thesis, we identified that TRPM2 is required for NMDAR-dependent LTD. No change in NMDAR expression or function was observed following genetic deletion of TRPM2. Instead, the loss of NMDAR-LTD in TRPM2 knockout mice results from diminished GSK-3β activation. We next examined whether age *in vitro* could facilitate TRPM2 currents. We demonstrate that diminished glutathione with age results in the loss of basal TRPM2 channel inhibition. We subsequently demonstrate that TRPM2 currents are enhanced by oligomeric Aβ, a peptide proposed to initiate the majority of toxic effects observed in Alzheimer's disease. Potentiation of TRPM2 may involve Fyn, a tyrosine kinase implicated in oxidative stress and neurotoxicity. We demonstrate that Fyn is capable of interacting with and phosphorylating TRPM2. Acute application of Fyn through the patch pipette potentiates TRPM2 currents, and a Fyn(39-57) mimetic peptide significantly attenuates currents in cultured hippocampal neurons. These results are the first to establish a role for TRPM2 in neurons, and also implicate TRPM2 in neurodegenerative disorders such as Alzheimer's disease.

KEYWORDS:

TRPM2, calcium, synaptic plasticity, LTD, NMDA, GSK-3β, aging, glutathione, Fyn, Alzheimer's disease

CO-AUTHORSHIP STATEMENT

Chapter 2

Dr. Yu-Feng Xie designed and performed recordings from slice preparations. Dr. Gang Lei designed and performed immunoblotting experiments. Dr. Yasuo Mori generated TRPM2$^{-/-}$ mice. John MacDonald and Michael Jackson conceptualized and supervised the project, contributed to the design of experiments and wrote the manuscript.

Chapter 3

Lynn Gierszewski assisted with real-time quantitative PCR analysis. Drs. Yu-Feng Xie, John MacDonald, and Michael Jackson conceptualized and supervised the project and contributed to the design of experiments.

Chapter 4

Matthew Johnson performed co-immunoprecipitation and Western blotting experiments to assess tyrosine phosphorylation of TRPM2, and interactions with Fyn. Dr. Hongbin Li performed Fyn inhibitory peptide experiments in neurons. Dr. Fabiana Caetano performed preliminary experiments which assisted in design and development of several electrophysiological experiments. Drs. John MacDonald, and Michael Jackson conceptualized and supervised the project and contributed to the design of experiments.

Chapter 5

Matthew Johnson performed the western blotting experiment to assess TRPM2 expression. Drs. John MacDonald and Michael Jackson conceptualized and supervised the project and contributed to the design of these preliminary experiments.

ACKOWLEDGEMENTS

My sincere gratitude is owed to my supervisors, Dr. John MacDonald and Dr. Michael Jackson, for their constructive feedback, support, encouragement. I have really enjoyed my time in your lab, and cannot express how grateful I am to have had you both as supervisors.

I would also like to thank my supervisory committee: Dr. Jane Rylett, Dr. Marco Prado, and Dr. Arthur Brown. Your expertise, detailed feedback, and guidance have been greatly beneficial toward me completing my PhD studies.

My sincere gratitude is due to all of my colleagues in the lab. Specifically, I'd like to thank Brian Lockhart, Yu-Feng Xie, Matthew Johnston, Hongbin Li, Kai Yang, Gang Lei, Catherine Trepanier, Rohit Kesarwani, Oies Hussein, Kristen Condie, and Fabiana Caetano for their assistance, friendship, and support throughout my project. I owe many thanks to Natalie Lavine for the hours spent discussing my project, and being an amazing source of support, especially when I felt overwhelmed. I would also like to express my gratitude to Lidia Brandes for many memorable moments inside and outside the lab, and her invaluable help with neuronal cultures. These studies could not have been done without you!

I would like to thank all of my family and friends for their loving support and optimism throughout my project. Most importantly, I owe thanks to my husband, PJ Belrose, for his patience, kind words, and sense of humour which have helped me stay motivated and keep perspective.

Lastly, the funding required to complete this project was provided through the Canadian Institute of Health Research (CIHR). This assistance is gratefully acknowledged.

TABLE OF CONTESTS

LIST OF TABLES

LIST OF FIGURES

LIST OF APPENDICES

LIST OF ABBREVIATIONS

aa	amino acids
Aβ	amyloid beta
AD	Alzheimer's disease
ADPR	adenosine diphosphate ribose
ALS	amyotrophic lateral sclerosis
AMPA	α-amino-3-hyroxy-5-methyl-4-isoazoleproprionic acid
AMPAR	AMPA Receptor
AP2	adaptor protein 2
APP	amyloid precursor protein
ATP	adenosine triphosphate
BDNF	brain derived neurotrophic factor
Ca^{2+}	calcium
cADPR	cyclic adenosine diphosphate ribose
CaMKII	calcium/calmodulin-dependent protein kinase II
CD	cluster of differentiation
CNS	central nervous system
DRG	dorsal root ganglion
EC_{50}	half maximal concentration for activation
EFHC1	EF-hand domain containing protein 1
EPSP	excitatory post-synaptic potential
ER	endoplasmic reticulum
GSH	glutathione

GSK--3β	glycogen synthase kinase-3 beta
HEK293	human embryonic kidney 293
HEK293-TRPM2	HEK-293 cells expressing inducible flag-tagged human TRPM2
IC_{50}	half-maximal inhibitory concentration
IL	interleukin
IP	intraparitoneal
I-V	current-voltage
LTD	long-term depression
LTP	long-term potentiation
LTRPC2	long Transient Receptor Potential Channel 2
MAPK	mitogen-activated protein kinase
mRNA	messenger RNA
MTT	3-(4,5-Dimethylthiazol-2-yl)-2,5-diphenyltetrazolium bromide
Na^+	sodium
NAADP	nicotinic acid adenine dinucleotide phosphate
N-ACA	N-(p-amycinnamoyl)anthranilic acid
NAD^+	nicotinamide adenine dinucleotide
NMDA	N-methyl-□-aspartate
NMDAR	NMDA Receptor
NUDT9-H	nucleoside diphosphate-linked moiety X-type homology motif
OGD	oxygen glucose deprivation
PARG	polyADPRglycohydrolase
PARP	polyADPRpolymerase

P_{Ca}:P_{Na}	permeability ratio of Ca^{2+} to Na^{+}
PD	Parkinson's disease
PDGF	platelet derived growth factor
PI3K	phosphatidylinositol 3-kinase
PKA	protein kinase A
PKC	protein kinase C
PP1	protein phosphatase 1
PP2B	protein phosphatase 2B (also known as calcineurin)
PSD-93	post-synaptic density 93
PSD-95	post-synaptic density 95
qRT-PCR	quantitative real-time polymerase chain reaction
ROS	reactive oxygen species
RNS	reactive nitrogen species
SFKs	Src family kinases
SH domain	Src homology domain
shRNA	short hairpin RNA
SNP	single nucleotide polymorphism
SOD	superoxide dismutase
SSF-TRPM2	striatum short form Transient Receptor Potential 2
tMCAO	transient middle cerebral artery occlusion
TNF-α	tumor necrosis factor alpha
TRP	Transient Receptor Potential Channel
TRPC7	Transient Receptor Potential Channel 7

TRPM2	Transient Receptor Potential Melastatin Type 2 Channel
TRPM2-S	TRPM2(1-995). Truncated form of TRPM2; dominant negative
VDCC	voltage-dependent calcium channel

CHAPTER 1

1.1 INTRODUCTION

Transient receptor potential melastatin type 2 (TRPM2) is a non-selective cation channel permeable to calcium (Ca^{2+}), which belongs to the TRP family of ion channels. TRPM2 mRNA is the most abundant of TRP channels in the Central Nervous System (CNS) (Fonfria, Murdock et al., 2006). Several studies have demonstrated a clear role for TRPM2 in cell death in response to oxidative stress in a variety of cell types, including neurons (Takahashi et al., 2011); however, a physiological role for TRPM2 in the CNS has not yet been elucidated. TRPM2 was first cloned and characterized in 2001 (Perraud et al., 2001). Although several factors which activate, inhibit, and modulate TRPM2 have been identified over the past decade, research into the regulation of TRPM2 and potential implications for normal function and pathology is still in its infancy. The purpose of this PhD thesis is to investigate the role of TRPM2, and how this channel is regulated in hippocampal pyramidal neurons.

1.2 TRANSIENT RECEPTOR POTENTIAL MELASTATIN 2 (TRPM2)

The Transient receptor potential (TRP) family of ion channels are non-selective cation channels. The first TRP gene was originally identified in *Drosophila*, where TRP participates in phototransduction (Montell & Rubin, 1989). To date, 28 TRP channels have been discovered in mammals, which are divided into six subfamilies including the canonical (C), vanilloid (V), polycystin (P), mucolipin (ML), ankyrin (A), and melastatin (M) subfamilies (Clapham, 2007; Nilius & Owsianik, 2011).

The first member of the TRPM subfamily to be described, TRPM1, was originally identified in melanomas, where its expression is negatively correlated with

tumour cell proliferation and metastasis (Duncan et al., 1998). Since this time, eight different TRPM family members (TRPM1-TRPM8) have been described in mammals (Clapham, 2007). TRPM2, previously known as TRPC7 and LTRPC2, is located on chromosome 21q22.3 in humans (Nagamine et al., 1998). The gene contains 33 exons over 90kb, and produces a 5876bp full-length transcript which codes for a 1503 amino acid protein. In addition to the full length form of the protein, several splice variants of TRPM2 have also been identified. These include: TRPM2-ΔN, a variant with deletion of amino acids 538-557; TRPM2-ΔC, a variant with a deletion of amino acids 1292-1325; TRPM2-ΔNΔC, missing both regions 538-557 and 1292-1325; striatum short form TRPM2 (SSF-TRPM2), a variant identified in the striatum in which the first N-terminal 214 amino acids are deleted; TRPM2-S, a variant in which a stop codon is introduced at amino acid 995, producing a non-functional protein which is truncated after the second transmembrane domain (Uemura et al., 2005; Wehage et al., 2002; Zhang et al., 2003). TRPM2 mRNA assessed by quantitative real-time polymerase chain reaction (qRT-PCR) demonstrates a near ubiquitous expression in all tissues examined, with the exception of bone and cartilage. TRPM2 mRNA is most abundant in the brain (Fonfria, Murdock et al., 2006).

The structure of TRPM2 is proposed to include 6 transmembrane domains, with a pore-forming re-entry loop between transmembrane domains 5 and 6. The amino and carboxy terminal regions of the protein are cytoplasmic, and contain regulatory features for the channel (Figure 1.1). The amino-terminus of TRPM2 contains a TRPM homology domain, a region of approximately 700 amino acids (aa) which is largely conserved across all TRPM family members (Kraft & Harteneck, 2005). Additionally,

an IQ-like motif identified to be involved in Ca^{2+}-Calmodulin binding to the channel participates in TRPM2 activation (Tong et al., 2006). In the C-terminal portion of TRPM2, the coiled-coiled motif is predicted to participate in interactions between TRPM2 proteins and formation of the functional tetrameric form of the channel (Jiang, 2007). Importantly, the C-terminus of TRPM2 also includes a nucleoside diphosphate-linked moiety X-type homology motif (NUDT9-H) which is required for gating of the channel by adenosine diphosphate ribose (ADPR), an intracellular ligand for TRPM2. The NUDT9-H region shares 39% sequence homology to NUDT9, a mitochondrial ADPR hydrolase that converts ADPR to adenosine monophosphate (AMP) and ribose-5-phosphate, but demonstrates less than 1% of the enzymatic activity (Perraud et al., 2001; Shen et al., 2003). The reduction in activity has been attributed to amino acid substitutions in the NUDT9-H motif at E1405I/F1406L. Indeed, when these residues are replaced in TRPM2, gating of TRPM2 by ADPR is lost (Kuhn & Luckhoff, 2004).

The TRPM2 channel has a single channel conductance of approximately 60-80pS and a linear current-voltage relationship, with a reversal potential of 0mV (Heiner et al., 2003; Perraud et al., 2001; Sano et al., 2001). These characteristics demonstrate that the channel is not gated by voltage, and is a non-selective cation channel. The permeability ratio of Ca^{2+} to Na^{+} (P_{Ca}:P_{Na}) is approximately 0.7, demonstrating that the inward current is predominantly carried by Na^{+} (Kraft et al., 2004; Sano et al., 2001); however, the long open time of several hundred milliseconds allows for substantial Ca^{2+} influx into the cell (Kraft et al., 2004; Perraud et al., 2001; Sano et al., 2001).

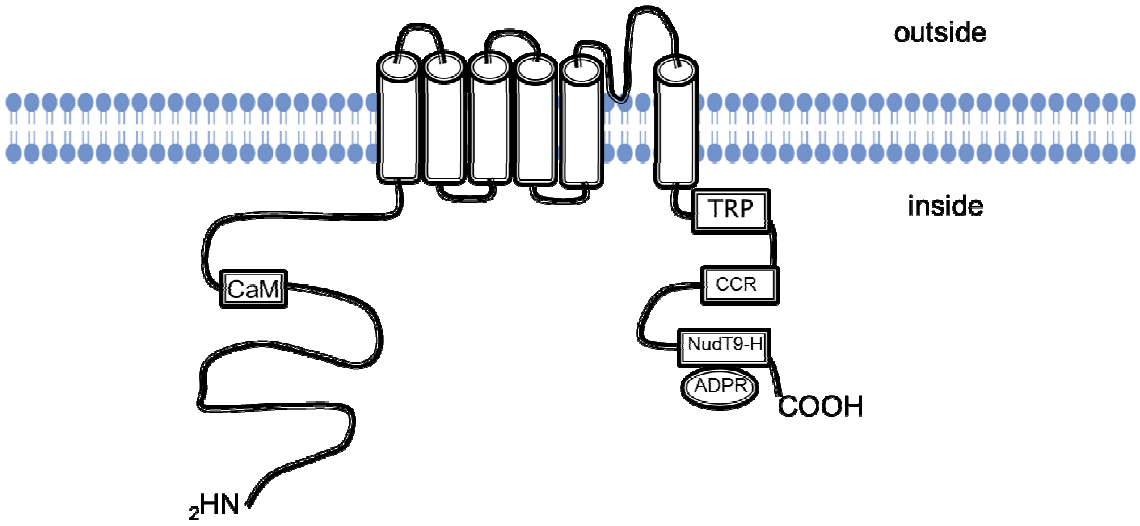

FIGURE 1.1 TRPM2 Structure.

TRPM2 is a 1503aa protein, comprised of intracellular amino and carboxy terminal regions, and six transmembrane segments with a re-entry pore forming loop between segments 5 and 6. The amino-terminus contains a Ca^{2+}-Calmodulin binding motif (CaM) which participates in channel activation. The carboxy terminus contains a highly conserved TRP box (TRP), a coiled-coiled region (CCR) which may participate in tetrameric assembly, and the nucleoside diphosphate-linked moiety X-type homology motif (NUDT9-H) which binds adenosine diphosphate ribose (ADPR), the intracellular agonist for TRPM2.

TRPM2 represents a particularly unique channel in that it is activated in response to reactive oxygen and nitrogen species (ROS/RNS) (Takahashi et al., 2011). In a variety of cell types, several groups have demonstrated that TRPM2 activation by ROS/RNS can elicit a toxic influx of Ca^{2+} which leads to cell death (Takahashi et al., 2011). The mechanism for channel activation following exposure to ROS/RNS has been attributed predominantly to generation of ADPR, a ligand of TRPM2 which was accurately predicted based on homology of the NUDT9-H domain of TRPM2 to NUDT9 (Perraud et al., 2001). Oxidative stress may generate ADPR through two cellular mechanisms. First, ROS/RNS exposure may lead to DNA damage and activation of polyADPR polymerase (PARP) and polyADPR glycohydrolase (PARG). These enzymes convert nicotinamide adenine dinucleotide (NAD^+) into polyADPR, and break down polyADPR into monomeric ADPR, which is then capable of activating TRPM2 channels (Blenn et al., 2011; Fonfria et al., 2004). The second proposed mechanism of ROS/RNS activation of TRPM2 involves the breakdown of NAD^+ into ADPR by NUDT9 ADPRase activity in the mitochondria. Indeed, when a mitochondrial targeted form of NUDT9 was expressed in human embryonic kidney-293 (HEK-293) cells stably expressing an inducible flag-tagged human TRPM2 (HEK293-TRPM2), activation of TRPM2 in response to H_2O_2 treatment was significantly suppressed (Perraud et al., 2005). The half maximal concentration for activation of TRPM2 by ADPR (EC_{50}) is estimated at 70 - 90μM (Perraud et al., 2001; Sano et al., 2001). Importantly, intracellular concentrations of ADPR fall within the range for endogenous TRPM2 activation at 5-80μM (Gasser & Guse, 2005; Heiner et al., 2006). A variant of TRPM2 (TRPM2-ΔC) which is insensitive to ADPR still responds to H_2O_2

exposure, raising the possibility that activation of TRPM2 by oxidative stress may also occur independent of ADPR production (Wehage et al., 2002).

In addition to ADPR, several studies have proposed that NAD^+ is capable of directly activating TRPM2 channels (Hara et al., 2002; Inamura et al., 2003; Sano et al., 2001); however, this finding has not been consistently reproduced in the literature (Perraud et al., 2001; Wehage et al., 2002). In comparison to activation of TRPM2 by ADPR, the time period between NAD^+ application and TRPM2 activation is significantly longer, raising the possibility that NAD^+ activates TRPM2 indirectly following the generation of ADPR (Sano et al., 2001). Similarly, whether Ca^{2+} is capable of directly activating TRPM2 channels or whether its actions on TRPM2 simply enhance response to ADPR is under debate. It is well accepted that intracellular Ca^{2+} facilitates TRPM2 currents generated by ADPR (Heiner et al., 2006; McHugh et al., 2003; Olah et al., 2009; Perraud et al., 2001; J. Starkus et al., 2007). The co-operativity between ADPR and Ca^{2+} has been attributed to the binding of 4 Ca^{2+} ions near the pore entrance of TRPM2, and also through an interaction between a Ca^{2+}/Calmodulin complex with the IQ-like motif on the N-terminus of TRPM2 (Csanady & Torocsik, 2009; Tong et al., 2006). In support of direct activation of TRPM2 by Ca^{2+}, TRPM2 splice variants which do not respond to ADPR (TRPM2-ΔN, TRPM2-ΔC, TRPM2-ΔNΔC, and SSF-TRPM2) are still activated by 10μM Ca^{2+} (Du, Xie, & Yue, 2009a). Importantly, intracellular Ca^{2+} in micro- and nano-domains are estimated to range as high as 1-100μM (Fakler & Adelman, 2008). Whether Ca^{2+} reaches this concentration near TRPM2 and could represent a physiologically relevant gating mechanism remains to be determined.

In addition to activation of TRPM2 by the above mechanisms, TRPM2 currents are augmented by cyclic ADPR (cADPR), nicotinic acid adenine dinucleotide phosphate (NAADP), arachidonic acid, and temperature. TRPM2 current potentiation by cADPR and NAADP has been demonstrated by several groups; however, whether they act as direct agonists, contribute to channel activation by conversion to ADPR, or co-activate the channel, shifting the concentration response curve of ADPR required for channel activation, is still unclear (Beck et al., 2006; Kolisek et al., 2005; Lange et al., 2008; Tao et al., 2011; Toth & Csanady, 2010). Arachidonic acid has also been demonstrated to facilitate TRPM2 currents, potentially in response to increased release of intracellular Ca^{2+} (Hara et al., 2002). Lastly, heat enhances the permeability of TRPM2 currents, augmenting currents elicited with β-NAD^+ or ADPR at physiological temperatures (Togashi et al., 2006).

In addition to endogenously occurring agonists of TRPM2, an acidic environment has been shown to inhibit the channel. An extracellular acidic environment reversibly suppresses TRPM2 currents at a half-maximal inhibitory concentration (IC_{50}) ranging from pH 4.7 - 6.5, depending on the concentration of Ca^{2+} used in solutions. These studies suggest that extracellular pH inhibits TRPM2 channels by binding to external residues and/or permeation of H^+ and subsequent competition for intracellular Ca^{2+} binding sites on the channel, resulting in reduced channel conductance (Du, Xie, & Yue, 2009b; J. G. Starkus, Fleig, & Penner, 2010; W. Yang et al., 2010). Similarly, an intracellular acidic environment also inhibits TRPM2 currents with an IC_{50} of pH 6.7 by inducing channel closure, through an interaction with Asp^{933} located on the intracellular side of the channel between transmembrane domains 4 and 5 and/or competing for

intracellular Ca^{2+} binding sites (Du, Xie, & Yue, 2009b; J. G. Starkus et al., 2010; W. Yang et al., 2010).

Preliminary evidence also implicates glutathione (GSH), a naturally occurring antioxidant, as an endogenous inhibitor of TRPM2 channels. Extracellular GSH inhibits cell death induced by H_2O_2 and TNF-α in insulinoma and monocyte cell lines (Hara et al., 2002). Furthermore, chemical depletion of intracellular GSH induces an increase in intracellular Ca^{2+} through TRPM2 channels in glia and dorsal root ganglion sensory neurons (Lee et al., 2010; Naziroglu et al., 2011). These studies propose that depletion of GSH activates TRPM2 through a subsequent increase in oxidative stress, but do not establish a mechanism of inhibition nor do they determine whether or not endogenously occurring changes in GSH modulate TRPM2 currents.

At present, there are no specific antagonists to TRPM2. The channel is inhibited, albeit non-selectively, by various pharmacological agents, including N-(p-amycinnamoyl) anthranilic acid (N-ACA), econazole, clotrimazole, and flufenamic acid (Eisfeld & Luckhoff, 2007; Olah et al., 2009). Research elucidating physiological roles of TRPM2 has been hindered by the lack of a specific antagonist. In order to specifically assess the role of TRPM2 in various processes, TRPM2 knockout mice have been generated (Yamamoto et al., 2008). Studies employing a pharmacological and/or genetic approach to inhibiting TRPM2 currents have increased our understanding of the pathological and physiological roles of TRPM2.

Cell death in response to oxidative stress is the best characterized role for TRPM2. Initial evidence using heterologous expression of TRPM2 in HEK cells, and endogenous expression of TRPM2 in insulinoma and monocyte cell line cells revealed

that TRPM2 conferred susceptibility to cell death in response to treatment with H_2O_2 (Hara et al., 2002). A role for TRPM2 in cell death has since been confirmed in a variety of cell types including neuronal cell populations in response to H_2O_2, TNFα, and Aβ peptide (Fonfria et al., 2005; Jia et al., 2011; Kaneko et al., 2006; Takahashi et al., 2011; Xie, Macdonald, & Jackson, 2010).

In addition to the established role of TRPM2 in oxidative stress-mediated cell death, physiological roles for TRPM2 are being actively investigated. For example, TRPM2 has been implicated in insulin secretion from pancreatic β-cells (Inamura et al., 2003; Togashi et al., 2006; Uchida et al., 2011). A role for TRPM2 in cytokine production in monocytes/macrophages has also been established. In particular, activation of TRPM2 leads to the production of cytokines including CXCL8 (previously known as interleukin-8 [IL-8]), IL-6, IL-10, and TNF-α (Wehrhahn et al., 2010; Yamamoto et al., 2008). Increased cytokine production through activation of TRPM2 promotes inflammation. Interestingly, TRPM2 also appears to dampen the inflammatory response through cellular depolarization and subsequent reduction of ROS production in phagocytes, thereby minimizing excess inflammation (Di et al., 2011). Lastly, oxidative stress acts on TRPM2 to enhance endothelial cell permeability by opening interendothelial junctions, although the precise mechanism(s) involved requires further investigation (Hecquet et al., 2008). Although the highest level of TRPM2 expression is found in the brain, a physiological role for TRPM2 in neuronal cells has not yet been identified. Investigation into the physiological role of TRPM2 in neurons and regulatory pathways in these cells is therefore of critical importance.

1.3 TRPM2 IN THE CENTRAL NERVOUS SYSTEM

TRPM2 mRNA is most abundant in brain tissue (Fonfria, Murdock et al., 2006). At present, TRPM2 expression in the CNS has been demonstrated in microglia, astrocytes, and in neuronal populations in the hippocampus, substantia nigra, striatum, cortex, and dorsal root ganglion (DRG) sensory neurons in the spinal cord (Fonfria et al., 2006; Hill et al., 2006; Kaneko et al., 2006; Kraft et al., 2004; Lee et al., 2010; Olah et al., 2009). The role of TRPM2 in normal physiological functions and its involvement in CNS disease is gaining increasing attention.

Activation of TRPM2 by oxidative stress and role in cell death implicates TRPM2 in various neurological disorders. Genetic studies have associated single nucleotide polymorphisms (SNPs) in TRPM2 to an increased susceptibility for bipolar disorder (Kostyrko et al., 2006; McQuillin et al., 2006; Xu et al., 2006; Xu et al., 2009). A single SNP (P1018L) in TRPM2 has also been identified in tissue from Guamanian amyotrophic lateral sclerosis (ALS) and Parkinson's disease (PD) subjects (Hermosura et al., 2008). Whether other neurological disorders are associated with TRPM2 mutations requires further investigation.

Stroke is associated with increased oxidative stress and calcium dysregulation, which implicates TRPM2 in the neurodegenerative processes following ischemia. In cultured cortical neurons, cell death following treatment with H_2O_2 (50μM for 6 hours, or 1mM for 20 minutes) was greatly attenuated by knockdown of TRPM2, providing evidence that TRPM2 promotes cell death in neurons in response to oxidative stress (Kaneko et al., 2006). In a transient middle cerebral artery occlusion (tMCAO) rat model of ischemia, expression of TRPM2 mRNA is elevated from 1-4 weeks following

induction of the stroke. This was attributed to transcriptional upregulation of TRPM2 in microglia in response to oxidative stress and the cytokine IL-1β (Fonfria et al., 2006). Pharmacological inhibitors and RNA interference with shRNA targeting TRPM2 reduced infarct volume *in vivo* and decreased neuronal cell death *in vitro* following oxygen glucose deprivation (OGD). Interestingly, this protection appears to be specific to males, suggesting a potential gender difference in contributions of TRPM2 to ischemic cell death (Jia et al., 2011).

In addition to a potential role in stroke, TRPM2 has also been implicated in Alzheimer's disease (AD). Primary striatal cultures exposed to 20μM monomeric β-amyloid, the main component of senile plaques in AD, demonstrate an increase in intracellular calcium and cell death which was partially blocked when cultures were transfected with a dominant negative splice variant of TRPM2 (Fonfria et al., 2005). Of note, these experiments were performed in striatal cultures; however, AD presents with degeneration of the basal forebrain cholinergic neurons, entorhinal cortex, hippocampus, and cortex (Coyle, Price, & DeLong, 1983; Gomez-Isla et al., 1996) and therefore the validity of a striatal culture system to model AD is questionable. Furthermore, 20μM of Aβ which had not been oligomerized was used to induce calcium influx and cell death; however, it is the oligomeric form of Aβ that has been shown to induce an influx of intracellular calcium, significantly increase oxidative stress, and be particularly toxic to neurons (De Felice et al., 2007; Demuro et al., 2005; Lambert et al., 1998). Although this study implicates TRPM2 in Alzheimer's pathology, further research into the role of TRPM2 is required to validate and expand upon this preliminary study.

Recent evidence also suggests that TRPM2 may play a role in spinal cord injury and neuropathic pain. In a rat model of spinal cord injury, intraperitoneal (IP) injection of clotrimazole conjugated to polyethylene glycol significantly reduced lipid peroxidation, an indicator of oxidative stress, when administered 5 minutes after spinal cord compression (Usul et al., 2006). It is unclear whether inhibition or knockdown of TRPM2 results in higher functional performance compared to untreated controls in a spinal cord injury model. Additionally, a recent study demonstrated that TRPM2 mRNA is elevated following sciatic nerve injury. When compared with WT littermate controls, TRPM2 knockout mice show a reduced immune response and attenuation of the heightened mechanical and thermal pain responses elicited by sciatic nerve injury, suggesting that TRPM2 plays a role in neuropathic pain (Haraguchi et al., 2012).

Combined, the above data provides genetic, *in vitro*, and *in vivo* evidence that TRPM2 may be a key player in a variety of CNS disorders. Importantly, a role for TRPM2 in non-pathological processes in the CNS has not yet been elucidated. To determine potential physiological roles of TRPM2, it is important to consider location of expression and channel characteristics. For example, the permeability of TRPM2 to Ca^{2+} and activation by oxidative stress are defining characteristics of TRPM2. In the CNS, Ca^{2+} plays important roles in development, signal transduction, protein expression, neurotransmitter release, and synaptic plasticity. As mentioned earlier, TRPM2 is expressed in neuronal populations in the hippocampus, substantia nigra, striatum, cortex, and DRG sensory neurons (Chung, Freestone, & Lipski, 2011; Fonfria et al., 2005; Fonfria et al., 2006; Hill et al., 2006; Kaneko et al., 2006; Kraft et al., 2004; Lee et al., 2010; Naziroglu et al., 2011; Olah et al., 2009; Uemura et al., 2005).

Expression of TRPM2 in the hippocampus is particularly interesting because this region of the brain is critically involved in learning and memory, and neurons in this region of the brain also demonstrate a selective vulnerability to various pathological insults (Mattson, Guthrie, & Kater, 1989; Wang & Michaelis, 2010). Within the hippocampus, TRPM2 mRNA is localized to the pyramidal cell layer, and preliminary evidence demonstrates a predominantly extrasynaptic distribution in cultured hippocampal neurons (Olah et al., 2009). TRPM2 currents in these cells can be activated by ROS/RNS exposure, or by calcium influx through voltage-dependent calcium channels (VDCC) or NMDARs in the presence of intracellular ADPR (Olah et al., 2009). Therefore, a greater understanding of VDCCs, NMDARs, and synaptic plasticity may help to establish a potential physiological role for TRPM2 in hippocampal pyramidal neurons.

1.4 VOLTAGE-DEPENDENT CALCIUM CHANNELS

Voltage-dependent calcium channels (VDCCs) allow for the influx of Ca^{2+} following neuronal depolarization. Strong depolarization will activate L-type, N-type, P/Q-type, and R-type VDCCs, while a more modest depolarization will activate T-type VDCCs (Benarroch, 2010). VDCC all contain an obligate pore-forming α-subunit which determines gating properties of the channel. VDCC α subunits include the Ca_v1, Ca_v2, and Ca_v3 subunits. The Ca_v1 α subunit is expressed in L-type VDCCs, the Ca_v2 α subunit is expressed in N-, P/Q-, and R-type channels, and the Ca_v3 α subunit is expressed in T-type channels. The α subunit of most VDCCs are also found in complex

with a β-, $\alpha_2\delta$, and γ- subunits which modulate trafficking and channel gating (Arikkath & Campbell, 2003; Benarroch, 2010).

Within hippocampal neurons, VDCCs are involved in both pre- and post-synaptic functions (Catterall, 2011). L-type VDCC are expressed predominantly on the neuronal soma and proximal dendrites where they participate in incorporating synaptic input and coupling Ca^{2+} influx to gene transcription (Bading, Ginty, & Greenberg, 1993; Christie et al., 1995; Christie, Schexnayder, & Johnston, 1997; Deisseroth, Heist, & Tsien, 1998; Hell et al., 1993; Murphy, Worley, & Baraban, 1991; Weisskopf, Bauer, & LeDoux, 1999). In contrast, N, P/Q-, and R-type channels demonstrate a presynaptic distribution and are mainly involved in neurotransmitter release (Catterall & Few, 2008). Due to the low threshold of depolarization required for activation of T-type VDCC and their transient kinetics, T-type VDCC channels are associated with rhythmic bursting in neurons (Perez-Reyes et al., 1998). Whether TRPM2 channels uniquely couple to specific VDCC has not yet been investigated.

1.5 GLUTAMATE RECEPTORS

Glutamate is the major excitatory neurotransmitter in the nervous system, and is also a key mediator of neurotoxicity. Glutamate receptors are classified as either metabotropic or ionotropic. The metabotropic glutamate receptors (mGluR1-8) couple to G-proteins to activate downstream signaling cascades. The ionotropic glutamate receptors are ligand-gated non-selective cation-permeable ion channels, allowing for the movement of Na^+, K^+, and sometimes Ca^{2+}. These receptors include the N-methyl-□-aspartate (NMDA), α-amino-3-hyroxy-5-methyl-4-isoazoleproprionic acid (AMPA),

and 2-carboxy-3-carboxymethyl-4-isopropenylpyrrolidine (kainate) receptors (Kew & Kemp, 2005).

AMPA Receptors (AMPARs) in the CNS are tetramers. Subunits are termed GluR1-4. In the hippocampus, AMPARs are contain GluR2 in combination with GluR1 or GluR3 subunits, with GluR2-GluR1 being the most common at CA3-CA1 synapses (W. Lu et al., 2009). In the adult CNS, presence of the GluR2 subunit abolishes Ca^{2+} permeability of AMPA Receptors; therefore, the majority of AMPAR current is attributed to influx of Na^{+} and efflux of K^{+} ions (Geiger et al., 1995; Hollmann, Hartley, & Heinemann, 1991). Synaptic transmission in the hippocampus is predominantly mediated through these receptors (Derkach et al., 2007).

NMDARs are comprised of two obligate GluN1 subunits in combination with two GluN2 subunits (GluN2 A-D) or two GluN3 subunits (GluN3 A or B) (Kew & Kemp, 2005). Under normal physiological conditions, the release of glutamate during synaptic transmission results in the activation of AMPARs, depolarizing the post-synaptic cell. This change in voltage relieves the Mg^{2+} block of NMDA channels, permitting cation influx following co-activation by glutamate and glycine. This results in an acute, non-toxic rise in intracellular Ca^{2+} that is buffered by a variety of mechanisms (Derkach et al., 2007; Mattson, 2007). In pathological conditions, excessive Ca^{2+} entry via NMDARs has been shown to be particularly neurotoxic (MacDonald, Xiong, & Jackson, 2006; Sattler et al., 1998; Tymianski et al., 1993).

In the adult hippocampus, GluN2A and GluN2B containing NMDARs are the most abundant. GluN2B-containing NMDAR demonstrate a largely extrasynaptic distribution, while synaptic NMDARs are comprised predominantly of GluN2A-

containing NMDARs (Monyer et al., 1994). Interestingly, NMDARs have been associated with dichotomous signaling toward survival and apoptosis pathways, and also in synaptic plasticity. Although still a matter of debate, some explanations for the differences in signaling include synaptic vs. extrasynaptic localization of NMDARs, stimulus intensity, and subunit specific differences between GluN2B and GluN2A (Choi, 1985; Dudek & Bear, 1992; Hardingham, Fukunaga, & Bading, 2002; Ikonomidou et al., 1999; Ikonomidou, Stefovska, & Turski, 2000; L. Liu et al., 2004; Y. Liu et al., 2007; Mulkey & Malenka, 1992; Sattler et al., 2000).

1.6 SYNAPTIC PLASTICITY

Synaptic plasticity describes the strengthening or weakening of connections between neurons. These experience-dependent changes are implicated in learning and memory (Ho, Lee, & Martin, 2011; Malenka & Bear, 2004; Whitlock et al., 2006). A strong stimulus results in the strengthening of synaptic connections (potentiation), whereas a weak stimulus will produce a weakening of the synaptic connection (depression). When these changes are maintained for minutes to hours, the changes are termed long-term potentiation (LTP) or long-term depression (LTD). Long-term changes in synaptic strength require the synthesis of new proteins (Greer & Greenberg, 2008; Kandel, 2001). Furthermore, pre-synaptic, trans-synaptic, and post-synaptic modifications are also involved in the induction and maintenance of experience-dependent synaptic changes (Ho et al., 2011; Malenka & Bear, 2004). Pre-synaptic mechanisms of synaptic plasticity often alter the likelihood of neurotransmitter release (Catterall & Few, 2008). At the synaptic cleft, release of trans-synaptic signaling

molecules can activate a variety of signaling cascades in the pre-synaptic neuron (Regehr, Carey, & Best, 2009). Furthermore, LTP and LTD both involve alterations to adhesion molecules which alter signaling cascades and promote remodeling of the synapse (Dalva, McClelland, & Kayser, 2007). Post-synaptic changes underlying LTP and LTD include post-translational modifications and altered protein trafficking (Ho et al., 2011; Santos et al., 2009).

LTP and LTD require influx of Ca^{2+} (Cavazzini, Bliss, & Emptage, 2005; Greer & Greenberg, 2008; Lisman, Schulman, & Cline, 2002; MacDonald, Jackson, & Beazely, 2006). Importantly, calcium-permeable TRPM2 channels are expressed and functional in hippocampal pyramidal neurons (Olah et al., 2009); therefore, a greater understanding of synaptic plasticity at these synapses is required to explore a potential physiological role for TRPM2.

NMDAR-dependent LTP and LTD is the major form of synaptic plasticity at hippocampal CA3-CA1 glutamatergic synapses (MacDonald et al., 2006). In the hippocampus, LTP and LTD are experimentally induced by stimulation of the Schaffer collateral pathway. This activates axon collaterals of glutamatergic neurons in the CA3 area of the hippocampus which synapse upon CA1 pyramidal neurons. The resulting excitatory post-synaptic potential (EPSP) can then be recorded by field recordings extracellular of the CA1 neurons (Figure 1.2). Basal stimulation (~0.1Hz) results in an EPSP mediated predominantly by AMPAR. When a low-frequency (1Hz) or high-frequency (100Hz) stimulation is applied, NMDAR are also activated, allowing for influx of Ca^{2+} and induction of LTD or LTP, respectively (Collingridge, Kehl, & McLennan, 1983; Collingridge, Herron, & Lester, 1988; MacDonald et al., 2006).

Activation of NMDAR is required for synaptic plasticity *in vitro* and *in vivo* (Collingridge et al., 1983; Davis, Butcher, & Morris, 1992; Morris et al., 1986).

The bidirectional plasticity induced by activation of NMDARs suggests that the amount of glutamate released, distribution or subtype of activated NMDARs, and/or the amount, kinetics, or subcellular location of Ca^{2+} influx may activate different downstream pathways and uniquely alter the post-synaptic response to stimulation (MacDonald et al., 2006). The large increase in intracellular Ca^{2+} following a high frequency stimulation activates calcium/calmodulin-dependent protein kinase II (CaMKII), which phosphorylates AMPARs, increasing conductance of the receptor (Lisman et al., 2002; Malenka & Bear, 2004). Several other kinases including protein kinase C (PKC), mitogen-activated protein kinase (MAPK), and phosphatidylinositol 3-kinase (PI3K) also participate in phosphorylation of AMPAR, trafficking of AMPAR to the synapse, and structural modifications to synapses which increase basal synaptic transmission (W. Lu et al., 2001; Malenka & Bear, 2004). Furthermore, the tyrosine kinase Fyn is required for induction of LTP, and the tyrosine kinase Src is activated during LTP and participates in enhancing NMDAR function (Grant et al., 1992; Salter & Kalia, 2004; K. Yang et al., 2011).

The mechanisms underlying NMDAR-dependent LTD are less well established (Collingridge et al., 2010). Briefly, a modest increase in Ca^{2+} during NMDAR-dependent LTD promotes the Ca^{2+} dependent activation of calcineurin, also known as protein phosphatase 2B (PP2B). This leads to activation of protein phosphatase 1 (PP1), which dephosphorylates AMPAR and decreases receptor conductance. PP1 also de-phosphorylates and activates glycogen synthase kinase-3β (GSK-3β), which in turn

plays a role in the endocytosis of the scaffolding protein post-synaptic density-95 (PSD-95). Additionally, Ca^{2+} activates hippocalcin which targets adaptor protein 2 (AP2) to the synapse, further increasing AMPAR endocytosis (Collingridge et al., 2010). Fyn also participates in enhancing LTD through phosphorylation and subsequent potentiation of GluN2B-containing NMDARs (L. Liu et al., 2004; Nakazawa et al., 2001; K. Yang et al., 2011).

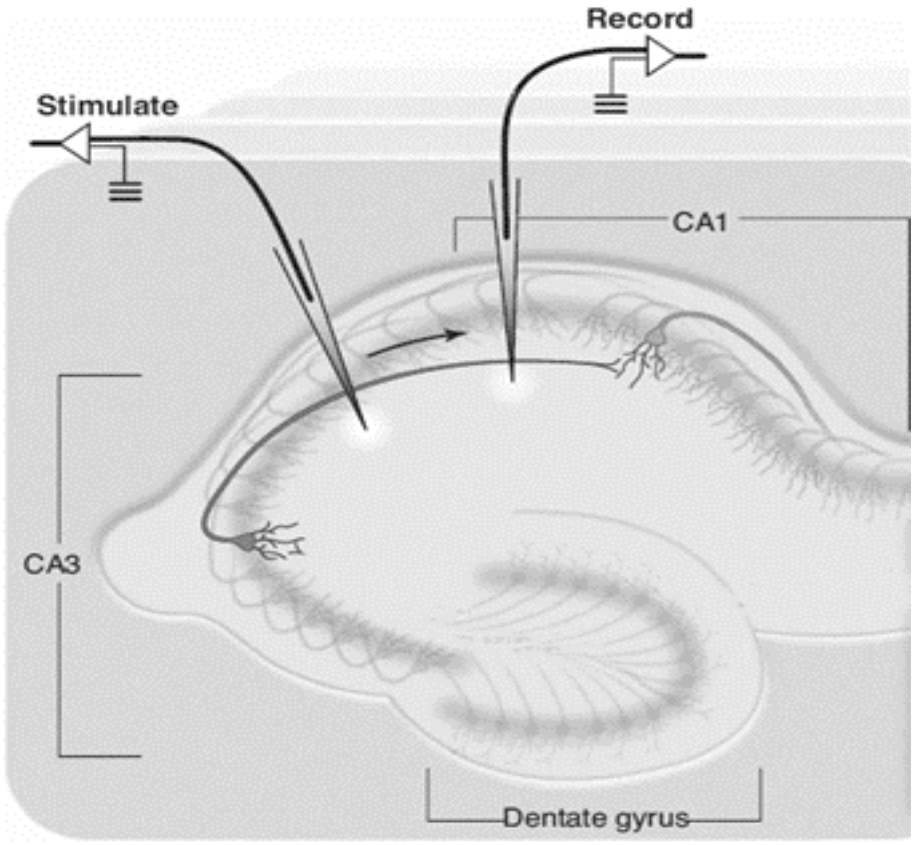

Figure 1.2. Hippocampal slice preparation.

Shown above is a transverse section of the hippocampus, used to assess synaptic plasticity at hippocampal CA3-CA1 synapses. Neurons from the CA3 region of the hippocampus project axon collaterals to CA1 pyramidal cells; this is known as the Schaffer collateral pathway. Stimulation of the Schaffer collateral pathway depolarizes CA3 axons, resulting in glutamate release which acts upon the post-synaptic CA1 neurons. A recording electrode placed extracellular to the CA1 neurons is used to quantify the resulting field excitatory post-synaptic potential (fEPSP). An increase or decrease in the fEPSP which is maintained for one hour following various stimulation protocols is termed long-term potentiation (LTP) or long-term depression (LTD), respectively. *Adapted from Ho et al (2011).*

1.7 AGING AND CALCIUM DYNAMICS

Homeostatic control of intracellular Ca^{2+} is important to maintain normal physiological function of neurons, including regulation of synaptic plasticity. Prolonged or excessive alterations in Ca^{2+} concentrations can lead to cytotoxicity (Choi, 1985; Dirnagl, Iadecola, & Moskowitz, 1999; Orrenius, Zhivotovsky, & Nicotera, 2003). A sudden and excessive increase in intracellular calcium triggers necrotic death in neurons, while milder but sustained elevations in calcium promotes delayed cell death through a combination of apoptotic and necrotic pathways. We previously reviewed the variety of pathways through which Ca^{2+} levels are altered following ischemia (Belrose et al., 2012). In addition to a dysregulation of Ca^{2+} in pathology, control of Ca^{2+} levels can also be compromised during normal aging in response to energy impairment and increased oxidative stress (Figure 1.3) (Mattson, 2007).

The primary theory underlying the increase in oxidative stress with age was described in 1972 and termed the "mitochondrial free radical theory of aging" (Harman, 1972). Mitochondria are the site of ATP production in the cell, and use the majority of the cell's oxygen for the oxidative phosphorylation process. ROS are a byproduct of this process. Oxidative stress in the aging brain leads to lipid peroxidation, DNA damage, modifications to ligand and voltage gated Ca^{2+} channels, and endoplasmic reticulum (ER) dysfunction promoting aberrant release of Ca^{2+} from internal stores (Mattson, 1998; Mattson, 2007). Furthermore, oxidative stress contributes to mitochondrial dysfunction, resulting in diminished ATP levels, and impairing ion-motive ATPases which participate in regulating intracellular Ca^{2+} levels (Mattson, 2007; Mattson, 2007; Navarro & Boveris, 2007). This creates a positive feedback loop whereby ROS

produced by the mitochondria contribute to cellular dysfunction and reduce efficiency of the mitochondria, ultimately resulting in enhanced ROS production. The energy impairment and oxidative stress converge on multiple pathways to promote dysregulation of neuronal Ca^{2+} levels during normal aging.

The consequence of elevated intracellular Ca^{2+} includes changes in synaptic plasticity and cell viability. Interestingly, although NMDAR-dependent LTP is impaired with age, the total magnitude of LTP is largely preserved during normal aging, potentially through a compensatory upregulation in VDCC-dependent LTP (Robillard et al., 2011). LTD, in contrast, is enhanced with normal aging (Norris, Korol, & Foster, 1996). Combined, these changes in synaptic plasticity produce an age-dependent decrease in synaptic strength which may underlie memory impairment with normal aging. Furthermore, normal aging also results in a reduction in brain volume in several regions of the brain, including the hippocampus (Long et al., 2012; Scahill et al., 2003; Sowell et al., 2003). An increase in intracellular Ca^{2+} levels may underlie the age-dependent changes in neuronal structure, function, and viability that contribute to the observed reduction in brain volume, and altered synaptic plasticity (Foster, 2007; Gant et al., 2006; Mattson, 2007; Ouanounou et al., 1999; Villalba et al., 1995). The pathway(s) leading to increased intracellular Ca^{2+} with age is therefore of critical importance to our understanding of the age-dependent decrease in synaptic strength and increase in susceptibility to neurodegeneration.

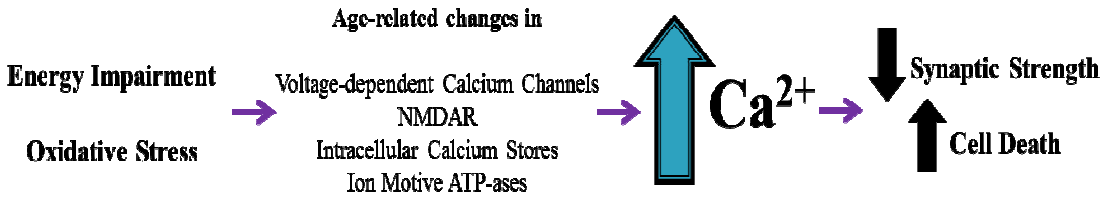

Figure 1.3. Aging and Calcium Dynamics.

In the brain, normal aging results in a decrease in ATP production resulting in energy impairment, and an increase in oxidative stress. These converge to increase intracellular Ca^{2+} concentrations in response to changes to several pathways/channels which participate in Ca^{2+} homeostasis including voltage-dependent calcium channels, NMDARs, intracellular calcium stores, and ion motive ATP-ases. The increase in intracellular Ca^{2+} promotes the decreased synaptic strength and increased susceptibility to cell death observed with age.

1.8 GLUTATHIONE

Endogenous mechanisms to protect against ROS mediated damage include the endogenously occurring antioxidants superoxide dismutase (SOD), superoxide reductase, catalase, and glutathione. These antioxidants may participate in the age-dependent increase in Ca^{2+} influx through their modulation of the oxidative stress status of the cell. Interestingly, the concentration of glutathione (GSH) decreases with age *in vitro* and *in vivo*, and therefore represents an interesting potential player in the Ca^{2+} dysregulation observed with age (Chen, Richie, & Lang, 1989; R. M. Liu, 2002; Parihar, Kunz, & Brewer, 2008; Rebrin, Forster, & Sohal, 2007; Sasaki et al., 2001).

GSH is a tripeptide of glutamate, cysteine, and glycine. It is synthesized by the enzymes γ-glutamylcysteine followed by glutathione synthases. Both of these steps require ATP. The rate limiting step in GSH synthesis is carried out by γ-glutamylcysteine, due to the limited availability of the cysteine substrate. The intracellular concentration of GSH typically ranges from 0.2 - 10mM (Anderson, 1998). In the brain, evidence from cultured cells suggests that GSH levels are higher in glial cells than in neurons (Dringen & Hamprecht, 1998; Hirrlinger et al., 2002; Raps et al., 1989). It is less clear whether this is also true *in vivo* (Miller et al., 2009).

In the CNS, the primary role of GSH is to decrease oxidative damage by reacting with the ROS/RNS superoxide, nitric oxide, hydroxyl radical, and peroxynitrite (Clancy et al., 1994; Koppal et al., 1999; Nauser, Koppenol, & Gebicki, 2005; Winterbourn & Metodiewa, 1994). The cysteine residue in GSH is also important in minimizing protein oxidation. GSH is capable of forming protein adducts through a process known as S-glutathionylation to prevent irreversible disulphide bonds between

oxidized proteins (Dalle-Donne et al., 2007). The depletion of GSH with age not only increases the oxidative stress status of the cell, but may also be associated with increased intracellular calcium and subsequent toxicity (Aoyama et al., 2006; Bains & Shaw, 1997; Gabby et al., 1996; Jurma, Hom, & Andersen, 1997; Thanislass, Raveendran, & Devaraj, 1995).

1.9 FYN KINASE

A version of this section has been published:

Yang, K.*, **Belrose, J.***, Trepanier, C.H., Lei, G., Jackson, M.F., & MacDonald, J.F. (2011). Fyn, a potential target for Alzheimer's disease. REVIEW. *Journal of Alzheimer's Disease, 27*(2): 243-252. **these authors contributed equally to this work*

The Fyn gene is located at chromosome 6q21. Isoform 1 is a 59kDa protein that has the most ubiquitous expression pattern among the three identified Fyn isoforms and is highly expressed in the brain (Cooke & Perlmutter, 1989; Goldsmith, Hall, & Atkinson, 2002). Homology modeling revealed that the structure is similar to that of other Src family kinases (SFKs) such as Src. The structure includes the regulatory domain at the C terminus, the catalytic domain (SH1) domain, the linker region, the Src homology 2 (SH2) domain, the Src homology 3 (SH3) domain, the unique domain, and the Src homology 4 (SH4) domain at the N terminus (Ingley, 2008; Roskoski, 2005; Salter & Kalia, 2004; Thomas & Brugge, 1997; Vatish et al., 2009).

The role of each structural domain has been investigated in Fyn and other SFK family members. The SH4 domain of Fyn is a very short motif, containing the signals for lipid modification such as myristoylation and palmitoylation that are responsible for membrane targeting (Resh, 1993). The importance of this domain was illustrated by

observations that the specificity of Fyn in cell signaling depended on its subcellular locations (Sicheri & Kuriyan, 1997). This region is followed by the unique N-terminal domain, a region of low relative homology to other Src family members (Jelic et al., 2007). The role of the unique domain remains relatively unexplored; however, it may serve as a site for selective interactions with proteins that are specific for each family member (Salter & Kalia, 2004). The Fyn SH3 domain is a 60 amino acid sequence that interacts with proline rich motifs in a number of signaling molecules and mediates various protein-protein interactions. The SH2 domain binds to phosphorylated tyrosine residues of interacting proteins (Ingley, 2008; Roskoski, 2005; Salter & Kalia, 2004; Thomas & Brugge, 1997; Vatish et al., 2009). The catalytic SH1 domain is highly conserved among SFKs. It includes an ATP binding site which is required for the phosphoryation of Fyn substrates. The SFK inhibitor PP2 binds to this site, inhibiting the phosphorylation of Fyn substrates (Osterhout et al., 1999).

As with other SFK members, the catalytic function of Fyn is tightly regulated by phosphorylation. Foremost, phosphorylation of Y_{420}, located in the activation loop of the SH1 domain, is necessary for Fyn activation (Cheng et al., 1991). The degree of Fyn activation is often measured by the level of phosphorylated Y_{420} normalized to total Fyn expression. In addition to Y_{420}, phosphorylation of S_{21} is also involved in the regulation of Fyn. Mutation of this site blocked protein kinase A (PKA) phosphorylation of Fyn and diminished kinase activity (Yeo et al., 2011). Basal Fyn activity is low due to intramolecular interactions between the SH2 domain and phosphorylated Y_{531} in the C-terminus and/or between the SH3 domain and the linker region of Fyn. Phosphorylation of Fyn at Y_{531} leads to an inhibition of Fyn activity (Relucio et al., 2009). When this site

is dephosphorylated by phosphatases including protein tyrosine phosphatase α (PTPα) and Src homology-2-domain-containing phosphatase (SHP1/2), Fyn activity is enhanced (Samayawardhena & Pallen, 2010; X. Yang, Dutta, & Shaw, 2010).

Fyn is an important player in synaptic plasticity. As mentioned previously, Fyn is required for induction of LTP at the CA3/CA1 synapse. The requirement for Fyn in LTP induction is unique amongst the Src family kinases since knockout of Src -/-, Yes -/-, and Abl -/- mice show no change in LTP (Grant et al., 1992; Kojima et al., 1997). The requirement for Fyn in synaptic plasticity is, at least in part, attributed to regulation of NMDA and AMPA Receptors. Potential sites of Fyn phosphorylation on the GluN2B subunit of NMDARs include Y1252, Y1336, and Y1472 (Nakazawa et al., 2001). Phosphorylation of GluN2B at Y1472 by Fyn enhances GluN2B-NMDAR currents, and facilitates LTD (K. Yang et al., 2011). Phosphorylation at these sites may also differentially alter NMDAR activity by enhancing degradation of the NMDAR, promoting truncation of GluN2 subunits, or by increasing insertion of NMDARs to the plasma membrane (Hu et al., 2010; Jurd et al., 2008; Lau & Zukin, 2007; Rong et al., 2001; Wu et al., 2007). Interestingly, it appears that scaffolding proteins such as post synaptic density 93 (PSD-93) or PSD-95 might promote the phosphorylation of NMDARs by Fyn (Sato et al., 2008; Tezuka et al., 1999). Furthermore, Fyn phosphorylation of GluN2A and GluN2B facilitates the binding of NMDARs to PSD-95, an interaction that has been linked to toxicity in stroke and in Alzheimer's disease (Aarts et al., 2002; Ittner et al., 2010; Rong et al., 2001).

Regulation of AMPARs is a crucial mechanism in synaptic plasticity (Santos et al., 2009). In neocortical neurons, both BDNF and platelet derived growth factor

(PDGF) enhanced surface expression of AMPARs via Fyn. The increase of AMPAR was blocked by a PTK inhibitor and was also absent in Fyn -/-mice (Narisawa-Saito et al., 1999). Transgenic mice overexpressing either wild type Fyn or constitutively activated Fyn have also been generated. Mice overexpressing constitutively active Fyn demonstrate enhanced basal synaptic transmission, and facilitated LTP using a weak theta-burst stimulation protocol. In contrast, the basal synaptic transmission and the threshold for the induction of LTP were not altered in the slices overexpressing wild type Fyn (Y. F. Lu et al., 1999). The regulation of NMDARs, AMPARs, and LTP induction outlined here demonstrate that Fyn plays a role in synaptic plasticity.

Importantly, Fyn kinase also plays a role in pathological conditions. For example, ROS increases autophosphorylation of Fyn in fibroblasts, and upregulates expression of Fyn in a model of chronic myelogenous leukemia (Gao et al., 2009; Sanguinetti, Cao, & Corley Mastick, 2003). Whether TRPM2 is also a target of Fyn kinase has not yet been explored; however, a recent paper has demonstrated that TRPM2 is tyrosine phosphorylated following exposure to oxidative stress. Inhibition of Src family kinases with PP2 decreases TRPM2 mediated Ca^{2+} influx in response to H_2O_2 treatment (Zhang et al., 2007). Combined, this data implicates Fyn in the regulation of TRPM2 channels.

1.10 HYPOTHESIS AND OBJECTIVES

TRPM2 is a Ca^{2+} permeable non-selective ion channel which is activated by oxidative stress and participates in cell death in a wide variety of cell types (Takahashi et al., 2011). TRPM2 exhibits the highest level of expression in the brain, where it is expressed in a variety of cell types including hippocampal pyramidal neurons (Fonfria, Murdock et al., 2006; Olah et al., 2009). The physiological role for TRPM2 in these cells, and mechanisms which regulate TRPM2 channels, requires investigation.

Preliminary evidence suggests that TRPM2 may be predominantly localized extrasynaptically on these neurons (Olah et al., 2009). Interestingly, some studies report that synaptic localization of NMDARs is more closely associated with LTP, while extrasynaptically localized NMDARs are more closely associated with LTD (W. Lu et al., 2001). Furthermore, substantial evidence supports a role for TRPM2 in cell death (Takahashi et al., 2011), and activation of extrasynaptic localization of NMDAR is associated with neurotoxicity (Hardingham et al., 2002; Sattler et al., 2000). Therefore, **we hypothesized that TRPM2 participates in NMDAR-dependent LTD at hippocampal CA3-CA1 synapses**.

TRPM2 may also represent a potential mediator of age-dependent Ca^{2+} dysregulation. First, TRPM2 is activated by oxidative stress. Second, it is permeable to Ca^{2+}, and TRPM2-mediated calcium-influx leads to cell death in a variety of cell types. Third, it is expressed in hippocampal pyramidal neurons which are not only critical for learning and memory, but are also particularly susceptible to cell death during ischemia and age-dependent neurodegenerative diseases such as Alzheimer's disease. Therefore,

we hypothesized that the expression or activity of TRPM2 is increased with age *in vitro* in cultured hippocampal pyramidal neurons.

Lastly, TRPM2 is implicated in neuronal cell death in response to oxidative stress and Aβ (Fonfria et al., 2005; Kaneko et al., 2006). Whether knockout of TRPM2 protects against Aβ oligomer-mediated toxicity has not yet been investigated. **We hypothesized that genetic deletion of TRPM2 will attenuate Aβ oligomer-induced reduction in cell viability in cultured hippocampal neurons.** Pathways which regulate TRPM2 during oxidative stress and/or following exposure to Aβ have not yet been elucidated. One potential mediator may be the non-receptor tyrosine kinase, Fyn. Oxidative stress induces tyrosine phosphorylation of TRPM2 (Zhang et al., 2007). Fyn kinase SH3 domain participates in protein-protein interactions between Fyn and several of its substrates via interactions with proline rich (PxxP) motifs in other proteins. Importantly, TRPM2 contains several proline rich motifs (PxxP) in the N- and C-terminal portions of TRPM2. **We hypothesized that Fyn kinase phosphorylates and interacts with TRPM2, and augments TRPM2 currents**.

REFERENCES

Aarts, M., Liu, Y., Liu, L., Besshoh, S., Arundine, M., Gurd, J. W., Wang, Y. T., Salter, M. W., & Tymianski, M. , 2002. Treatment of ischemic brain damage by perturbing NMDA receptor- PSD-95 protein interactions.Science298(5594), 846-850.

Anderson, M. E. , 1998. Glutathione: An overview of biosynthesis and modulation.Chem.Biol.Interact.111-112, 1-14.

Aoyama, K., Suh, S. W., Hamby, A. M., Liu, J., Chan, W. Y., Chen, Y., & Swanson, R. A. , 2006. Neuronal glutathione deficiency and age-dependent neurodegeneration in the EAAC1 deficient mouse.Nat.Neurosci.9(1), 119-126.

Arikkath, J., & Campbell, K. P. , 2003. Auxiliary subunits: Essential components of the voltage-gated calcium channel complex.Curr.Opin.Neurobiol.13(3), 298-307.

Bading, H., Ginty, D. D., & Greenberg, M. E. , 1993. Regulation of gene expression in hippocampal neurons by distinct calcium signaling pathways.Science260(5105), 181-186.

Bains, J. S., & Shaw, C. A. , 1997. Neurodegenerative disorders in humans: The role of glutathione in oxidative stress-mediated neuronal death.Brain Res.Brain Res.Rev.25(3), 335-358.

Beck, A., Kolisek, M., Bagley, L. A., Fleig, A., & Penner, R. , 2006. Nicotinic acid adenine dinucleotide phosphate and cyclic ADP-ribose regulate TRPM2 channels in T lymphocytes.FASEB J.20(7), 962-964.

Belrose, J. C., Cateano, F. A., Yang, K., Lockhart, B. M. W., Jackson, M. F., & MacDonald, J. F. (2012). Mechanisms of calcium influx following stroke. In Li, Y.V. & Zhang, J.H (Eds), *Metal Ion in Stroke*. New York, NY: Springer. (ISBN 978-1-4419-9662-6

Benarroch, E. E. , 2010. Neuronal voltage-gated calcium channels: Brief overview of their function and clinical implications in neurology.Neurology74(16), 1310-1315.

Blenn, C., Wyrsch, P., Bader, J., Bollhalder, M., & Althaus, F. R. , 2011. Poly(ADP-ribose)glycohydrolase is an upstream regulator of Ca2+ fluxes in oxidative cell death.Cell Mol.Life Sci.68(8), 1455-1466.

Catterall, W. A. , 2011. Voltage-gated calcium channels.Cold Spring Harb Perspect.Biol.3(8), a003947.

Catterall, W. A., & Few, A. P. , 2008. Calcium channel regulation and presynaptic plasticity.Neuron59(6), 882-901.

Cavazzini, M., Bliss, T., & Emptage, N. , 2005. Ca2+ and synaptic plasticity.Cell Calcium38(3-4), 355-367.

Chen, T. S., Richie, J. P.,Jr, & Lang, C. A. , 1989. The effect of aging on glutathione and cysteine levels in different regions of the mouse brain.Proc.Soc.Exp.Biol.Med.190(4), 399-402.

Cheng, S. H., Espino, P. C., Marshall, J., Harvey, R., Merrill, J., & Smith, A. E. , 1991. Structural elements that regulate pp59c-fyn catalytic activity, transforming potential, and ability to associate with polyomavirus middle-T antigen.J.Virol.65(1), 170-179.

Choi, D. W. , 1985. Glutamate neurotoxicity in cortical cell culture is calcium dependent.Neurosci.Lett.58(3), 293-297.

Christie, B. R., Eliot, L. S., Ito, K., Miyakawa, H., & Johnston, D. , 1995. Different Ca2+ channels in soma and dendrites of hippocampal pyramidal neurons mediate spike-induced Ca2+ influx.J.Neurophysiol.73(6), 2553-2557.

Christie, B. R., Schexnayder, L. K., & Johnston, D. , 1997. Contribution of voltage-gated Ca2+ channels to homosynaptic long-term depression in the CA1 region in vitro.J.Neurophysiol.77(3), 1651-1655.

Chung, K. K., Freestone, P. S., & Lipski, J. , 2011. Expression and functional properties of TRPM2 channels in dopaminergic neurons of the substantia nigra of the rat.J.Neurophysiol.106(6), 2865-2875.

Clancy, R. M., Levartovsky, D., Leszczynska-Piziak, J., Yegudin, J., & Abramson, S. B. , 1994. Nitric oxide reacts with intracellular glutathione and activates the hexose monophosphate shunt in human neutrophils: Evidence for S-nitrosoglutathione as a bioactive intermediary.Proc.Natl.Acad.Sci.U.S.A.91(9), 3680-3684.

Clapham, D. E. , 2007. SnapShot: Mammalian TRP channels.Cell129(1), 220.

Collingridge, G. L., Herron, C. E., & Lester, R. A. , 1988. Synaptic activation of N-methyl-D-aspartate receptors in the schaffer collateral-commissural pathway of rat hippocampus.J.Physiol.399, 283-300.

Collingridge, G. L., Kehl, S. J., & McLennan, H. , 1983. Excitatory amino acids in synaptic transmission in the schaffer collateral-commissural pathway of the rat hippocampus.J.Physiol.334, 33-46.

Collingridge, G. L., Peineau, S., Howland, J. G., & Wang, Y. T. , 2010. Long-term depression in the CNS.Nat.Rev.Neurosci.11(7), 459-473.

Cooke, M. P., & Perlmutter, R. M. , 1989. Expression of a novel form of the fyn proto-oncogene in hematopoietic cells.New Biol.1(1), 66-74.

Coyle, J. T., Price, D. L., & DeLong, M. R. , 1983. Alzheimer's disease: A disorder of cortical cholinergic innervation.Science219(4589), 1184-1190.

Csanady, L., & Torocsik, B. , 2009. Four Ca2+ ions activate TRPM2 channels by binding in deep crevices near the pore but intracellularly of the gate.J.Gen.Physiol.133(2), 189-203.

Dalle-Donne, I., Rossi, R., Giustarini, D., Colombo, R., & Milzani, A. , 2007. S-glutathionylation in protein redox regulation.Free Radic.Biol.Med.43(6), 883-898.

Dalva, M. B., McClelland, A. C., & Kayser, M. S. , 2007. Cell adhesion molecules: Signalling functions at the synapse.Nat.Rev.Neurosci.8(3), 206-220.

Davis, S., Butcher, S. P., & Morris, R. G. , 1992. The NMDA receptor antagonist D-2-amino-5-phosphonopentanoate (D-AP5) impairs spatial learning and LTP in vivo at intracerebral concentrations comparable to those that block LTP in vitro.J.Neurosci.12(1), 21-34.

De Felice, F. G., Velasco, P. T., Lambert, M. P., Viola, K., Fernandez, S. J., Ferreira, S. T., & Klein, W. L. , 2007. Abeta oligomers induce neuronal oxidative stress through an N-methyl-D-aspartate receptor-dependent mechanism that is blocked by the alzheimer drug memantine.J.Biol.Chem.282(15), 11590-11601.

Deisseroth, K., Heist, E. K., & Tsien, R. W. , 1998. Translocation of calmodulin to the nucleus supports CREB phosphorylation in hippocampal neurons.Nature392(6672), 198-202.

Demuro, A., Mina, E., Kayed, R., Milton, S. C., Parker, I., & Glabe, C. G. , 2005. Calcium dysregulation and membrane disruption as a ubiquitous neurotoxic mechanism of soluble amyloid oligomers.J.Biol.Chem.280(17), 17294-17300.

Derkach, V. A., Oh, M. C., Guire, E. S., & Soderling, T. R. , 2007. Regulatory mechanisms of AMPA receptors in synaptic plasticity.Nat.Rev.Neurosci.8(2), 101-113.

Di, A., Gao, X. P., Qian, F., Kawamura, T., Han, J., Hecquet, C., Ye, R. D., Vogel, S. M., & Malik, A. B. , 2011. The redox-sensitive cation channel TRPM2 modulates phagocyte ROS production and inflammation.Nat.Immunol.13(1), 29-34.

Dirnagl, U., Iadecola, C., & Moskowitz, M. A. , 1999. Pathobiology of ischaemic stroke: An integrated view.Trends Neurosci.22(9), 391-397.

Dringen, R., & Hamprecht, B. , 1998. Glutathione restoration as indicator for cellular metabolism of astroglial cells.Dev.Neurosci.20(4-5), 401-407.

Du, J., Xie, J., & Yue, L. , 2009a. Intracellular calcium activates TRPM2 and its alternative spliced isoforms.Proc.Natl.Acad.Sci.U.S.A.106(17), 7239-7244.

Du, J., Xie, J., & Yue, L. , 2009b. Modulation of TRPM2 by acidic pH and the underlying mechanisms for pH sensitivity.J.Gen.Physiol.134(6), 471-488.

Dudek, S. M., & Bear, M. F. , 1992. Homosynaptic long-term depression in area CA1 of hippocampus and effects of N-methyl-D-aspartate receptor blockade.Proc.Natl.Acad.Sci.U.S.A.89(10), 4363-4367.

Duncan, L. M., Deeds, J., Hunter, J., Shao, J., Holmgren, L. M., Woolf, E. A., Tepper, R. I., & Shyjan, A. W. , 1998. Down-regulation of the novel gene melastatin correlates with potential for melanoma metastasis.Cancer Res.58(7), 1515-1520.

Eisfeld, J., & Luckhoff, A. , 2007. Trpm2.Handb.Exp.Pharmacol.(179)(179), 237-252.

Fakler, B., & Adelman, J. P. , 2008. Control of K(ca) channels by calcium nano/microdomains.Neuron59(6), 873-881.

Fonfria, E., Marshall, I. C., Benham, C. D., Boyfield, I., Brown, J. D., Hill, K., Hughes, J. P., Skaper, S. D., & McNulty, S. , 2004. TRPM2 channel opening in response to oxidative stress is dependent on activation of poly(ADP-ribose) polymerase.Br.J.Pharmacol.143(1), 186-192.

Fonfria, E., Marshall, I. C., Boyfield, I., Skaper, S. D., Hughes, J. P., Owen, D. E., Zhang, W., Miller, B. A., Benham, C. D., & McNulty, S. , 2005. Amyloid beta-peptide(1-42) and hydrogen peroxide-induced toxicity are mediated by TRPM2 in rat primary striatal cultures.J.Neurochem.95(3), 715-723.

Fonfria, E., Mattei, C., Hill, K., Brown, J. T., Randall, A., Benham, C. D., Skaper, S. D., Campbell, C. A., Crook, B., Murdock, P. R., Wilson, J. M., Maurio, F. P., Owen, D. E., Tilling, P. L., & McNulty, S. , 2006. TRPM2 is elevated in the tMCAO stroke model, transcriptionally regulated, and functionally expressed in C13 microglia.J.Recept.Signal Transduct.Res.26(3), 179-198.

Fonfria, E., Murdock, P. R., Cusdin, F. S., Benham, C. D., Kelsell, R. E., & McNulty, S. , 2006. Tissue distribution profiles of the human TRPM cation channel family.J.Recept.Signal Transduct.Res.26(3), 159-178.

Foster, T. C. , 2007. Calcium homeostasis and modulation of synaptic plasticity in the aged brain.Aging Cell.6(3), 319-325.

Gabby, M., Tauber, M., Porat, S., & Simantov, R. , 1996. Selective role of glutathione in protecting human neuronal cells from dopamine-induced apoptosis.Neuropharmacology35(5), 571-578.

Gant, J. C., Sama, M. M., Landfield, P. W., & Thibault, O. , 2006. Early and simultaneous emergence of multiple hippocampal biomarkers of aging is mediated by Ca2+-induced Ca2+ release.J.Neurosci.26(13), 3482-3490.

Gao, Y., Howard, A., Ban, K., & Chandra, J. , 2009. Oxidative stress promotes transcriptional up-regulation of fyn in BCR-ABL1-expressing cells.J.Biol.Chem.284(11), 7114-7125.

Gasser, A., & Guse, A. H. , 2005. Determination of intracellular concentrations of the TRPM2 agonist ADP-ribose by reversed-phase HPLC.J.Chromatogr.B.Analyt Technol.Biomed.Life.Sci.821(2), 181-187.

Geiger, J. R., Melcher, T., Koh, D. S., Sakmann, B., Seeburg, P. H., Jonas, P., & Monyer, H. , 1995. Relative abundance of subunit mRNAs determines gating and Ca2+ permeability of AMPA receptors in principal neurons and interneurons in rat CNS.Neuron15(1), 193-204.

Goldsmith, J. F., Hall, C. G., & Atkinson, T. P. , 2002. Identification of an alternatively spliced isoform of the fyn tyrosine kinase.Biochem.Biophys.Res.Commun.298(4), 501-504.

Gomez-Isla, T., Price, J. L., McKeel, D. W.,Jr, Morris, J. C., Growdon, J. H., & Hyman, B. T. , 1996. Profound loss of layer II entorhinal cortex neurons occurs in very mild alzheimer's disease.J.Neurosci.16(14), 4491-4500.

Grant, S. G., O'Dell, T. J., Karl, K. A., Stein, P. L., Soriano, P., & Kandel, E. R. , 1992. Impaired long-term potentiation, spatial learning, and hippocampal development in fyn mutant mice.Science258(5090), 1903-1910.

Greer, P. L., & Greenberg, M. E. , 2008. From synapse to nucleus: Calcium-dependent gene transcription in the control of synapse development and function.Neuron59(6), 846-860.

Hara, Y., Wakamori, M., Ishii, M., Maeno, E., Nishida, M., Yoshida, T., Yamada, H., Shimizu, S., Mori, E., Kudoh, J., Shimizu, N., Kurose, H., Okada, Y., Imoto, K., & Mori, Y. , 2002. LTRPC2 Ca2+-permeable channel activated by changes in redox status confers susceptibility to cell death.Mol.Cell9(1), 163-173.

Haraguchi, K., Kawamoto, A., Isami, K., Maeda, S., Kusano, A., Asakura, K., Shirakawa, H., Mori, Y., Nakagawa, T., & Kaneko, S. , 2012. TRPM2 contributes to inflammatory and neuropathic pain through the aggravation of pronociceptive inflammatory responses in mice.J.Neurosci.32(11), 3931-3941.

Hardingham, G. E., Fukunaga, Y., & Bading, H. , 2002. Extrasynaptic NMDARs oppose synaptic NMDARs by triggering CREB shut-off and cell death pathways.Nat.Neurosci.5(5), 405-414.

Harman, D. , 1972. The biologic clock: The mitochondria?J.Am.Geriatr.Soc.20(4), 145-147.

Hecquet, C. M., Ahmmed, G. U., Vogel, S. M., & Malik, A. B. , 2008. Role of TRPM2 channel in mediating H2O2-induced Ca2+ entry and endothelial hyperpermeability.Circ.Res.102(3), 347-355.

Heiner, I., Eisfeld, J., Halaszovich, C. R., Wehage, E., Jungling, E., Zitt, C., & Luckhoff, A. , 2003. Expression profile of the transient receptor potential (TRP) family in neutrophil granulocytes: Evidence for currents through long TRP channel 2 induced by ADP-ribose and NAD.Biochem.J.371(Pt 3), 1045-1053.

Heiner, I., Eisfeld, J., Warnstedt, M., Radukina, N., Jungling, E., & Luckhoff, A. , 2006. Endogenous ADP-ribose enables calcium-regulated cation currents through TRPM2 channels in neutrophil granulocytes.Biochem.J.398(2), 225-232.

Hell, J. W., Westenbroek, R. E., Warner, C., Ahlijanian, M. K., Prystay, W., Gilbert, M. M., Snutch, T. P., & Catterall, W. A. , 1993. Identification and differential subcellular localization of the neuronal class C and class D L-type calcium channel alpha 1 subunits.J.Cell Biol.123(4), 949-962.

Hermosura, M. C., Cui, A. M., Go, R. C., Davenport, B., Shetler, C. M., Heizer, J. W., Schmitz, C., Mocz, G., Garruto, R. M., & Perraud, A. L. , 2008. Altered functional properties of a TRPM2 variant in guamanian ALS and PD.Proc.Natl.Acad.Sci.U.S.A.105(46), 18029-18034.

Hill, K., Tigue, N. J., Kelsell, R. E., Benham, C. D., McNulty, S., Schaefer, M., & Randall, A. D. , 2006. Characterisation of recombinant rat TRPM2 and a TRPM2-like conductance in cultured rat striatal neurones.Neuropharmacology50(1), 89-97.

Hirrlinger, J., Resch, A., Gutterer, J. M., & Dringen, R. , 2002. Oligodendroglial cells in culture effectively dispose of exogenous hydrogen peroxide: Comparison with cultured neurones, astroglial and microglial cells.J.Neurochem.82(3), 635-644.

Ho, V. M., Lee, J. A., & Martin, K. C. , 2011. The cell biology of synaptic plasticity.Science334(6056), 623-628.

Hollmann, M., Hartley, M., & Heinemann, S. , 1991. Ca2+ permeability of KA-AMPA--gated glutamate receptor channels depends on subunit composition.Science252(5007), 851-853.

Hu, J. L., Liu, G., Li, Y. C., Gao, W. J., & Huang, Y. Q. , 2010. Dopamine D1 receptor-mediated NMDA receptor insertion depends on fyn but not src kinase pathway in prefrontal cortical neurons.Mol.Brain3, 20.

Ikonomidou, C., Bosch, F., Miksa, M., Bittigau, P., Vockler, J., Dikranian, K., Tenkova, T. I., Stefovska, V., Turski, L., & Olney, J. W. , 1999. Blockade of NMDA receptors and apoptotic neurodegeneration in the developing brain.Science283(5398), 70-74.

Ikonomidou, C., Stefovska, V., & Turski, L. , 2000. Neuronal death enhanced by N-methyl-D-aspartate antagonists.Proc.Natl.Acad.Sci.U.S.A.97(23), 12885-12890.

Inamura, K., Sano, Y., Mochizuki, S., Yokoi, H., Miyake, A., Nozawa, K., Kitada, C., Matsushime, H., & Furuichi, K. , 2003. Response to ADP-ribose by activation of TRPM2 in the CRI-G1 insulinoma cell line.J.Membr.Biol.191(3), 201-207.

Ingley, E. , 2008. Src family kinases: Regulation of their activities, levels and identification of new pathways.Biochim.Biophys.Acta1784(1), 56-65.

Ittner, L. M., Ke, Y. D., Delerue, F., Bi, M., Gladbach, A., van Eersel, J., Wolfing, H., Chieng, B. C., Christie, M. J., Napier, I. A., Eckert, A., Staufenbiel, M., Hardeman, E., & Gotz, J. , 2010. Dendritic function of tau mediates amyloid-beta toxicity in alzheimer's disease mouse models.Cell

Jelic, D., Mildner, B., Kostrun, S., Nujic, K., Verbanac, D., Culic, O., Antolovic, R., & Brandt, W. , 2007. Homology modeling of human fyn kinase structure: Discovery of rosmarinic acid as a new fyn kinase inhibitor and in silico study of its possible binding modes.J.Med.Chem.50(6), 1090-1100.

Jia, J., Verma, S., Nakayama, S., Quillinan, N., Grafe, M. R., Hurn, P. D., & Herson, P. S. , 2011. Sex differences in neuroprotection provided by inhibition of TRPM2 channels following experimental stroke.J.Cereb.Blood Flow Metab.

Jiang, L. H. , 2007. Subunit interaction in channel assembly and functional regulation of transient receptor potential melastatin (TRPM) channels.Biochem.Soc.Trans.35(Pt 1), 86-88.

Jurd, R., Thornton, C., Wang, J., Luong, K., Phamluong, K., Kharazia, V., Gibb, S. L., & Ron, D. , 2008. Mind bomb-2 is an E3 ligase that ubiquitinates the N-methyl-D-aspartate receptor NR2B subunit in a phosphorylation-dependent manner.J.Biol.Chem.283(1), 301-310.

Jurma, O. P., Hom, D. G., & Andersen, J. K. , 1997. Decreased glutathione results in calcium-mediated cell death in PC12.Free Radic.Biol.Med.23(7), 1055-1066.

Kandel, E. R. , 2001. The molecular biology of memory storage: A dialogue between genes and synapses.Science294(5544), 1030-1038.

Kaneko, S., Kawakami, S., Hara, Y., Wakamori, M., Itoh, E., Minami, T., Takada, Y., Kume, T., Katsuki, H., Mori, Y., & Akaike, A. , 2006. A critical role of TRPM2 in neuronal cell death by hydrogen peroxide.J.Pharmacol.Sci.101(1), 66-76.

Kew, J. N., & Kemp, J. A. , 2005. Ionotropic and metabotropic glutamate receptor structure and pharmacology.Psychopharmacology (Berl)179(1), 4-29.

Kojima, N., Wang, J., Mansuy, I. M., Grant, S. G., Mayford, M., & Kandel, E. R. , 1997. Rescuing impairment of long-term potentiation in fyn-deficient mice by introducing fyn transgene.Proc.Natl.Acad.Sci.U.S.A.94(9), 4761-4765.

Kolisek, M., Beck, A., Fleig, A., & Penner, R. , 2005. Cyclic ADP-ribose and hydrogen peroxide synergize with ADP-ribose in the activation of TRPM2 channels.Mol.Cell18(1), 61-69.

Koppal, T., Drake, J., Yatin, S., Jordan, B., Varadarajan, S., Bettenhausen, L., & Butterfield, D. A. , 1999. Peroxynitrite-induced alterations in synaptosomal membrane proteins: Insight into oxidative stress in alzheimer's disease.J.Neurochem.72(1), 310-317.

Kostyrko, A., Hauser, J., Rybakowski, J. K., & Trzeciak, W. H. , 2006. Screening of chromosomal region 21q22.3 for mutations in genes associated with neuronal Ca2+ signalling in bipolar affective disorder.Acta Biochim.Pol.53(2), 317-320.

Kraft, R., Grimm, C., Grosse, K., Hoffmann, A., Sauerbruch, S., Kettenmann, H., Schultz, G., & Harteneck, C. , 2004. Hydrogen peroxide and ADP-ribose induce TRPM2-mediated calcium influx and cation currents in microglia.Am.J.Physiol.Cell.Physiol.286(1), C129-37.

Kraft, R., & Harteneck, C. , 2005. The mammalian melastatin-related transient receptor potential cation channels: An overview.Pflugers Arch.451(1), 204-211.

Kuhn, F. J., & Luckhoff, A. , 2004. Sites of the NUDT9-H domain critical for ADP-ribose activation of the cation channel TRPM2.J.Biol.Chem.279(45), 46431-46437.

Lambert, M. P., Barlow, A. K., Chromy, B. A., Edwards, C., Freed, R., Liosatos, M., Morgan, T. E., Rozovsky, I., Trommer, B., Viola, K. L., Wals, P., Zhang, C., Finch, C. E., Krafft, G. A., & Klein, W. L. , 1998. Diffusible, nonfibrillar ligands

derived from Abeta1-42 are potent central nervous system neurotoxins.Proc.Natl.Acad.Sci.U.S.A.95(11), 6448-6453.

Lange, I., Penner, R., Fleig, A., & Beck, A. , 2008. Synergistic regulation of endogenous TRPM2 channels by adenine dinucleotides in primary human neutrophils.Cell Calcium44(6), 604-615.

Lau, C. G., & Zukin, R. S. , 2007. NMDA receptor trafficking in synaptic plasticity and neuropsychiatric disorders.Nat.Rev.Neurosci.8(6), 413-426.

Lee, M., Cho, T., Jantaratnotai, N., Wang, Y. T., McGeer, E., & McGeer, P. L. , 2010. Depletion of GSH in glial cells induces neurotoxicity: Relevance to aging and degenerative neurological diseases.FASEB J.24(7), 2533-2545.

Lisman, J., Schulman, H., & Cline, H. , 2002. The molecular basis of CaMKII function in synaptic and behavioural memory.Nat.Rev.Neurosci.3(3), 175-190.

Liu, L., Wong, T. P., Pozza, M. F., Lingenhoehl, K., Wang, Y., Sheng, M., Auberson, Y. P., & Wang, Y. T. , 2004. Role of NMDA receptor subtypes in governing the direction of hippocampal synaptic plasticity.Science304(5673), 1021-1024.

Liu, R. M. , 2002. Down-regulation of gamma-glutamylcysteine synthetase regulatory subunit gene expression in rat brain tissue during aging.J.Neurosci.Res.68(3), 344-351.

Liu, Y., Wong, T. P., Aarts, M., Rooyakkers, A., Liu, L., Lai, T. W., Wu, D. C., Lu, J., Tymianski, M., Craig, A. M., & Wang, Y. T. , 2007. NMDA receptor subunits have differential roles in mediating excitotoxic neuronal death both in vitro and in vivo.J.Neurosci.27(11), 2846-2857.

Long, X., Liao, W., Jiang, C., Liang, D., Qiu, B., & Zhang, L. , 2012. Healthy aging: An automatic analysis of global and regional morphological alterations of human brain.Acad.Radiol.19(7), 785-793.

Lu, W., Man, H., Ju, W., Trimble, W. S., MacDonald, J. F., & Wang, Y. T. , 2001. Activation of synaptic NMDA receptors induces membrane insertion of new AMPA receptors and LTP in cultured hippocampal neurons.Neuron29(1), 243-254.

Lu, W., Shi, Y., Jackson, A. C., Bjorgan, K., During, M. J., Sprengel, R., Seeburg, P. H., & Nicoll, R. A. , 2009. Subunit composition of synaptic AMPA receptors revealed by a single-cell genetic approach.Neuron62(2), 254-268.

Lu, Y. F., Kojima, N., Tomizawa, K., Moriwaki, A., Matsushita, M., Obata, K., & Matsui, H. , 1999. Enhanced synaptic transmission and reduced threshold for LTP induction in fyn-transgenic mice.Eur.J.Neurosci.11(1), 75-82.

MacDonald, J. F., Jackson, M. F., & Beazely, M. A. , 2006. Hippocampal long-term synaptic plasticity and signal amplification of NMDA receptors.Crit.Rev.Neurobiol.18(1-2), 71-84.

MacDonald, J. F., Xiong, Z. G., & Jackson, M. F. , 2006. Paradox of Ca2+ signaling, cell death and stroke.Trends Neurosci.29(2), 75-81.

Malenka, R. C., & Bear, M. F. , 2004. LTP and LTD: An embarrassment of riches.Neuron44(1), 5-21.

Mattson, M. P. , 1998. Modification of ion homeostasis by lipid peroxidation: Roles in neuronal degeneration and adaptive plasticity.Trends Neurosci.21(2), 53-57.

Mattson, M. P. , 2007. Calcium and neurodegeneration.Aging Cell.6(3), 337-350.

Mattson, M. P., Guthrie, P. B., & Kater, S. B. , 1989. Intrinsic factors in the selective vulnerability of hippocampal pyramidal neurons.Prog.Clin.Biol.Res.317, 333-351.

McHugh, D., Flemming, R., Xu, S. Z., Perraud, A. L., & Beech, D. J. , 2003. Critical intracellular Ca2+ dependence of transient receptor potential melastatin 2 (TRPM2) cation channel activation.J.Biol.Chem.278(13), 11002-11006.

McQuillin, A., Bass, N. J., Kalsi, G., Lawrence, J., Puri, V., Choudhury, K., Detera-Wadleigh, S. D., Curtis, D., & Gurling, H. M. , 2006. Fine mapping of a susceptibility locus for bipolar and genetically related unipolar affective disorders, to a region containing the C21ORF29 and TRPM2 genes on chromosome 21q22.3.Mol.Psychiatry11(2), 134-142.

Miller, V. M., Lawrence, D. A., Mondal, T. K., & Seegal, R. F. , 2009. Reduced glutathione is highly expressed in white matter and neurons in the unperturbed mouse brain--implications for oxidative stress associated with neurodegeneration.Brain Res.1276, 22-30.

Montell, C., & Rubin, G. M. , 1989. Molecular characterization of the drosophila trp locus: A putative integral membrane protein required for phototransduction.Neuron2(4), 1313-1323.

Monyer, H., Burnashev, N., Laurie, D. J., Sakmann, B., & Seeburg, P. H. , 1994. Developmental and regional expression in the rat brain and functional properties of four NMDA receptors.Neuron12(3), 529-540.

Morris, R. G., Anderson, E., Lynch, G. S., & Baudry, M. , 1986. Selective impairment of learning and blockade of long-term potentiation by an N-methyl-D-aspartate receptor antagonist, AP5.Nature319(6056), 774-776.

Mulkey, R. M., & Malenka, R. C. , 1992. Mechanisms underlying induction of homosynaptic long-term depression in area CA1 of the hippocampus.Neuron9(5), 967-975.

Murphy, T. H., Worley, P. F., & Baraban, J. M. , 1991. L-type voltage-sensitive calcium channels mediate synaptic activation of immediate early genes.Neuron7(4), 625-635.

Nagamine, K., Kudoh, J., Minoshima, S., Kawasaki, K., Asakawa, S., Ito, F., & Shimizu, N. , 1998. Molecular cloning of a novel putative Ca2+ channel protein (TRPC7) highly expressed in brain.Genomics54(1), 124-131.

Nakazawa, T., Komai, S., Tezuka, T., Hisatsune, C., Umemori, H., Semba, K., Mishina, M., Manabe, T., & Yamamoto, T. , 2001. Characterization of fyn-mediated tyrosine phosphorylation sites on GluR epsilon 2 (NR2B) subunit of the N-methyl-D-aspartate receptor.J.Biol.Chem.276(1), 693-699.

Narisawa-Saito, M., Silva, A. J., Yamaguchi, T., Hayashi, T., Yamamoto, T., & Nawa, H. , 1999. Growth factor-mediated fyn signaling regulates alpha-amino-3-hydroxy-5-methyl-4-isoxazolepropionic acid (AMPA) receptor expression in rodent neocortical neurons.Proc.Natl.Acad.Sci.U.S.A.96(5), 2461-2466.

Nauser, T., Koppenol, W. H., & Gebicki, J. M. , 2005. The kinetics of oxidation of GSH by protein radicals.Biochem.J.392(Pt 3), 693-701.

Navarro, A., & Boveris, A. , 2007. The mitochondrial energy transduction system and the aging process.Am.J.Physiol.Cell.Physiol.292(2), C670-86.

Naziroglu, M., Ozgul, C., Cig, B., Dogan, S., & Uguz, A. C. , 2011. Glutathione modulates ca(2+) influx and oxidative toxicity through TRPM2 channel in rat dorsal root ganglion neurons.J.Membr.Biol.242(3), 109-118.

Nilius, B., & Owsianik, G. , 2011. The transient receptor potential family of ion channels.Genome Biol.12(3), 218.

Norris, C. M., Korol, D. L., & Foster, T. C. , 1996. Increased susceptibility to induction of long-term depression and long-term potentiation reversal during aging.J.Neurosci.16(17), 5382-5392.

Olah, M. E., Jackson, M. F., Li, H., Perez, Y., Sun, H. S., Kiyonaka, S., Mori, Y., Tymianski, M., & MacDonald, J. F. , 2009. Ca2+-dependent induction of TRPM2 currents in hippocampal neurons.J.Physiol.587(Pt 5), 965-979.

Orrenius, S., Zhivotovsky, B., & Nicotera, P. , 2003. Regulation of cell death: The calcium-apoptosis link.Nat.Rev.Mol.Cell Biol.4(7), 552-565.

Osterhout, D. J., Wolven, A., Wolf, R. M., Resh, M. D., & Chao, M. V. , 1999. Morphological differentiation of oligodendrocytes requires activation of fyn tyrosine kinase.J.Cell Biol.145(6), 1209-1218.

Ouanounou, A., Zhang, L., Charlton, M. P., & Carlen, P. L. , 1999. Differential modulation of synaptic transmission by calcium chelators in young and aged hippocampal CA1 neurons: Evidence for altered calcium homeostasis in aging.J.Neurosci.19(3), 906-915.

Parihar, M. S., Kunz, E. A., & Brewer, G. J. , 2008. Age-related decreases in NAD(P)H and glutathione cause redox declines before ATP loss during glutamate treatment of hippocampal neurons.J.Neurosci.Res.86(10), 2339-2352.

Perez-Reyes, E., Cribbs, L. L., Daud, A., Lacerda, A. E., Barclay, J., Williamson, M. P., Fox, M., Rees, M., & Lee, J. H. , 1998. Molecular characterization of a neuronal low-voltage-activated T-type calcium channel.Nature391(6670), 896-900.

Perraud, A. L., Fleig, A., Dunn, C. A., Bagley, L. A., Launay, P., Schmitz, C., Stokes, A. J., Zhu, Q., Bessman, M. J., Penner, R., Kinet, J. P., & Scharenberg, A. M. , 2001. ADP-ribose gating of the calcium-permeable LTRPC2 channel revealed by nudix motif homology.Nature411(6837), 595-599.

Perraud, A. L., Takanishi, C. L., Shen, B., Kang, S., Smith, M. K., Schmitz, C., Knowles, H. M., Ferraris, D., Li, W., Zhang, J., Stoddard, B. L., & Scharenberg, A. M. , 2005. Accumulation of free ADP-ribose from mitochondria mediates oxidative stress-induced gating of TRPM2 cation channels.J.Biol.Chem.280(7), 6138-6148.

Raps, S. P., Lai, J. C., Hertz, L., & Cooper, A. J. , 1989. Glutathione is present in high concentrations in cultured astrocytes but not in cultured neurons.Brain Res.493(2), 398-401.

Rebrin, I., Forster, M. J., & Sohal, R. S. , 2007. Effects of age and caloric intake on glutathione redox state in different brain regions of C57BL/6 and DBA/2 mice.Brain Res.1127(1), 10-18.

Regehr, W. G., Carey, M. R., & Best, A. R. , 2009. Activity-dependent regulation of synapses by retrograde messengers.Neuron63(2), 154-170.

Relucio, J., Tzvetanova, I. D., Ao, W., Lindquist, S., & Colognato, H. , 2009. Laminin alters fyn regulatory mechanisms and promotes oligodendrocyte development.J.Neurosci.29(38), 11794-11806.

Resh, M. D. , 1993. Interaction of tyrosine kinase oncoproteins with cellular membranes.Biochim.Biophys.Acta1155(3), 307-322.

Robillard, J. M., Gordon, G. R., Choi, H. B., Christie, B. R., & MacVicar, B. A. , 2011. Glutathione restores the mechanism of synaptic plasticity in aged mice to that of the adult.PLoS One6(5), e20676.

Rong, Y., Lu, X., Bernard, A., Khrestchatisky, M., & Baudry, M. , 2001. Tyrosine phosphorylation of ionotropic glutamate receptors by fyn or src differentially modulates their susceptibility to calpain and enhances their binding to spectrin and PSD-95.J.Neurochem.79(2), 382-390.

Roskoski, R.,Jr. , 2005. Src kinase regulation by phosphorylation and dephosphorylation.Biochem.Biophys.Res.Commun.331(1), 1-14.

Salter, M. W., & Kalia, L. V. , 2004. Src kinases: A hub for NMDA receptor regulation.Nat.Rev.Neurosci.5(4), 317-328.

Samayawardhena, L. A., & Pallen, C. J. , 2010. PTPalpha activates lyn and fyn and suppresses hck to negatively regulate FcepsilonRI-dependent mast cell activation and allergic responses.J.Immunol.185(10), 5993-6002.

Sanguinetti, A. R., Cao, H., & Corley Mastick, C. , 2003. Fyn is required for oxidative- and hyperosmotic-stress-induced tyrosine phosphorylation of caveolin-1.Biochem.J.376(Pt 1), 159-168.

Sano, Y., Inamura, K., Miyake, A., Mochizuki, S., Yokoi, H., Matsushime, H., & Furuichi, K. , 2001. Immunocyte Ca2+ influx system mediated by LTRPC2.Science293(5533), 1327-1330.

Santos, S. D., Carvalho, A. L., Caldeira, M. V., & Duarte, C. B. , 2009. Regulation of AMPA receptors and synaptic plasticity.Neuroscience158(1), 105-125.

Sasaki, T., Senda, M., Kim, S., Kojima, S., & Kubodera, A. , 2001. Age-related changes of glutathione content, glucose transport and metabolism, and mitochondrial electron transfer function in mouse brain.Nucl.Med.Biol.28(1), 25-31.

Sato, Y., Tao, Y. X., Su, Q., & Johns, R. A. , 2008. Post-synaptic density-93 mediates tyrosine-phosphorylation of the N-methyl-D-aspartate receptors.Neuroscience153(3), 700-708.

Sattler, R., Charlton, M. P., Hafner, M., & Tymianski, M. , 1998. Distinct influx pathways, not calcium load, determine neuronal vulnerability to calcium neurotoxicity.J.Neurochem.71(6), 2349-2364.

Sattler, R., Xiong, Z., Lu, W. Y., MacDonald, J. F., & Tymianski, M. , 2000. Distinct roles of synaptic and extrasynaptic NMDA receptors in excitotoxicity.J.Neurosci.20(1), 22-33.

Scahill, R. I., Frost, C., Jenkins, R., Whitwell, J. L., Rossor, M. N., & Fox, N. C. , 2003. A longitudinal study of brain volume changes in normal aging using serial registered magnetic resonance imaging.Arch.Neurol.60(7), 989-994.

Shen, B. W., Perraud, A. L., Scharenberg, A., & Stoddard, B. L. , 2003. The crystal structure and mutational analysis of human NUDT9.J.Mol.Biol.332(2), 385-398.

Sicheri, F., & Kuriyan, J. , 1997. Structures of src-family tyrosine kinases.Curr.Opin.Struct.Biol.7(6), 777-785.

Sowell, E. R., Peterson, B. S., Thompson, P. M., Welcome, S. E., Henkenius, A. L., & Toga, A. W. , 2003. Mapping cortical change across the human life span.Nat.Neurosci.6(3), 309-315.

Starkus, J., Beck, A., Fleig, A., & Penner, R. , 2007. Regulation of TRPM2 by extra- and intracellular calcium.J.Gen.Physiol.130(4), 427-440.

Starkus, J. G., Fleig, A., & Penner, R. , 2010. The calcium-permeable non-selective cation channel TRPM2 is modulated by cellular acidification.J.Physiol.588(Pt 8), 1227-1240.

Takahashi, N., Kozai, D., Kobayashi, R., Ebert, M., & Mori, Y. , 2011. Roles of TRPM2 in oxidative stress.Cell Calcium

Tao, R., Sun, H. Y., Lau, C. P., Tse, H. F., Lee, H. C., & Li, G. R. , 2011. Cyclic ADP ribose is a novel regulator of intracellular Ca2+ oscillations in human bone marrow mesenchymal stem cells.J.Cell.Mol.Med.15(12), 2684-2696.

Tezuka, T., Umemori, H., Akiyama, T., Nakanishi, S., & Yamamoto, T. , 1999. PSD-95 promotes fyn-mediated tyrosine phosphorylation of the N-methyl-D-aspartate receptor subunit NR2A.Proc.Natl.Acad.Sci.U.S.A.96(2), 435-440.

Thanislass, J., Raveendran, M., & Devaraj, H. , 1995. Buthionine sulfoximine-induced glutathione depletion. its effect on antioxidants, lipid peroxidation and calcium homeostasis in the lung.Biochem.Pharmacol.50(2), 229-234.

Thomas, S. M., & Brugge, J. S. , 1997. Cellular functions regulated by src family kinases.Annu.Rev.Cell Dev.Biol.13, 513-609.

Togashi, K., Hara, Y., Tominaga, T., Higashi, T., Konishi, Y., Mori, Y., & Tominaga, M. , 2006. TRPM2 activation by cyclic ADP-ribose at body temperature is involved in insulin secretion.EMBO J.25(9), 1804-1815.

Tong, Q., Zhang, W., Conrad, K., Mostoller, K., Cheung, J. Y., Peterson, B. Z., & Miller, B. A. , 2006. Regulation of the transient receptor potential channel TRPM2 by the Ca2+ sensor calmodulin.J.Biol.Chem.281(14), 9076-9085.

Toth, B., & Csanady, L. , 2010. Identification of direct and indirect effectors of the transient receptor potential melastatin 2 (TRPM2) cation channel.J.Biol.Chem.285(39), 30091-30102.

Tymianski, M., Charlton, M. P., Carlen, P. L., & Tator, C. H. , 1993. Source specificity of early calcium neurotoxicity in cultured embryonic spinal neurons.J.Neurosci.13(5), 2085-2104.

Uchida, K., Dezaki, K., Damdindorj, B., Inada, H., Shiuchi, T., Mori, Y., Yada, T., Minokoshi, Y., & Tominaga, M. , 2011. Lack of TRPM2 impaired insulin secretion and glucose metabolisms in mice.Diabetes60(1), 119-126.

Uemura, T., Kudoh, J., Noda, S., Kanba, S., & Shimizu, N. , 2005. Characterization of human and mouse TRPM2 genes: Identification of a novel N-terminal truncated protein specifically expressed in human striatum.Biochem.Biophys.Res.Commun.328(4), 1232-1243.

Usul, H., Cakir, E., Arslan, E., Peksoylu, B., Alver, A., Sayin, O. C., Topbas, M., & Baykal, S. , 2006. Effects of clotrimazole on experimental spinal cord injury.Arch.Med.Res.37(5), 571-575.

Vatish, M., Yamada, E., Pessin, J. E., & Bastie, C. C. , 2009. Fyn kinase function in lipid utilization: A new upstream regulator of AMPK activity?Arch.Physiol.Biochem.115(4), 191-198.

Villalba, M., Pereira, R., Martinez-Serrano, A., & Satrustegui, J. , 1995. Altered cell calcium regulation in synaptosomes and brain cells of the 30-month-old rat: Prominent effects in hippocampus.Neurobiol.Aging16(5), 809-816.

Wang, X., & Michaelis, E. K. , 2010. Selective neuronal vulnerability to oxidative stress in the brain.Front.Aging Neurosci.2, 12.

Wehage, E., Eisfeld, J., Heiner, I., Jungling, E., Zitt, C., & Luckhoff, A. , 2002. Activation of the cation channel long transient receptor potential channel 2 (LTRPC2) by hydrogen peroxide. A splice variant reveals a mode of activation independent of ADP-ribose.J.Biol.Chem.277(26), 23150-23156.

Wehrhahn, J., Kraft, R., Harteneck, C., & Hauschildt, S. , 2010. Transient receptor potential melastatin 2 is required for lipopolysaccharide-induced cytokine production in human monocytes.J.Immunol.184(5), 2386-2393.

Weisskopf, M. G., Bauer, E. P., & LeDoux, J. E. , 1999. L-type voltage-gated calcium channels mediate NMDA-independent associative long-term potentiation at thalamic input synapses to the amygdala.J.Neurosci.19(23), 10512-10519.

Whitlock, J. R., Heynen, A. J., Shuler, M. G., & Bear, M. F. , 2006. Learning induces long-term potentiation in the hippocampus.Science313(5790), 1093-1097.

Winterbourn, C. C., & Metodiewa, D. , 1994. The reaction of superoxide with reduced glutathione.Arch.Biochem.Biophys.314(2), 284-290.

Wu, H. Y., Hsu, F. C., Gleichman, A. J., Baconguis, I., Coulter, D. A., & Lynch, D. R. , 2007. Fyn-mediated phosphorylation of NR2B tyr-1336 controls calpain-mediated NR2B cleavage in neurons and heterologous systems.J.Biol.Chem.282(28), 20075-20087.

Xie, Y. F., Macdonald, J. F., & Jackson, M. F. , 2010. TRPM2, calcium and neurodegenerative diseases.Int.J.Physiol.Pathophysiol.Pharmacol.2(2), 95-103.

Xu, C., Li, P. P., Cooke, R. G., Parikh, S. V., Wang, K., Kennedy, J. L., & Warsh, J. J. , 2009. TRPM2 variants and bipolar disorder risk: Confirmation in a family-based association study.Bipolar Disord.11(1), 1-10.

Xu, C., Macciardi, F., Li, P. P., Yoon, I. S., Cooke, R. G., Hughes, B., Parikh, S. V., McIntyre, R. S., Kennedy, J. L., & Warsh, J. J. , 2006. Association of the putative susceptibility gene, transient receptor potential protein melastatin type 2, with bipolar disorder.Am.J.Med.Genet.B.Neuropsychiatr.Genet.141B(1), 36-43.

Yamamoto, S., Shimizu, S., Kiyonaka, S., Takahashi, N., Wajima, T., Hara, Y., Negoro, T., Hiroi, T., Kiuchi, Y., Okada, T., Kaneko, S., Lange, I., Fleig, A., Penner, R., Nishi, M., Takeshima, H., & Mori, Y. , 2008. TRPM2-mediated Ca2+influx induces chemokine production in monocytes that aggravates inflammatory neutrophil infiltration.Nat.Med.14(7), 738-747.

Yang, K., Trepanier, C., Sidhu, B., Xie, Y. F., Li, H., Lei, G., Salter, M. W., Orser, B. A., Nakazawa, T., Yamamoto, T., Jackson, M. F., & Macdonald, J. F. , 2011. Metaplasticity gated through differential regulation of GluN2A versus GluN2B receptors by src family kinases.EMBO J.31(4), 805-816.

Yang, W., Zou, J., Xia, R., Vaal, M. L., Seymour, V. A., Luo, J., Beech, D. J., & Jiang, L. H. , 2010. State-dependent inhibition of TRPM2 channel by acidic pH.J.Biol.Chem.285(40), 30411-30418.

Yang, X., Dutta, U., & Shaw, L. M. , 2010. SHP2 mediates the localized activation of fyn downstream of the alpha6beta4 integrin to promote carcinoma invasion.Mol.Cell.Biol.30(22), 5306-5317.

Yeo, M. G., Oh, H. J., Cho, H. S., Chun, J. S., Marcantonio, E. E., & Song, W. K. , 2011. Phosphorylation of ser 21 in fyn regulates its kinase activity, focal adhesion targeting, and is required for cell migration.J.Cell.Physiol.226(1), 236-247.

Zhang, W., Chu, X., Tong, Q., Cheung, J. Y., Conrad, K., Masker, K., & Miller, B. A. , 2003. A novel TRPM2 isoform inhibits calcium influx and susceptibility to cell death.J.Biol.Chem.278(18), 16222-16229.

Zhang, W., Tong, Q., Conrad, K., Wozney, J., Cheung, J. Y., & Miller, B. A. , 2007. Regulation of TRP channel TRPM2 by the tyrosine phosphatase PTPL1.Am.J.Physiol.Cell.Physiol.292(5), C1746-58.

CHAPTER 2

A version of this chapter has been published:

Xie, Y.F.*, **Belrose, J.C.*,** Tymianski, M., Mori, Y., MacDonald, J.F., Jackson, M.F. (2011). Dependence of NMDA/GSK3β mediated metaplasticity on TRPM2 channels at hippocampal CA3-CA1 synapses. *Molecular Brain, 4*:44. **these authors contributed equally to this work*

2. DEPENDENCE OF NMDA/GSK-3β MEDIATED METAPLASTICITY ON TRPM2 CHANNELS AT HIPPOCAMPAL CA3-CA1 SYNAPSES

2.1 Introduction

The transient receptor potential melastatin 2 channel (TRPM2) is a novel non-selective cation channel that was initially cloned from the brain, and was subsequently identified as an effector of calcium fluxes following oxidative stress (Takahashi et al., 2011). Functionally, TRPM2 has been linked to cell death, cytokine production, and insulin secretion (Takahashi et al., 2011). Interestingly, TRPM2 expression is greatest in the central nervous system (CNS) where it may contribute to neurodegenerative disease (Takahashi et al., 2011; Xie et al., 2011). We recently demonstrated functional expression of TRPM2 in CA1 pyramidal neurons (Olah et al., 2009), in culture and in situ. TRPM2 is unique among known ion channels in that it contains a cryptic C-terminal enzyme domain homologous to the NUDT9 ADP-ribose (ADPR) hydrolase. This channel motif serves primarily as the ligand binding domain for ADPR, which is required for Ca^{2+}-dependent gating of the channel (Scharenberg, 2005). In hippocampal neurons, TRPM2 currents can be activated by voltage-ramps that generate inward Ca^{2+} currents or by strong stimulation of NMDA receptors (NMDARs) (Olah et al., 2009). Indeed, high concentrations of ADPR are unable to evoke these currents until activated by an influx of Ca^{2+}. The coupling of channel activity to Ca^{2+} signaling downstream of voltage-gated Ca^{2+} channels and NMDARs suggests that TRPM2 could play a role in neuronal signaling or synaptic transmission. Given the lack of selective antagonists, we have examined the hypothesis that these channels contribute to synaptic plasticity by

employing TRPM2 deficient mice (Yamamoto et al., 2008).

2.1 Methods

Experimental animals

TRPM2 knockout (KO) mice, generated as described previously(Yamamoto et al., 2008), were provided by Dr Y Mori. Wild-type (WT) and KO mice used for experimentation were derived from heterozygous matings and mouse genotyping was performed as previously described (Yamamoto et al., 2008). Mice were kept in a pathogen-free environment, and analyses were performed using mice that were matched for age. All animal experiments were performed in accordance with protocols approved by the University of Western Ontario Animal Use Subcommittee of the University Council on Animal Care.

Whole-cell recording from primary culture

Mouse hippocampal primary neuronal cultures were prepared from E17-19 embryos using homozygously bred time pregnant TRPM2 KO mice or WT mice according to previously described procedures (MacDonald et al., 1989). Currents were recorded at 21-28 days in vitro. Whole-cell voltage-clamp recordings were performed as described previously (Olah et al., 2009), with minor adjustments. Briefly, standard intracellular solution (ICS) contained (in mM): 150 cesium gluconate, 10 Hepes, and 2 MgCl2. To record NMDA currents, 11 mM EGTA, 1 mM CaCl2, and 2 mM K2-ATP was added to the ICS. TRPM2 currents were recorded with 1 mM ADPR added to the ICS. Standard extracellular solution (ECS) contained (in mM): 140 NaCl, 5.4 KCl, 25 Hepes, 33 glucose, 2 CaCl2, and 0.2 μM TTX. To generate NMDA currents, 50 μM

NMDA and 0.5 μM glycine was added to the standard ECS and applied for 3 seconds every minute using a multibarrelled rapid perfusion system (SF77B; Warner Instruments). For experiments examining the contribution of GluN2B receptor, 1 μM Ro 25-6981 (Tocris) was applied after having obtained 3 stable control sweeps in its absence. ADPR-primed TRPM2 currents were generated with voltage ramps (± 100 mV over 500ms, applied every 10 sec) in the presence of standard ECS supplemented with 1 mM $MgCl_2$ and 1 mM $BaCl_2$. After the TRPM2 current stabilized, or after 10 minutes of voltage ramps, calcium-free solution was applied (total divalent concentration maintained by replacing $CaCl_2$ with equimolar $BaCl_2$). Voltage-clamp recordings (Vhold = -60 mV) were performed at room temperature (20-22°C) using a Multiclamp 700A amplifier (Molecular Devices). Data were filtered at 2 kHz, digitized, and acquired using pCLAMP and Axoscope software (Molecular Devices).

Hippocampal slices preparation

Hippocampal slices were prepared from age-matched TRPM2$^{-/-}$ and wild type mice (post-natal day 20-30). Briefly, mice were decapitated after isoflurane anesthesia, and brains were quickly removed and placed in ice-cold oxygenated (95% O2,5%CO2) artificial CSF (ACSF) containing: 124 mM NaCl, 3 mM KCl, 1.25 mM NaH2PO4, 1.3 mM MgCl2, 2.6 mM CaCl2, 26 mM NaHCO3 and 10 mM glucose (osmolality between 300 and 310 mOsm). Whole-brain coronal slices (300 μm) containing transverse sections of the hippocampus were prepared using a vibrating microtome (VT100E; Leica). After a recovery period of 1 h in oxygenated ACSF, hippocampal slices were transferred to a recording chamber continuously perfused with oxygenated ACSF (3 ml/ min), warmed to 31°C through an in-line solution heater.

Field excitatory postsynaptic potentials (fEPSP) recording from Schaffer collateral-CA1 synapses. fEPSPs were evoked every 30 s (0.033 Hz) by electrical stimulation (100 μs duration) delivered to the Schaffercollateral pathway using a concentric bipolar stimulating electrode (25 μm exposed tip) and recorded using glass microelectrodes (3-5 MΩ, filled with ACSF) positioned in the stratum radiatum of the CA1 area. The stimuli intensity was adjusted to evoke fEPSPs corresponding to 30~50% of the maximal response evoked in the absence of a contaminating spike discharge. The paired-pulse ratio was determined in each slice by delivering pairs of stimuli at varying interstimulus intervals (10-1000 ms). For LTD/LTP experiments, baseline fEPSPs were monitored for at least 20 min to ensure stability, following which synaptic plasticity was induced by repetitive stimulation at the Schaffer collaterals delivered at 1, 10, 20, 50 Hz (900 pulses at each frequency) or 100 Hz (four 1 sec trains delivered 20 sec apart). Following repetitive stimulation, fEPSP slopes were monitored for 1 h. Signals were amplified (Axoclamp 700B, Molecular Devices), recorded digitally (Digidata 1440A) and analyzed offline using Clampfit 10.

Whole-cell patch clamp recordings from hippocampal slices

Visual patch recordings from CA1 pyramidal neurons were performed using the whole-cell configuration with holding potential at -60 mV. Patch pipettes, pulled from borosilicate glass (4-6 MΩ), were filled with an internal solution containing (in mM): Cs-gluconate 132.5, CsCl 17.5, HEPES 10, EGTA 0.2, Mg-ATP 2 and GTP 0.3 (pH 7.25, 290 mOsm). Synaptic responses were evoked with a concentric bipolar tungsten electrode located about 50 μm from the cell body layer in CA1. In some recordings, NMDAR-mediated EPSCs were pharmacologically isolated by supplementing our

aCSF with CNQX (10 μM). The AMPAR-and NMDAR-mediated EPSCs were measured at -70 mV and +40 mV, respectively. For NMDAR-EPSCs, the amplitude was measured 20 ms after the start of the stimulus artifact (von Engelhardt et al., 2010). Signals were amplified using multiclamp 700B, sampled at 5 kHz, and analyzed with Clampfit 10 software (Molecular Devices).

Western Blotting

For the basal protein expression and protein phosphorylation assays, hippocampal tissue from wild type and TRPM2 KO mice (post-natal day 20-30) was used for Western blot. For experiments involving quinpirole treatment, hippocampal slices were incubated in ECS solution bubbled with 95%O2 and 5%CO2 at room temperature for at least 1 h, followed by exposing to quinpirole (10 μM) or vehicle for 30 min in aCSF. After 3 times wash with cold PBS, hippocampal tissue was homogenized in ice-cold RIPA buffer (50 mM Tris-HCl pH 7.4, 150 mM NaCl, 1 mM EDTA, 0.1% SDS, 0.5% Triton-X100, and 1% Sodium Deoxycholate) containing protease and phosphatase inhibitors. These samples were subjected to SDS-PAGE, transferred to a nitrocellulose membrane, which was subjected to repeated probing and stripping with antibodies as described. The signals were quantified using VersaDoc Imaging System (BioRad). The antibodies PSD-95, pGSK-3β^{Ser9}, GSK-3β, GluN2A and GluN2B were purchased from Cell Signaling Technology, and GluR1 and GluR2 from Santa Cruz Biotechnology, Inc.

Statistics

Data are expressed as mean ± SEM. Statistical comparisons were made using

either unpaired t-test or one-way ANOVA followed by Bonferroni post-hoc test, depending on the experimental protocol.

2.3 Results

Hippocampal neurons were cultured from wildtype (WT) and knockout (KO) mice using standard procedures outlined in the methods. This allowed us to compare the activation of TRPM2 currents in cultured pyramidal neurons from both genotypes. Whole-cell voltage clamp recordings were performed with 1 mM ADPR in the patch solution. Under these recording conditions TRPM2 currents were absent until multiple voltage-ramps are used to evoke these slowly developing currents (Figure 2.1). Large TRPM2 inward currents were generated at a holding potential of -60 mV in neurons from WT mice (Figure 2.1a, c; 553.4 ± 132 pA, n = 5) but were entirely absent in those from KO mice (Figure 2.1b; 7.9±7.2pA, n=6; unpaired t-test, p=0.001). Importantly, no genotypic difference in peak Ca^{2+} currents were detected (3648 ± 715 pA in WT, 2836 ± 390 pA in KO; unpaired t-test, p=0.3234; Figure 2.1d). Furthermore, there were no changes in peak responses (or steady-state to peak ratios) to applications of NMDA (Figure 2.1e, f) or in the GluN2B mediated component of this response determined by application of 1 μM Ro-256981, a highly selective antagonist of GluN2B containing receptors (Figure 2.1g). These results confirm the functional identification of TRPM2 currents in hippocampal pyramidal neurons, the absence of TRPM2 currents in neurons cultured from TRPM2 deficient mice, and that the absence of TRPM2 does not alter either voltage-dependent or NMDAR-dependent Ca^{2+} currents.

Next, acute transverse hippocampal slices were prepared from TRPM2 KO and WT mice at 3-4 weeks of age using standard approaches described in the methods. Field

excitatory postsynaptic potentials (fEPSPs) were recorded from CA3-CA1. We noted no difference in the paired-pulse ratios between WT and KO mice (Figure 2.2a). We then examined the effects of a short period of oxygen-glucose deprivation (OGD) on fEPSPs in slices from both genotypes. In WT slices, OGD resulted in a strong depression of the fEPSPs. This depression was greatly diminished in TRPM2 KO slices, consistent with a phenotype of a reduced responsiveness to the oxidative stress mediated by TRPM2 channels (Figure 2.2b).

TRPM2 currents can be activated by NMDAR stimulation; therefore, we examined whether TRPM2 might contribute to NMDAR-dependent synaptic plasticity. We first examined the induction of long-term potentiation (LTP) using a standard 100 Hz stimulation. No difference in LTP was observed in slices from TRPM2$^{-/-}$ mice (Figure 2.3a) suggesting that TRPM2 plays little or no role in this form of synaptic plasticity. However, NMDARs are also required for one form of long-term depression (LTD) at these synapses so we extended our studies to include low frequency stimulation. Applying 900 pulses at 1 Hz induced LTD in WT mice (0.84 ± 0.021, n =10) but failed to do so in TRPM2 KO mice (Figure 2.3b; 0.98 ± 0.025, n = 10; p = 0.017). Acute applications of the TRPM2 blocker clotrimazole also blocked LTD induced using this protocol (Figure 2.3c). Clotrimazole did not inhibit the induction of LTP (data not shown).

Figure 2.1. NMDAR and Ca^{2+} current function is preserved in TRPM2 KO cultured hippocampal neurons.

(a,b) ADPR-primed TRPM2 currents are facilitated by voltage ramps (± 100 mV, 1/10 sec) in WT (a), but not in cultured neurons from TRPM2-/- mice (b); (c) Summary bar graph of ADPR-primed peak current amplitude in WT and TRPM2-/- neurons. (unpaired t-test p = 0.001, 553.4 ± 132 pA in WT, n = 5; 7.9 ± 7.2 pA in KO, n = 6); (d) Peak Ca^{2+} currents elicited by the voltage ramp protocol are not altered by disruption of TRPM2 channel expression; Neither NMDAR peak currents (e), nor NMDAR steady state to peak ratios (f) generated in response to rapid applications of NMDA to cultured hippocampal neurons are affected by loss of TRPM2 expression; (g) Representative traces and summary bar graph of GluN2B subtype NMDAR inhibition with Ro 25-6981. Results demonstrate that the contribution of GluN2B subtype receptors to total NMDAR charge transfer is unaltered in cultured TRPM2 KO hippocampal neurons relative to control.

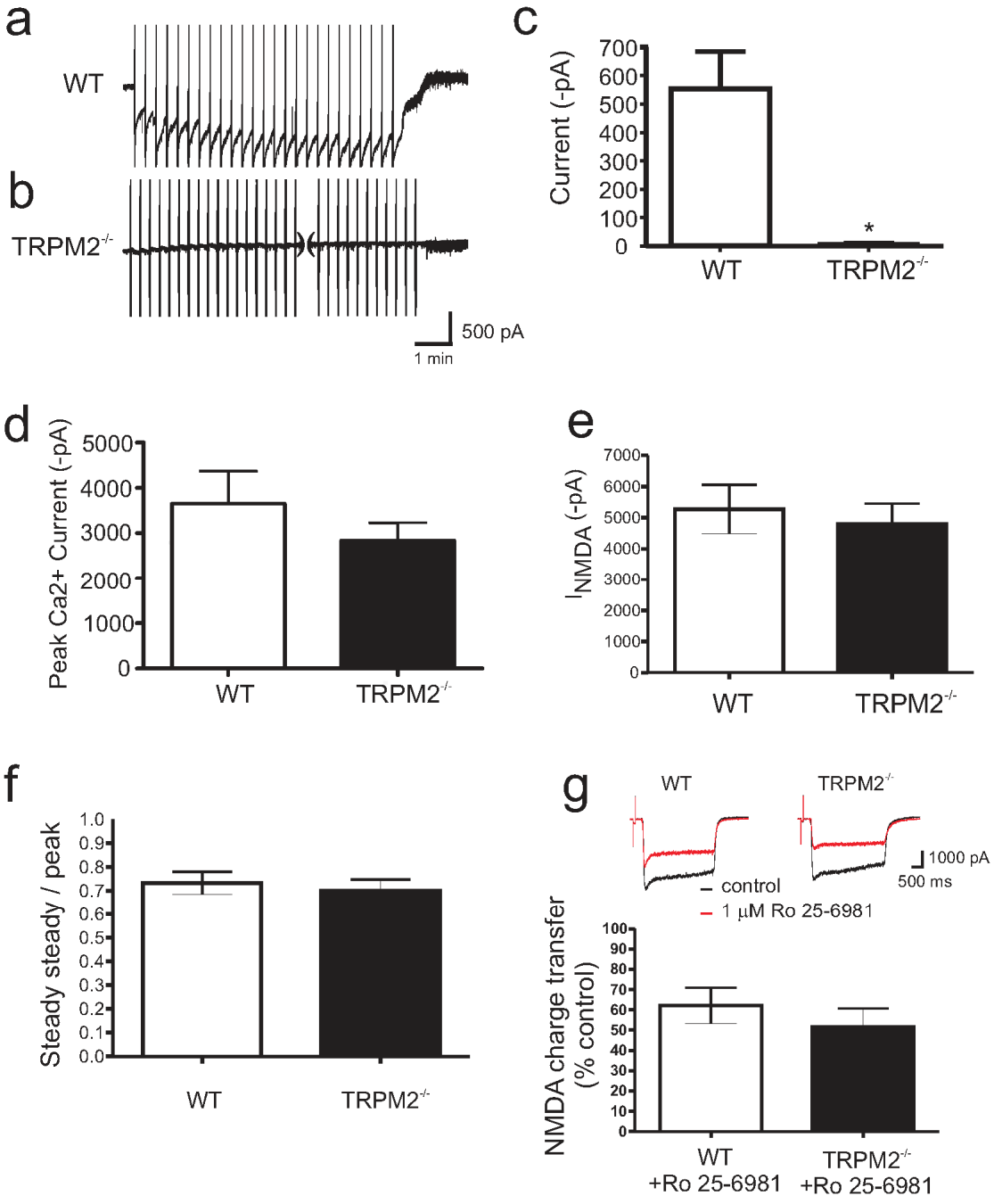
a
WT
b
TRPM2-/-
500 pA
1 min
c
Current (-pA)
700
600
500
400
300
200
100
0
*
WT
TRPM2-/-
d
Peak Ca2+ Current (-pA)
5000
4000
3000
2000
1000
0
WT
TRPM2-/-
e
INMDA (-pA)
7000
6000
5000
4000
3000
2000
1000
0
WT
TRPM2-/-
f
Steady steady / peak
1.0
0.9
0.8
0.7
0.6
0.5
0.4
0.3
0.2
0.1
0.0
WT
TRPM2-/-
g
WT
TRPM2-/-
1000 pA
500 ms
control
1 μM Ro 25-6981
NMDA charge transfer (% control)
100
90
80
70
60
50
40
30
20
10
0
WT +Ro 25-6981
TRPM2-/- +Ro 25-6981

Figure 2.2 OGD-mediated LTD is impaired in the absence of TRPM2

(a) The response to a paired-pulse protocol is identical in hippocampal slices derived from TRPM2 KO mice and WT controls (n=11 per group), demonstrating that pre-synaptic short-term plasticity is unaltered in the absence of TRPM2; (b) Transient oxygen-glucose deprivation (5 min OGD) causes long-lasting depression of fEPSP slopes in slices from WT (n = 12) but not TRPM2-/- (n = 6).

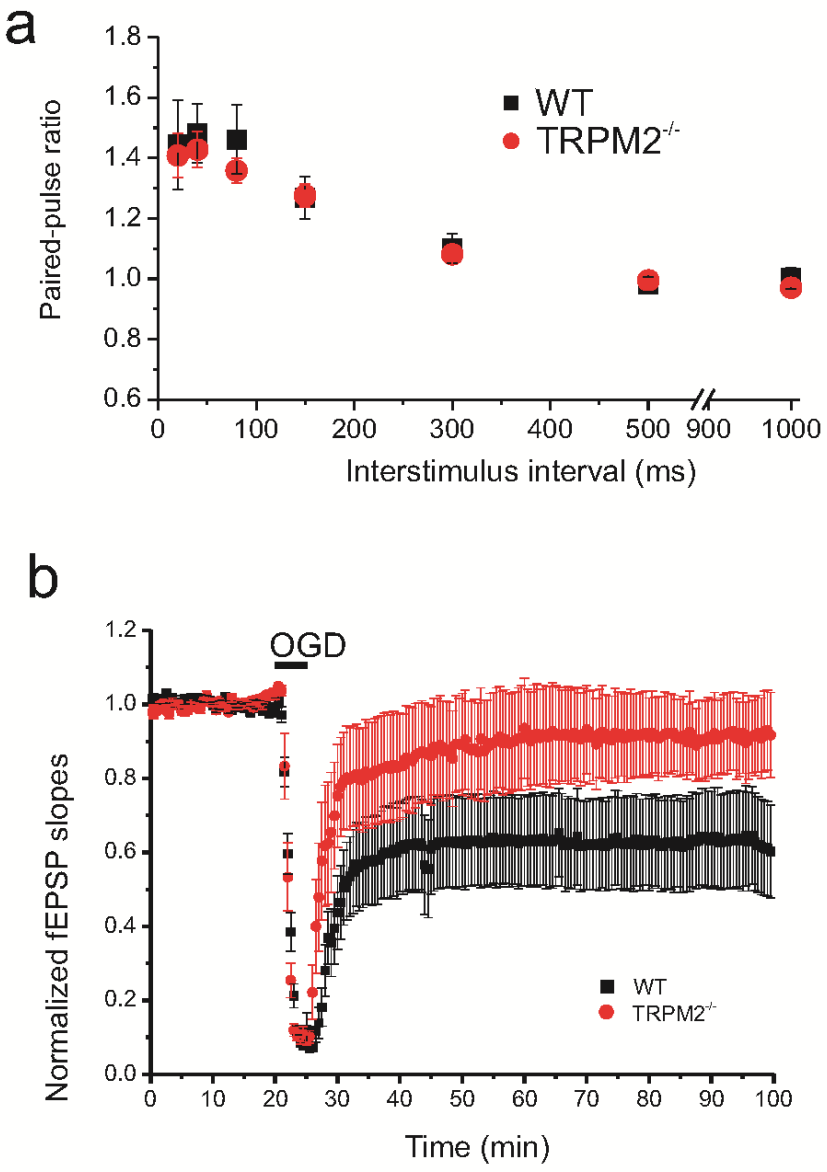
a
Paired-pulse ratio
1.8
1.6
1.4
1.2
1.0
0.8
0.6
WT
TRPM2-/-
0
100
200
300
400
500
900
1000
Interstimulus interval (ms)
b
OGD
Normalized fEPSP slopes
1.2
1.0
0.8
0.6
0.4
0.2
0.0
WT
TRPM2-/-
0
10
20
30
40
50
60
70
80
90
100
Time (min)

LTD at these synapses can also depend upon activation of group 1 mGluRs rather than NMDARs (Collingridge et al., 2010), we therefore examined responses to a bath exposure to NMDA (10 μM, 5 min) or DHPG (10 μM, 20 min) in slices of both genotypes. The LTD induced by DHPG was similar in WT and TRPM2 KO mice (Figure 2.3d; 0.85 ± 0.043, n = 6 in WT vs 0.80 ± 0.031, n = 7 in TRPM2 KO mice, respectively; $p > 0.05$). Conversely, NMDA application induced LTD in slices from WT (n = 6) but failed to do so in TRPM2 KO mice (Figure 2.3e; n = 6). When plasticity induced by a range of repetitive stimulation frequencies was examined it was clear that TRPM2 KO slices demonstrated a substantial impairment in NMDA-dependent LTD (Figure 2.3f).

The expression of NMDAR-dependent LTD at CA3-CA1 synapses requires the endocytosis of AMPA Receptors (AMPARs) (Collingridge et al., 2010; Sanderson, Collingridge, & Fitzjohn, 2011). To determine if there was a change in the functional expression of AMPARs in TRPM2 KO mice we used whole cell voltage clamp recordings to measure the ratio of AMPAR to NMDAR mediated EPSCs. By holding the membrane potential at -70 and +40 mV the relative contribution of each receptor type was determined. This ratio was significantly reduced in TRPM2 KO (n = 10) neurons compared to WT (n = 10, $p < 0.01$; Figure 2.4a). These results suggest that a reduction of synaptic AMPARs or alternatively an enhancement of NMDARs may underlie the deficiency of LTD in TRPM2 KO mice. A change in AMPARs was supported by our observation of a reduction of mEPSC amplitude but not frequency in TRPM2 KO mice (Figure 2.4b,c,d).

Figure 2.3 LTD is impaired in hippocampal slices derived from TRPM2 KO mice. (a) LTP is unaffected by knockout of TRPM2 (WT, n = 6; TRPM2-/-, n = 8); (b) LTD of fEPSPs evoked by repetitive stimulation (900 stimuli at 1 Hz) in WT slices (n = 10) is absent in slices from TRPM2 KO mice (n = 10); (c) LTD of fEPSPs was inhibited by application of clotrimazole, a TRPM2 inhibitor. Timing of clotrimazole application in treated slices is indicated by the black bar. (d) Metabotropic-glutamate receptor dependent LTD is unimpaired by deletion of TRPM2 (WT, n = 6; TRPM2 KO, n = 7); (e) Chem-LTD, evoked by 5 min application of NMDA (10 μM) is abolished in slices from TRPM2 KO (n = 6) but not WT (n = 6) slices; (f) Summary graph for a series of recordings from WT and TRPM2 KO slices in which plasticity was induced by repetitive stimulation delivered at 1, 10, 20, 50 Hz (900 pulses at each frequency) or 100 Hz (four 1 sec trains delivered 20 sec apart). For each induction frequency, normalized fEPSP slopes, measured at the end of recording from each of the two populations of slices, are plotted. Numbers in parentheses represents the number of recordings at each point. *denotes $p = 0.016$.

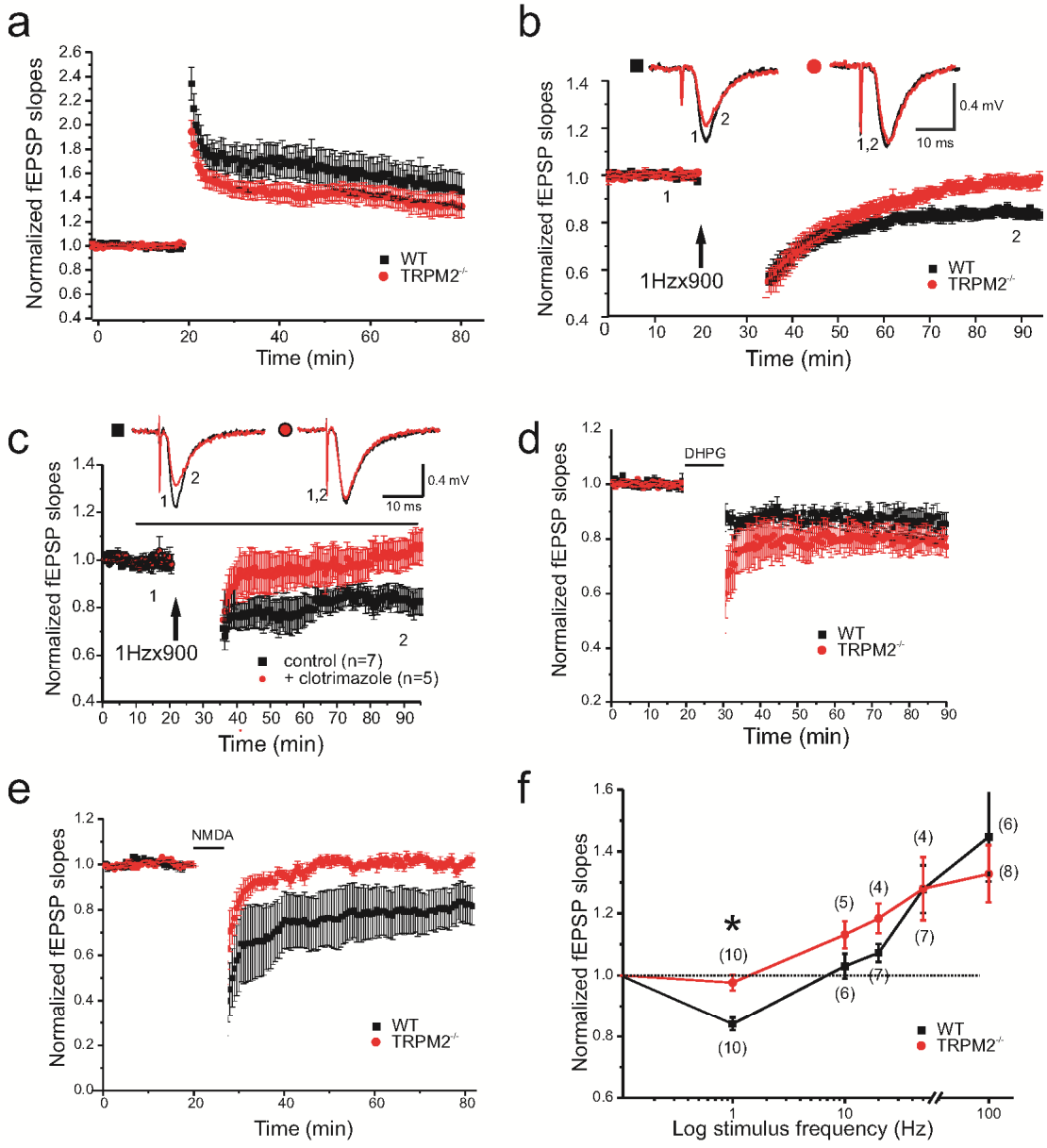
a
Normalized fEPSP slopes
Time (min)
WT
TRPM2-/-
b
Normalized fEPSP slopes
0.4 mV
10 ms
1
2
1,2
1Hzx900
Time (min)
WT
TRPM2-/-
c
Normalized fEPSP slopes
0.4 mV
10 ms
1Hzx900
control (n=7)
+ clotrimazole (n=5)
Time (min)
d
DHPG
Normalized fEPSP slopes
Time (min)
WT
TRPM2-/-
e
NMDA
Normalized fEPSP slopes
Time (min)
WT
TRPM2-/-
f
Normalized fEPSP slopes
Log stimulus frequency (Hz)
WT
TRPM2-/-

We also examined the relative contribution of NMDARs composed of GluN2A or GluN2B subunits to synaptic currents by measuring EPSC NMDAR before and after application of the selective GluN2B antagonist, Ro-256981. The relative block was the same regardless of genotype (Figure 2.4e).

During LTD there is some loss of postsynaptic density 95 protein (PSD-95) from the synapses followed by endocytosis of AMPAR (Bhattacharyya et al., 2009). Therefore, we used western blotting to examine if there was a change in PSD-95 expression in TRPM2 KO mice. Consistent with the change in AMPARs, we observed a significant reduction in PSD-95 expression (Figure 2.5a). Previous reports link the level of PSD-95 expression with AMPAR number without an overall change in synaptic number (Bhattacharyya et al., 2009; Chen et al., 2011). We examined the total expression of GluR1 in TRPM2 KO slices versus those from WT mice, and as anticipated observed a reduction in the expression of GluR1 (Figure 2.5b). In contrast, the expression levels of GluR2 and NMDAR subunits were the same regardless of genotype (Figure 2.5b,c,).

To further explore the mechanism of the loss of NMDAR-dependent LTD in TRPM2 KO mice we examined the activity of glycogen synthase kinase-3β (GSK-3β), which is required for this form of LTD (Peineau et al., 2007; Peineau et al., 2009). We compared the expression levels and phosphorylation of this kinase at Ser9, which is indicative of inactivation of GSK-3β (Frame, Cohen, & Biondi, 2001). Expression of GSK-3β was unaltered; however, there was an increase in Ser9 phosphorylation (GSK-3β inactivation) in TRPM2 KO slices (Figure 2.5d) suggesting that impaired LTD in TRPM2 KO mice results from inhibition of GSK-3β (Peineau et al., 2007).

Figure 2.4. AMPA/NMDA Receptor Contribution to EPSCs, and mEPSC amplitude are diminished in TRPM2 KO slices.

(a) The ratio of AMPAR- to NMDAR-mediated EPSCs is reduced in TRPM2-/- neurons. (b,c,d) Representative mEPSC traces (b) and summary bar graphs demonstrating that the amplitude (c), but not the frequency (d) of mEPSCs is reduced in slices from TRPM2 KO mice; (e) The relative contribution of GluN2B NMDAR subtype to NMDAR EPSC, quantified by application of the selective antagonist Ro 25-6981, is unaltered in TRPM2 KO slices, confirming previous results in culture.

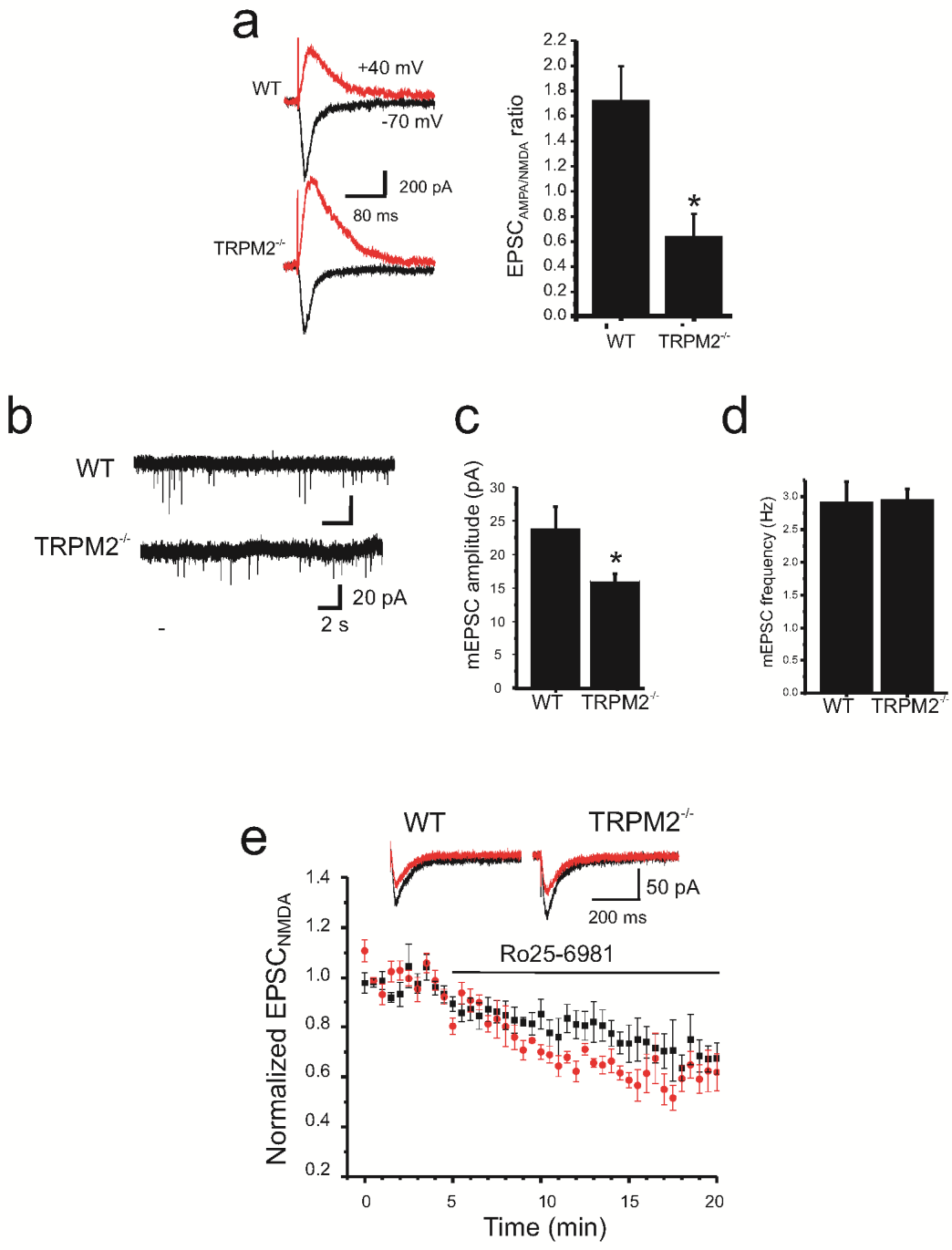
a
WT
+40 mV
-70 mV
200 pA
80 ms
TRPM2-/-
EPSCAMPA/NMDA ratio
WT
TRPM2-/-
b
WT
TRPM2-/-
20 pA
2 s
c
mEPSC amplitude (pA)
WT
TRPM2-/-
d
mEPSC frequency (Hz)
WT
TRPM2-/-
e
WT
TRPM2-/-
50 pA
200 ms
Ro25-6981
Normalized EPSCNMDA
Time (min)

Insulin also acts via stimulation of Akt/PKB to inactivate GSK-3β via Ser9 phosphorylation, resulting in a long lasting depression of AMPAR-mediated synaptic transmission, which in turn occludes low frequency induced LTD (Man et al., 2000). We therefore examined the effect of insulin on WT and TRPM2 KO slices. The long-lasting depression induced by applications of insulin was lacking in TRPM2 KO slices (Figure 2.5e) suggesting that insulin-induced LTD was occluded in this genotype due to the pre-existing inactivation of GSK-3β. To determine if the loss of LTD in TRPM2 KO is attributable to the consistent inhibition of GSK-3β we applied the D2 agonist quinpirole in order to stimulate Akt GSK-3β signaling (Beaulieu, Gainetdinov, & Caron, 2007) and observed an enhanced activation of GSK-3β (Figure 2.5f) and rescue of LTD in TRPM2 KO mice (Figure 2.5g).

2.4 Discussion

Our results show that loss of TRPM2 expression modifies NMDAR-dependent synaptic plasticity, specifically LTD, but they do not implicate TRPM2 channels directly in excitatory synaptic transmission. Instead, the presence of TRPM2 channels seems to be associated with maintenance of the appropriate level of GSK-3β activation as well as full expression of PSD-95 and AMPARs. In the absence of the TRPM2 expression there is a reduction in the relative contribution of AMPA receptors to synaptic transmission at CA1 synapses along with a reduction of LTD and a shift to lower thresholds for the induction of LTP. This metaplastic shift towards LTP in TRPM2 KO slices seems to result from enhanced phosphorylation and inactivation of GSK-3β.

Figure 2.5 Inhibition of GSK-3β phosphorylation and reduced PSD-95 and AMPAR expression contributes to impaired LTD in TRPM2 KO mice.

The expression of (a) PSD-95 (normalized to β-actin loading control) and (b) the AMPAR subunit, GluR1, is depressed in slices from TRPM2 KO mice. (b,c) Expression of the AMPAR subunit, GluR2, and the NMDAR subunits GluN2A, GluN2B, and GluN1 are unchanged in the absence of TRPM2; (d) Knockout of TRPM2 is correlated with an increase in GSK-3β phosphorylation at its inhibitory site (Ser9, n = 3); (e) Insulin application to hippocampal slices depresses AMPAR-mediated fEPSPs in slices from TRPM2 KO, but not WT, slices. (f) Simulation of dopamine D2 receptors by quinpirole (10 μM) reduces GSK-3β phosphorylation at Ser9 (n = 3); (g) D2 receptor stimulation by quinpirole rescues LTD in slices from TRPM2 KO mice.

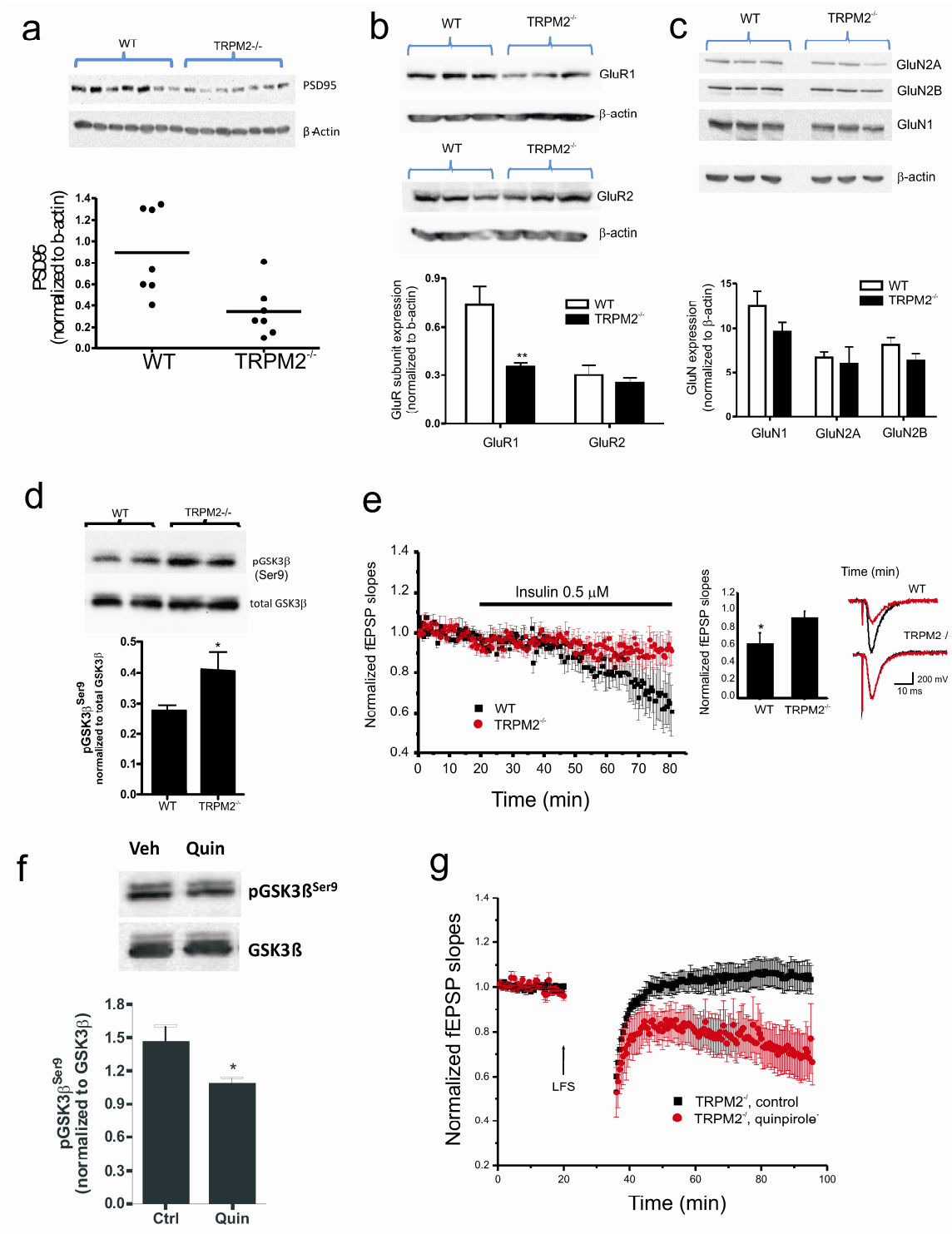
a
WT
TRPM2-/-
PSD95
β-Actin
PSD95 (normalized to b-actin)
WT
TRPM2-/-
b
WT
TRPM2-/-
GluR1
β-actin
GluR2
β-actin
GluR subunit expression (normalized to b-actin)
WT
TRPM2-/-
GluR1
GluR2
c
GluN2A
GluN2B
GluN1
β-actin
GluN expression (normalized to β-actin)
GluN1
GluN2A
GluN2B
d
pGSK3β (Ser9)
total GSK3β
pGSK3β Ser9 normalized to total GSK3β
e
Insulin 0.5 μM
Normalized fEPSP slopes
Time (min)
WT
TRPM2-/-
Time (min)
200 mV
10 ms
f
Veh
Quin
pGSK3ßSer9
GSK3ß
pGSK3β Ser9 (normalized to GSK3β)
Ctrl
Quin
g
Normalized fEPSP slopes
LFS
TRPM2-/-, control
TRPM2-/-, quinpirole
Time (min)

The resulting inactivation of GSK-3β prevented further depression of synaptic transmission by applications of insulin. Importantly, applications of quinpirole reduced GSK-3β phosphorylation in TRPM2 KO slices and effectively rescued LTD induction by repetitive low-frequency stimulation. Moreover, acute block of TRPM2 function by clotrimazole prevented LTD induction thereby mimicking TRPM2 loss of function by genetic deletion. Collectively, these findings argue that the reductions in GSK-3β activity, PSD-95 and GluR1 expression, as well as AMPAR-mediated synaptic transmission and plasticity observed in hippocampal slices derived from TRPM2 KO mice cannot simply be attributed to developmental compensations resulting from genetic deletion of TRPM2. Rather, in light of our findings, we propose that ongoing TRPM2 channel activity contributes to the regulation of AMPAR-mediated fast excitatory synaptic transmission through maintenance of constitutive GSK-3β activity.

The precise mechanism through which TRPM2 activity regulates GSK-3β remains to be determined; however the contribution of TRPM2 to Ca^{2+} signaling is likely to play an important role is this regard. Previous findings have proposed the Ca^{2+} dependent phosphatase, calcineurin (or PP2B), as a candidate for mediating dephosphorylation of GSK-3β at Ser9 (Y. Kim et al., 2009). Alternatively, the Ca^{2+}-dependent tyrosine kinase Pyk2 has been shown to associate and regulate GSK-3β activity through tyrosine phosphorylation (Sayas et al., 2006). Whether the activity of either calcineurin, Pyk2, or other kinases or phosphatases are altered by TRPM2-initiated Ca^{2+} signaling remains to be established. Similarly, the behavioural consequence of altered synaptic transmission and plasticity associated with the loss of TRPM2 function has yet to be investigated; however, a recent paper by Kim and

colleagues (2011) may offer some insight. These authors demonstrated that behavioural flexibility, evaluated by reversal learning in the Morris water maze and by the delayed non-match to place T-maze task, was reduced following genetic disruption of PI3Kγ, which also resulted in a selective loss of NMDAR dependent LTD (J. I. Kim et al., 2011). Additional research is required to assess whether these behaviours are similarly altered in TRPM2 KO mice.

Conclusions

The present study establishes that loss of TRPM2 function through genetic means provokes long lasting changes in excitatory synaptic transmission and plasticity at the CA3-CA1 hippocampal synapse. Specifically, we show that the ability to induce NMDAR-dependent LTD is impaired in TRPM2 KO mice. Such impairment was associated with increased phosphorylation and inactivation of GSK-3β. Consistent with previously reported changes associated with GSK-3β inhibition, we report reduced PSD-95 and GluR1 expression and identify a corresponding reduction in AMPAR-mediated synaptic transmission. Interestingly, both GSK-3β and TRPM2 channels have been implicated in a number of overlapping pathophysiological processes ranging from pancreatic insulin secretion to Alzheimer's disease (Bhat, Budd Haeberlein, & Avila, 2004; Takahashi et al., 2011). Accordingly, our results show the importance of continuing studies to determine the pathophysiological roles of GSK-3β and TRPM2 in neurodegenerative diseases (Jo et al., 2011).

References

Beaulieu, J. M., Gainetdinov, R. R., & Caron, M. G. , 2007. The akt-GSK-3 signaling cascade in the actions of dopamine.Trends Pharmacol.Sci.28(4), 166-172.

Bhat, R. V., Budd Haeberlein, S. L., & Avila, J. , 2004. Glycogen synthase kinase 3: A drug target for CNS therapies.J.Neurochem.89(6), 1313-1317.

Bhattacharyya, S., Biou, V., Xu, W., Schluter, O., & Malenka, R. C. , 2009. A critical role for PSD-95/AKAP interactions in endocytosis of synaptic AMPA receptors.Nat.Neurosci.12(2), 172-181.

Chen, X., Nelson, C. D., Li, X., Winters, C. A., Azzam, R., Sousa, A. A., Leapman, R. D., Gainer, H., Sheng, M., & Reese, T. S. , 2011. PSD-95 is required to sustain the molecular organization of the postsynaptic density.J.Neurosci.31(17), 6329-6338.

Collingridge, G. L., Peineau, S., Howland, J. G., & Wang, Y. T. , 2010. Long-term depression in the CNS.Nat.Rev.Neurosci.11(7), 459-473.

Frame, S., Cohen, P., & Biondi, R. M. , 2001. A common phosphate binding site explains the unique substrate specificity of GSK3 and its inactivation by phosphorylation.Mol.Cell7(6), 1321-1327.

Jo, J., Whitcomb, D. J., Olsen, K. M., Kerrigan, T. L., Lo, S. C., Bru-Mercier, G., Dickinson, B., Scullion, S., Sheng, M., Collingridge, G., & Cho, K. , 2011. Abeta(1-42) inhibition of LTP is mediated by a signaling pathway involving caspase-3, Akt1 and GSK-3beta.Nat.Neurosci.14(5), 545-547.

Kim, J. I., Lee, H. R., Sim, S. E., Baek, J., Yu, N. K., Choi, J. H., Ko, H. G., Lee, Y. S., Park, S. W., Kwak, C., Ahn, S. J., Choi, S. Y., Kim, H., Kim, K. H., Backx, P. H., Bradley, C. A., Kim, E., Jang, D. J., Lee, K., Kim, S. J., Zhuo, M., Collingridge, G. L., & Kaang, B. K. , 2011. PI3Kgamma is required for NMDA receptor-dependent long-term depression and behavioral flexibility.Nat.Neurosci.14(11), 1447-1454.

Kim, Y., Lee, Y. I., Seo, M., Kim, S. Y., Lee, J. E., Youn, H. D., Kim, Y. S., & Juhnn, Y. S. , 2009. Calcineurin dephosphorylates glycogen synthase kinase-3 beta at serine-9 in neuroblast-derived cells.J.Neurochem.111(2), 344-354.

MacDonald, J. F., Mody, I., & Salter, M. W. , 1989. Regulation of N-methyl-D-aspartate receptors revealed by intracellular dialysis of murine neurones in culture.J.Physiol.414, 17-34.

Man, H. Y., Lin, J. W., Ju, W. H., Ahmadian, G., Liu, L., Becker, L. E., Sheng, M., & Wang, Y. T. , 2000. Regulation of AMPA receptor-mediated synaptic transmission by clathrin-dependent receptor internalization.Neuron25(3), 649-662.

Olah, M. E., Jackson, M. F., Li, H., Perez, Y., Sun, H. S., Kiyonaka, S., Mori, Y., Tymianski, M., & MacDonald, J. F. , 2009. Ca2+-dependent induction of TRPM2 currents in hippocampal neurons.J.Physiol.587(Pt 5), 965-979.

Peineau, S., Nicolas, C. S., Bortolotto, Z. A., Bhat, R. V., Ryves, W. J., Harwood, A. J., Dournaud, P., Fitzjohn, S. M., & Collingridge, G. L. , 2009. A systematic investigation of the protein kinases involved in NMDA receptor-dependent LTD: Evidence for a role of GSK-3 but not other serine/threonine kinases.Mol.Brain2, 22.

Peineau, S., Taghibiglou, C., Bradley, C., Wong, T. P., Liu, L., Lu, J., Lo, E., Wu, D., Saule, E., Bouschet, T., Matthews, P., Isaac, J. T., Bortolotto, Z. A., Wang, Y. T., & Collingridge, G. L. , 2007. LTP inhibits LTD in the hippocampus via regulation of GSK3beta.Neuron53(5), 703-717.

Sanderson, T. M., Collingridge, G. L., & Fitzjohn, S. M. , 2011. Differential trafficking of AMPA receptors following activation of NMDA receptors and mGluRs.Mol.Brain4, 30.

Sayas, C. L., Ariaens, A., Ponsioen, B., & Moolenaar, W. H. , 2006. GSK-3 is activated by the tyrosine kinase Pyk2 during LPA1-mediated neurite retraction.Mol.Biol.Cell17(4), 1834-1844.

Scharenberg, A. M. , 2005. TRPM2 and TRPM7: Channel/enzyme fusions to generate novel intracellular sensors.Pflugers Arch.451(1), 220-227.

Takahashi, N., Kozai, D., Kobayashi, R., Ebert, M., & Mori, Y. , 2011. Roles of TRPM2 in oxidative stress.Cell Calcium

von Engelhardt, J., Mack, V., Sprengel, R., Kavenstock, N., Li, K. W., Stern-Bach, Y., Smit, A. B., Seeburg, P. H., & Monyer, H. , 2010. CKAMP44: A brain-specific protein attenuating short-term synaptic plasticity in the dentate gyrus.Science327(5972), 1518-1522.

Xie, Y. F., Belrose, J. C., Lei, G., Tymianski, M., Mori, Y., Macdonald, J. F., & Jackson, M. F. , 2011. Dependence of NMDA/GSK3beta mediated metaplasticity on TRPM2 channels at hippocampal CA3-CA1 synapses.Mol.Brain4(1), 44.

Yamamoto, S., Shimizu, S., Kiyonaka, S., Takahashi, N., Wajima, T., Hara, Y., Negoro, T., Hiroi, T., Kiuchi, Y., Okada, T., Kaneko, S., Lange, I., Fleig, A., Penner, R., Nishi, M., Takeshima, H., & Mori, Y. , 2008. TRPM2-mediated Ca2+influx

induces chemokine production in monocytes that aggravates inflammatory neutrophil infiltration.Nat.Med.14(7), 738-747.

CHAPTER 3

A version of this chapter has been published:

Belrose, J.C., Xie, Y.F., Gierszewski, L.J., MacDonald, J.F., Jackson, M.F. (2012). Loss of glutathione homeostasis associated with neuronal senescence facilitates TRPM2 channel activation in cultured hippocampal pyramidal neurons. *Molecular Brain, 5*:11.

3. Loss of glutathione homeostasis associated with neuronal senescence facilitates TRPM2 channel activation in cultured hippocampal pyramidal neurons

3.1 Introduction

Aging is a major risk factor for developing several neurodegenerative diseases. Although the precise reasons are poorly understood, a growing body of evidence suggests that age-related cognitive decline is associated with stereotypic changes in cellular homeostasis which ultimately lead to impaired neuronal function (Thibault, Gant, & Landfield, 2007). A leading hypothesis suggests that increased oxidative stress associated with aging predisposes neurons to dysregulated intracellular calcium (Ca^{2+}) homeostasis in response to disease causing factors (Camandola & Mattson, 2011). Accordingly, understanding the relation between oxidative stress and altered Ca^{2+} homeostasis may provide valuable insight into mechanisms underlying neurodegenerative disease. Glutathione (GSH), the most abundant intracellular reducing agent (Cooper & Kristal, 1997), plays an important role in limiting cellular damage by reactive oxygen and nitrogen species generated as a by-product of aerobic metabolism. Cellular levels of GSH are known to decrease with age (Chen, Richie, & Lang, 1989; Liu, 2002; Parihar, Kunz, & Brewer, 2008; Rebrin, Forster, & Sohal, 2007; Sasaki et al., 2001) and the resulting decline in antioxidant defence is viewed as a risk factor contributing to the increased susceptibility to neurodegenerative disease associated with aging. For example, a strong relationship has been demonstrated between reduced levels of GSH and Parkinson's disease (M. F. Anderson & Sims, 2002; Bragin et al., 2010;

Martin & Teismann, 2009; Perry, Godin, & Hansen, 1982; Rehncrona & Siesjo, 1979; Sian et al., 1994). Furthermore, a reduction in glutathione has also been associated with cerebral ischemia (M. F. Anderson & Sims, 2002; Bragin et al., 2010; Rehncrona & Siesjo, 1979; Salemi et al., 2009). Importantly, depletion of GSH itself leads to increased oxidative stress, altered Ca^{2+} homeostasis and increased neuronal cell death (de Bernardo et al., 2004; Khanna et al., 2003; Naziroglu et al., 2011; Wullner et al., 1999). It is unknown whether depletion of GSH promotes Ca^{2+} dysregulation directly (e.g. by altering Ca^{2+} permeation pathways) or through the induction of oxidative stress.

TRPM2 is a highly unique calcium permeable non-selective cation channel that is responsive to reactive oxygen and nitrogen species (ROS/RNS). Channel activation by ROS/RNS is proposed to occur following the generation of adenosine diphosphate ribose (ADPR), which serves as an intracellular agonist (Sumoza-Toledo & Penner, 2011). Notably, gating is also greatly facilitated by elevated concentrations of intracellular Ca^{2+} (McHugh et al., 2003; Olah et al., 2009). TRPM2 expression is highest within the brain (Fonfria et al., 2006) and recent work in our lab demonstrated that TRPM2 is expressed and functional in pyramidal neurons of the hippocampus (Olah et al., 2009), a subset of neurons that are particularly susceptible to oxidative stress-induced damage in stroke and neurodegenerative disease (Mattson, Guthrie, & Kater, 1989; X. Wang & Michaelis, 2010). This current was absent in primary hippocampal neurons cultured from TRPM2 knockout (KO) animals (Xie et al., 2011). Importantly, TRPM2 has been shown to contribute to cell death in response to oxidative stress, TNFα, amyloid-β peptide, and ischemia (Fonfria et al., 2005; Jia et al., 2011; Takahashi et al., 2011). These findings raise the possibility that TRPM2 may

play an important role in neurological diseases associated with aging, excitotoxicity and oxidative stress.

Recent evidence suggests that TRPM2 channels may be directly regulated by GSH. Indeed, GSH has been shown to inhibit TRPM2 currents in astrocytes, microglia, and dorsal root ganglion sensory neurons (Lee et al., 2010; Naziroglu et al., 2011). Importantly, these papers did not investigate the effects of glutathione on TRPM2 channels in neurons susceptible to degeneration. Furthermore, the mechanism responsible for the observed inhibition was not explored.

We now extend previous findings demonstrating GSH-mediated inhibition of TRPM2 currents by demonstrating that intrinsic, age-dependent, variations in the intracellular concentration of GSH is a key determinant in dictating the level of TRPM2 activation in neurons. Moreover, we demonstrate that the inhibition of TRPM2 function by GSH operates independently of its capacity as a reducing agent. These findings suggest that altered intracellular Ca^{2+} dynamics associated with GSH depletion, induced experimentally or with aging, may develop as a result of altered TRPM2 regulation.

3.2 Methods

Reagents

Trypsin-EDTA, 5-fluorodeoxyuridine, uridine, CsOH, Gluconic acid, MgCl2, CaCl2, BaCl2, EGTA, KCl, Mg-ATP, N-methyl-D-aspartate (NMDA), D-serine, Glucose, Glutathione (GSH), L-Buthionine sulfoximine (L-BSO), and N-acetyl-cysteine (NAC) were all purchased from Sigma (Oakville, Ontario, Canada). HEPES and NaCl

were purchased from Bioshop (Burlington, Ontario, Canada). Ophthalmic acid was obtained from Bachem (Bubendorf, Switzerland).

Cell culture

Mouse hippocampal primary neuronal cultures were prepared from CD-1 mice (Charles River, Wilmington, MA, USA) at E17-19 as described previously with minor adjustments (MacDonald, Mody, & Salter, 1989). Briefly, hippocampal tissue from embryonic day 17-18 mice were dissected, enzymatically and mechanically dissociation with 0.05% Trypsin-EDTA, and plated at a density of $< 1 \times 10^{6}$ cells ml^{-1} on collagen coated Nunc™ 35 mm culture dishes (Fisher, Rochester, NY). After 3-5 days, each plate was treated for 24hours with 0.08 mM 5-fluorodeoxyuridine and 0.2 mM uridine. Cells were maintained for 4 weeks in culture.

Whole-cell recordings: Primary culture

Currents were recorded from mouse hippocampal primary neuronal cultures at 14-28 days in vitro. Whole-cell voltage-clamp recordings were performed as described previously, with minor adjustments (Olah et al., 2009). Unless otherwise indicated, standard intracellular solution (ICS) contained (in mM): 150 cesium gluconate, 10 Hepes, and 2 MgCl2 and 1 ADPR. Standard extracellular solution (ECS) contained (in mM): 140 NaCl, 5.4 KCl, 25 Hepes, 33 glucose, 2 CaCl2, and 0.2 TTX. TRPM2 currents were generated with either repeated NMDAR activation or voltage ramps. NMDA currents were elicited with 100 μM NMDA and 3 μM d-serine added to the standard ECS and applied for 5 or 10 seconds every minute using a multibarrelled rapid perfusion system (SF-77B; Warner Instruments, Hamden, CT, USA). Voltage ramps

(±100 mV, 1/10 sec) were applied in the presence of standard ECS supplemented with 1 mM MgCl2 and 1 mM BaCl2. After the TRPM2 current stabilized, or after 10 minutes of recording, calcium free solution was applied (total divalent concentration was maintained by replacing CaCl2 with equimolar BaCl2). Data were filtered at 2 kHz, digitized, and acquired using pCLAMP and Axoscope software (Molecular Devices, Sunnyvale, CA, USA).

Whole-cell recordings: TRPM2-HEK293

HEK293 cells stably expressing an inducible flag-tagged human TRPM2 (TRPM2-HEK293) were generously provided by Dr. A. M. Sharenberg (University of Washington, Seattle, Washington). Cells were cultured at 37°C with 5% CO2 in DMEM (Sigma) supplemented with 10% fetal bovine serum and 1% penicillin/streptomycin (Invitrogen, Burlington, ON, Canada). TRPM2 expression was induced with doxycycline (1 μg ml^{-1}) 24 hours prior to experiments. Intracellular solution (ICS) contained (in mM): 130 CsGluconate, 10 HEPES, 2 MgCl2, 1 CaCl2, 10 EGTA, and 4 Mg-ATP. ICS was adjusted to a pH of 7.3 and osmolarity between 295 and 300 mOsm. The final resistance of ICS-filled electrodes was between 3 and 5 MΩ. The standard extracellular solution (ECS) was composed of (in mM): 140 NaCl, 5.4 KCl, 25 HEPES, 33 glucose, 1 MgCl2, 2 CaCl2, pH of 7.4 and osmolarity between 310 and 315 mOsm. Calcium-free ECS contained 2 mM BaCl2 in the place of CaCl2. Data were filtered at 2 kHz, digitized, and acquired using pCLAMP and Axoscope software (Molecular Devices). TRPM2-HEK293 cells were held at -60 mV during whole-cell voltage-clamp recordings. Currents were evoked through the intracellular application of ADPR at a concentration of 0.1 mM unless otherwise indicated. Calcium containing

ECS was applied for 5 minutes or until a current of -1000pA developed, followed by 2-3 minutes in calcium-free ECS. Calcium solution was then applied until the TRPM2 current began to inactivate, and the amplitude of the TRPM2 current was then determined after removal of extracellular Ca^{2+}.

Real-time quantitative polymerase chain reaction (QRT-PCR)

Total RNA was extracted from primary mouse hippocampal cultures at 15, 22, and 29 days in vitro (DIV) with Trizol™ (Invitrogen, Burlington, Canada) according to the manufacturer's protocol. RNA concentration was quantified using the Nanodrop Spectrophotometer ND1000 (Nanodrop technologies Inc., Wilmington, DE, USA). The OD260/280 ratio for all samples was greater than 1.7. Following quantification, RNA was reverse transcribed using Superscript™ II RT reagent according to the manufacturer's guidelines, including the optional treatment with 40 units of RNaseOUT™ (Invitrogen). "No RT" controls contained 1 μL H2O instead of Superscript™ II RT reagent. The reaction was carried out in an Eppendorf Mastercycler personal (Hamburg, Germany).

Primers were designed against the mouse TRPM2 coding strand (accession number NM_138301) and purchased from Sigma. To test primer efficiency, a standard curve was constructed from mouse hippocampal total cDNA using 10x serial dilutions, ranging from 100 ng to 0.1 ng. Inclusion criteria for primers were an efficiency of 90-110%, and an R^2 value >0.98.

To quantify TRPM2 mRNA, 100 ng of cDNA from each sample was run in duplicate with iQ™ SYBR green Supermix (Biorad, Mississauga, Ontario) according to the manufacturer's instructions. The BioRad MyiQTM iCycler was used for real-time

qPCR. Negative controls included the No RT samples from reverse transcription and a no-template control containing water instead of cDNA. Biorad MyIQ™ 2.0 software was used for quantification of cycle threshold. TRPM2 primers produced a 90 bp amplicon using the sense sequence 5'TGATCCTGATGGCTGTGGAC3' in combination with antisense sequence 5'AAGAGCAGAATGGCCCCA3'. The reaction was carried out at 95°C for 3minutes, followed by 40 cycles of 95°C for 1 minute and 55°C for 30 seconds. To control for potential variation in the number of neurons present in culture, cycle thresholds for TRPM2 mRNA were normalized to neuron specific enolase (ENO2) using the sense primer sequence 5'CTGCCTCTGAGTTTTACCGC3' and the antisense primer sequence 5'TCCGGACAAAGTCCTGGTAG3'. ENO2 was quantified with a thermal profile of 95°C for 3 minutes, followed by 40 cycles of 95°C for 1 minute and 62°C for 30 seconds. A dissociation curve was run for both primers using the following thermal profile: 95°C for 1 minute, 55°C for 1 minute, followed by a 2°C steps every 10 seconds from 70°C to 95°C.

Statistics

Data are expressed as mean ± SEM. Statistical analysis was undertaken using GraphPad Prism® (GraphPad Software, San Diego, CA). An unpaired two-tailed *t*-test, a one-way ANOVA followed by a Tukey's HSD post-hoc test, or a two-way ANOVA followed by Bonferroni post-hoc test was used to assess statistical significance. Data was considered significant when $p < 0.05$.

3.3 Results

TRPM2 currents increase with time in vitro

Primary neuronal cultures are often used to examine neuronal development; however, beyond 21 days in vitro, early neuronal markers such as nestin drastically diminishes in expression, and mature neuronal markers such as MAP-2 are expressed, indicative of a mature neuronal population (Bertrand et al., 2011). Furthermore, cultures maintained beyond 3 weeks in vitro recapitulate many of the characteristic cellular changes that have been associated with aging and neurodegeneration (Aksenova et al., 1999; Bertrand et al., 2011; Kim et al., 2007; Lesuisse & Martin, 2002). These include increased oxidative stress, lipid peroxidation, protein tyrosine nitration, mitochondrial injury, ER stress, DNA damage, Ca^{2+} dysregulation, calpain cleavage, endogenous Aβ accumulation, and susceptibility to neuronal cell death.

Importantly, in primary neuronal cultures the concentration of GSH has also been shown to decrease with time in vitro (Keelan et al., 2001; Sagara, Miura, & Bannai, 1993). Accordingly, long-term neuronal cultures serve as a valuable model system for the study of cellular changes associated with neuronal aging and senescence. With this in mind, we first sought to determine whether in vitro neuronal senescence correlates with altered TRPM2 function.

To rigorously examine TRPM2 function over time in culture, whole-cell voltage-clamp recordings were made from primary hippocampal neuronal cultures maintained in vitro for up to 28 days. Using a previously established protocol (Olah et al., 2009), TRPM2 currents were evoked by intracellular administration of ADPR paired with repeated N-methyl-D-aspartate receptor (NMDAR) stimulation.

Importantly, the currents generated using this protocol can be entirely attributed to TRPM2 channels as they are abolished by known blockers of TRPM2 (Olah et al., 2009). To ensure that the full complement of TRPM2 channels expressed at various time points are being activated in our recordings, a saturating concentration of ADPR (1 mM) was included in the patch pipette. Furthermore, as the neuronal cell surface area increases over time due to the continued extension of neuronal processes, TRPM2 currents were normalized to membrane capacitance, measurement of which correlates with cell surface area ($p < 0.05$, data not shown). As illustrated by the representative traces shown in Figure 3.1A and 2.1B, repeated applications of NMDA to pyramidal neurons loaded with ADPR caused the progressive development of large inward currents, the amplitudes of which stabilized within approximately 5-15 min. The amplitude of TRPM2 currents was then determined after removal of extracellular Ca^{2+}, a protocol known to abolish TRPM2-mediated currents (Olah et al., 2009; Xie et al., 2011). Recordings were made from neurons at 14, 20, and 26 days in vitro (DIV, n = 5/group). Results demonstrate that there is an increase in TRPM2 current density between 14 and 26 DIV in cultured hippocampal pyramidal neurons (Figure 3.1C, $p < 0.05$). Since activation of the NMDAR was used to elicit the TRPM2 current, we also analyzed whether the NMDAR current density is increased over time in vitro. No change was observed over this same time period ($p = 0.76$, Figure 3.1D). Furthermore, we assessed whether a change in NMDAR kinetics may explain the enhanced TRPM2 response by calculating the integral under the NMDAR application and normalized this measurement to capacitance (Q/pF). Similarly, no change was observed from 2 – 4 weeks in vitro (data not shown, $p = 0.39$).

Figure 3.1. TRPM2 currents are enhanced in hippocampal pyramidal neurons with time *in vitro*. With 1 mM ADPR included in the patch pipette, TRPM2 currents developed slowly following repeated (1/60 sec) applications of NMDA (100 μM, for 5 sec). TRPM2 currents were quantified by removing extracellular calcium and amplitude was normalized to cell capacitance. NMDA applications are indicated with solid lines. Calcium-free application is depicted as a dashed line (A) Representative trace of TRPM2 currents recorded at 14 DIV (B) Representative trace of TRPM2 currents recorded at 25 DIV. (C) Current density at 14, 20 , and 26 DIV (n = 5 per group) were compared by one-way ANOVA followed by *post-hoc* Tukey`s test. A significant increase in TRPM2 current density between 14 and 26 DIV was observed ($p < 0.05$). (D) NMDAR current density is not significantly increased over time *in vitro* ($p = 0.76$).

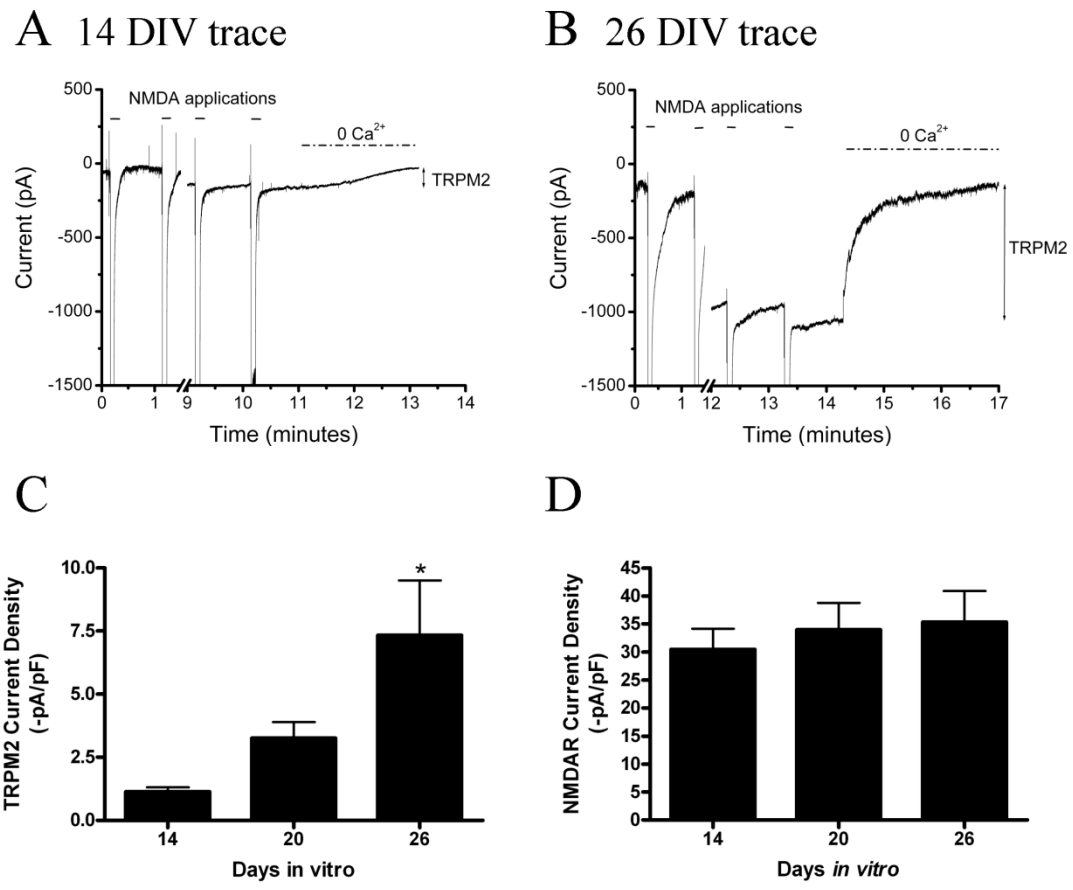
A 14 DIV trace
B 26 DIV trace
NMDA applications
0 Ca2+
TRPM2
Current (pA)
Time (minutes)
C
D
TRPM2 Current Density (-pA/pF)
Days in vitro
NMDAR Current Density (-pA/pF)
Days in vitro

TRPM2 mRNA does not change with time in vitro

Increased TRPM2 current density with time in vitro could be attributed to an increase in the function of TRPM2, potentially via a decrease in glutathione, or alternatively an increase in TRPM2 expression. Using real-time quantitative PCR (RT-QPCR), we tested whether TRPM2 mRNA increases with time in vitro in primary hippocampal cell culture. Total RNA from cells at 15 (n = 9), 22 (n = 8), and 29 (n = 9) DIV were run in duplicate and TRPM2 levels were quantified.

Results were normalized to neuron-specific enolase (Eno2) by calculating delta cycle threshold (ΔCT) values for each sample (NSE CT – TRPM2 CT) in order to control for any variability in neuronal content over time. Analysis by one-way ANOVA revealed no change in the TRPM2 cycle threshold (p = 0.89, Figure 3.2A), Eno2 (p = 0.9, Figure 3.2B) or normalized TRPM2 mRNA levels over time in vitro (p = 0.51, Figure 3.2C). These findings demonstrate that changes in mRNA expression levels are not responsible for the increase in TRPM2 current density observed over time in vitro.

Modulation of GSH alters TRPM2 currents in hippocampal pyramidal neurons

If decreased cellular GSH content is responsible for elevated TRPM2 function over time in vitro, then enhancing intracellular GSH levels should diminish TRPM2 current amplitude in older cultured neurons (~28 DIV). Conversely, reducing intracellular GSH levels should facilitate TRPM2 channel function in younger neuronal cultures (~14 DIV).

Figure 3.2. TRPM2 mRNA levels do not change in hippocampal primary cultures with time *in vitro*. (A) TRPM2 mRNA was measured at 14, 21, and 29 DIV (n=8 per group) by quantitative real-time PCR (qPCR). No significant change in cycle threshold values is observed (p = 0.89) (B) QPCR analysis of neuron specific enolase (ENO2) mRNA values used to control for neuronal content over time. No significant difference was observed ($\boldsymbol{p}$ = 0.9). (C) Normalized TRPM2 values for each sample (ENO2-TRPM2) were quantified. No difference in the normalized levels of TRPM2 mRNA is seen over time in culture (p = 0.51).

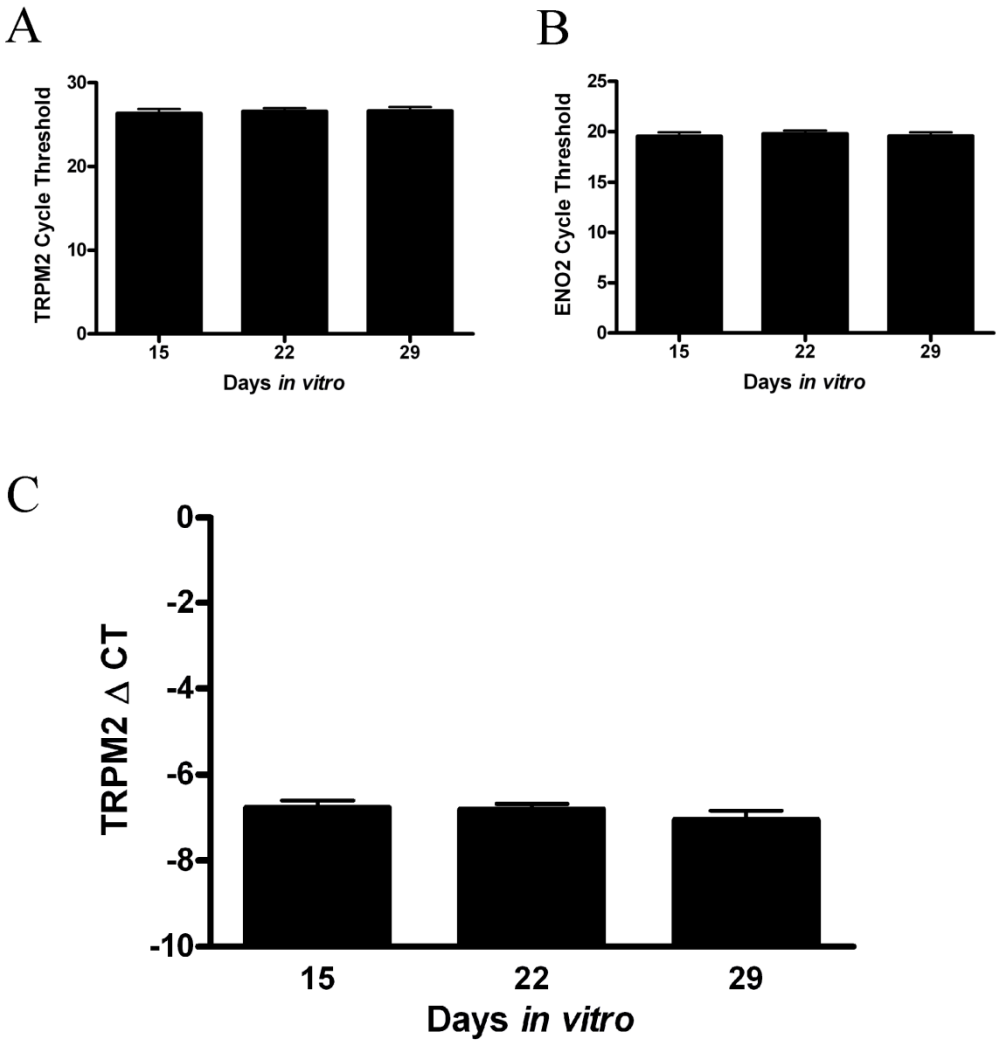
A
TRPM2 Cycle Threshold
30
20
10
0
15
22
29
Days in vitro
B
ENO2 Cycle Threshold
25
20
15
10
5
0
15
22
29
Days in vitro
C
TRPM2 Δ CT
0
-2
-4
-6
-8
-10
15
22
29
Days in vitro

We first examined the consequence of elevating the intracellular concentration of GSH in neurons at 4 weeks in vitro by exogenous application through the patch pipette. When compared with controls, GSH (10 mM) significantly inhibited TRPM2 currents activated in the presence of ADPR by the NMDAR stimulation protocol (Figure 3.3A, p = 0.04). In millimolar concentrations, extracellular GSH has been shown to enhance NMDAR function (Kohr et al., 1994; Oja et al., 2000). No difference in NMDAR amplitude was observed with intracellular delivery of GSH (p = 0.82, data not shown). Representative traces are shown in Figure 3.3B (control) and C (10mM GSH). To confirm the effects of GSH on TRPM2 currents, we also examined the effects of GSH delivered through the patch pipette on TRPM2 currents generated by a voltage ramp protocol. Using this alternative protocol, GSH similarly inhibited TRPM2 currents (Figure 3.3D, p = 0.01). Examples of representative traces for control and GSH voltage ramp recordings are shown in Figure 3.3E and 2.3F, respectively.

We next sought evidence that augmenting endogenous GSH content can similarly decrease TRPM2 function. We chronically treated neurons from 1-4 weeks in vitro with N-acetylcysteine (NAC), a precursor to GSH that has been shown to increase levels of endogenous GSH (M. F. Anderson & Sims, 2002; Aoyama, Watabe, & Nakaki, 2008; Gao et al., 2009; Jayalakshmi et al., 2005) and examined whether TRPM2 currents in cultures at 4 weeks in vitro were reduced. Treatment with 50 μM NAC beginning at 1 week in vitro significantly attenuated TRPM2 currents in cultures at 28 DIV (p= 0.04, Figure 3.4A-C). Previous studies have shown that NAC is able to act as a reactive oxygen scavenger independent of its ability to upregulate GSH (Aruoma et al., 1989).

Figure 3.3. GSH inhibits TRPM2 currents in hippocampal pyramidal neurons.

(A) 10 mM GSH in the patch pipette significantly inhibits TRPM2 currents generated by 1 mM ADPR with an NMDAR stimulation protocol (p = 0.04). (B, C) Representative traces of control and GSH inhibition with the NMDAR stimulation protocol. (D) 10 mM GSH in the patch pipette significantly inhibits TRPM2 currents generated by 1 mM ADPR with a voltage ramp protocol (p = 0.01). (E,F) Representative traces of control and GSH inhibition with the voltage ramp protocol

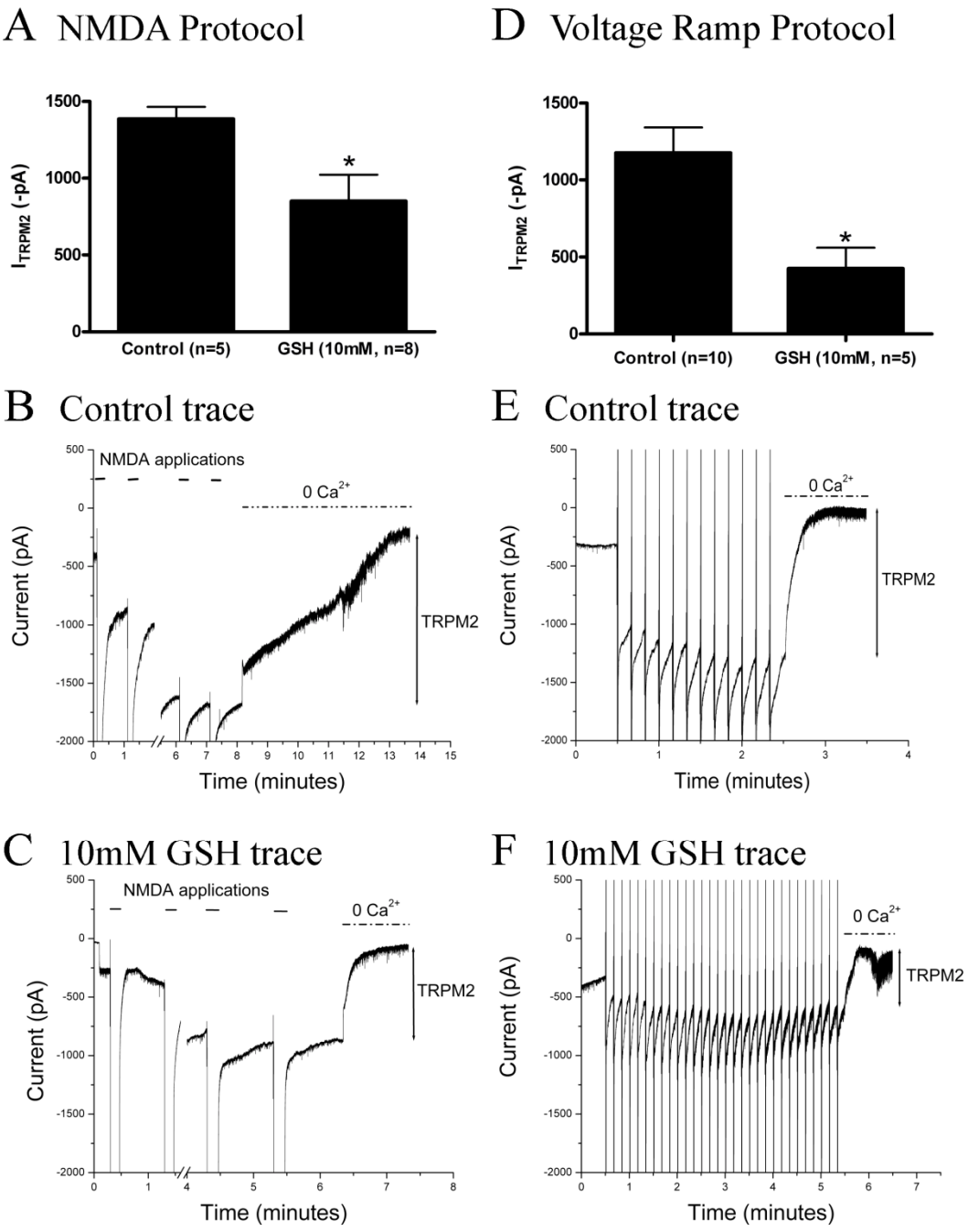
A NMDA Protocol
D Voltage Ramp Protocol
I_{TRPM2} (-pA)
Control (n=5)
GSH (10mM, n=8)
Control (n=10)
GSH (10mM, n=5)
B Control trace
E Control trace
C 10mM GSH trace
F 10mM GSH trace
NMDA applications
0 Ca^{2+}
TRPM2
Current (pA)
Time (minutes)

To confirm that the observed effect can be attributed to GSH and not to NAC itself, NAC (50 μM) was included in the patch pipette and TRPM2 currents were elicited with the NMDA activation protocol with 1 mM ADPR in the patch pipette. Compared to controls (1076 ± 204.9, n = 3), acute NAC (910.5 ± 142.8 n = 4) did not alter TRPM2 currents (p= 0.52, data not shown). These results confirm previous findings that GSH can inhibit TRPM2 currents, and are consistent with the notion that reduced GSH, at least in part, may underlie the increase in TRPM2 currents that we observed in hippocampal pyramidal neurons over time in vitro. These findings also imply that GSH constitutively suppresses TRPM2 function in younger cultured neurons.

Accordingly, we next examined whether depleting GSH could augment TRPM2 function in young cultures maintained for 2 weeks in vitro. L-buthionine-(S,R)-sulfoximine (L-BSO) inhibits the enzyme γ-glutamylcysteine synthetase, the rate limiting step in GSH synthesis (M. E. Anderson, 1998) and is effective in depleting GSH (M. F. Anderson & Sims, 2002; Aoyama et al., 2008; Keelan et al., 2001; Sebastia et al., 2003; Wullner et al., 1999). Consistent with our hypothesis, TRPM2 currents were significantly potentiated, when compared with controls (p= 0.01), in 2 week old cultured neurons depleted of GSH by treatment with 250 μM L-BSO for 48 hours (Figure 3.4D-F).

Figure 3.4. Modulation of Endogenous GSH Alters TRPM2 Currents

(A) Treatment from 1-4 weeks *in vitro* with 50 μM NAC significantly inhibited TRPM2 currents generated by 0.3 mM ADPR and an NMDAR stimulation protocol in cultures at 28 DIV (p= 0.04). (B, C) Representative control and NAC traces. (D) A 48 hour treatment with 250 μM L-BSO significantly enhances TRPM2 currents generated with 1 mM ADPR with an NMDAR stimulation protocol in hippocampal pyramidal neurons at 2 weeks *in vitro*. (E, F) Representative control and L-BSO traces.

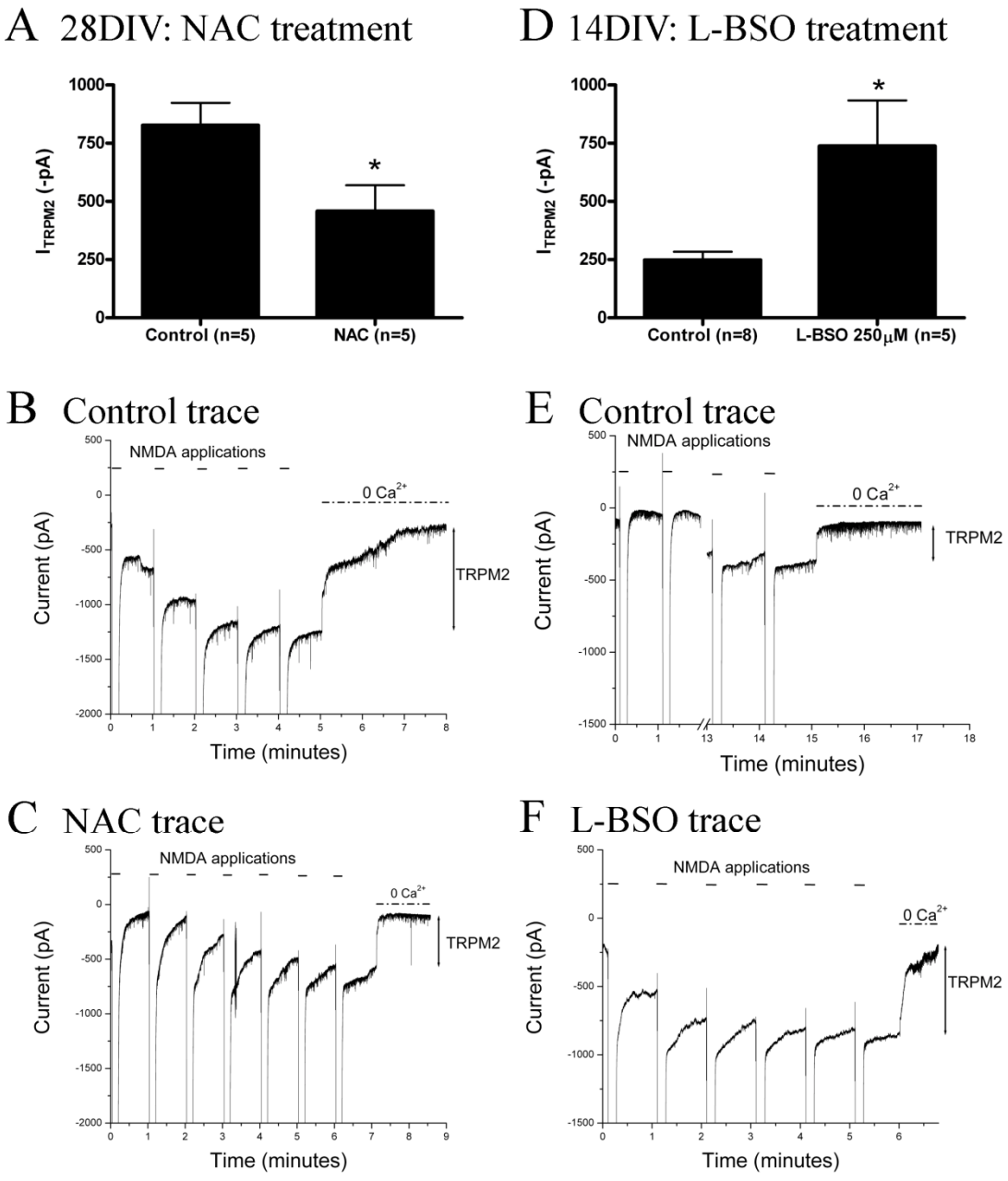
A 28DIV: NAC treatment
D 14DIV: L-BSO treatment
I_{TRPM2} (-pA)
Control (n=5)
NAC (n=5)
Control (n=8)
L-BSO 250μM (n=5)
B Control trace
E Control trace
C NAC trace
F L-BSO trace
NMDA applications
0 Ca^{2+}
TRPM2
Current (pA)
Time (minutes)

Mechanism of TRPM2 inhibition by GSH

HEK293 cells stably expressing TRPM2 under control of an inducible promoter (TRPM2-HEK293) were used to characterize the mechanism of GSH-mediated TRPM2 inhibition. To further validate our findings in hippocampal pyramidal neurons, and previous findings in glial and dorsal root ganglion cells [20,31], TRPM2 currents from TRPM2-HEK293 cells were recorded in the whole-cell patch clamp configuration with 0.1 mM ADPR in the patch pipette. Of note, HEK293 cells do not express NMDARs nor voltage-gated Ca^{2+} channels. In these cells, intracellular application of ADPR alone is sufficient to activate TRPM2 channels in this model system, presumably due to the much higher induced channel expression. Currents generated under control conditions were compared to those generated when 10 mM GSH was included in the patch pipette, and removal of extracellular Ca^{2+} was used to abolish the TRPM2 current. In these cells, intracellular delivery of GSH substantially attenuated the TRPM2 current (Figure 3.5, $p < 0.001$).

GSH may regulate channel function through a number of distinct mechanisms including redox mechanisms, or post-translational modification involving the formation of mixed protein disulfides (i.e. glutathionylation). Through its reducing potential GSH has been shown to regulate the function of other receptors and channels, including NMDARs (Bodhinathan, Kumar, & Foster, 2010; Kohr et al., 1994). To examine the possibility that TRPM2 is regulated through changes in its redox state, we examined whether the inhibitory effect of GSH could be mimicked by another reducing agent, dithiothreitol (DTT). DTT was included in the patch pipette and currents were recorded from TRPM2-HEK293 cells. At 10 mM DTT, no change

in TRPM2 amplitude was observed when compared to controls ($p > 0.05$; Figure 3.5), suggesting that the reducing ability of GSH is not responsible for the change in TRPM2 currents.

Figure 3.5. GSH inhibits TRPM2 in a thiol-independent mechanism. TRPM2 currents were elicited in HEK293-TRPM2 cells using a 2mM calcium extracellular solution and 0.1mM ADPR. TRPM2 currents were then inhibited and quantified following removal of extracellular calcium (A) Representative TRPM2 responses obtained in control (n=12), GSH (n=10), DTT (n=6) and ophthalmic acid (n=6) groups (B) TRPM2 currents are significantly inhibited with 10 mM GSH or 10 mM ophthalmic acid, but are not altered when 10 mM DTT is included in the patch pipette (One-way ANOVA followed by *post-hoc* Tukey's test, * $p < 0.05$).

A Representative TRPM2 Responses

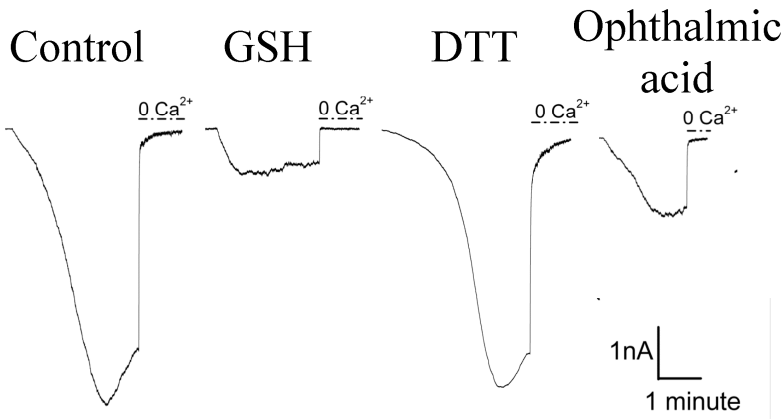

B

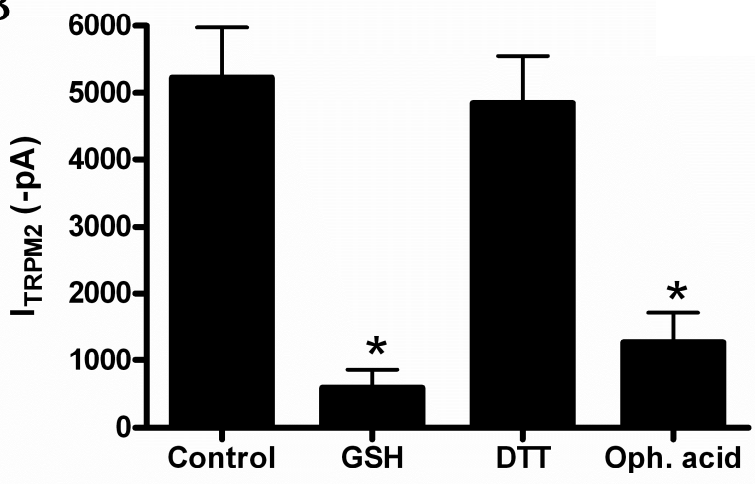

GSH has also been shown to inhibit currents through direct binding to channels, either at thiol residues, known as glutathionylation, or at other non-thiol containing binding sites (Herson & Ashford, 1999; W. Wang et al., 2005; Yang et al., 2010). Ophthalmic acid (γ-glutamyl-2-amino-*n*-butanoylglycine) is an analogue of GSH which contains L-2-aminobutyrate in place of the cysteine residue (WALEY, 1958). This analogue lacks both the ability to form disulphide bonds and the reducing potential of GSH. Interestingly, when ophthalmic acid (10 mM) was included in the patch pipette, TRPM2 currents were significantly inhibited in TRPM2-HEK293 cells ($p < 0.001$; Figure 3.5). This demonstrates that GSH acts in a thiol-independent manner to inhibit TRPM2 currents.

Potential mechanisms of TRPM2 inhibition by GSH were further studied by constructing a concentration-response relationship for ADPR with or without 10 mM GSH included in the patch pipette. TRPM2 currents were evoked with varying intracellular concentrations (0.03 - 3 mM) of ADPR. Each point on the curve represents the mean +/-SE of 6 -11 recordings (Figure 3.6). A two-way ANOVA followed by Bonferroni *post-hoc* test revealed an overall significant effect, with a highly significant inhibition by GSH for TRPM2 currents evoked with ADPR concentrations of 0.1, 0.3, and 1 mM ($p < 0.001$). No difference between groups was observed at the highest (3 mM) and lowest (0.03 mM) ADPR concentrations ($p > 0.05$). In control conditions, the EC50 of ADPR was 77 μM, consistent with a previous report (Perraud et al., 2001). In contrast, the EC50 of ADPR with 10 mM GSH was 269 μM, representing a ~3.5 fold change in sensitivity when GSH is included in the patch pipette.

Figure 3.6. GSH shifts the ADPR concentration-response curve of TRPM2 channels by 3.5 fold. TRPM2 currents were generated with or without 10 mM GSH included in the patch pipette. Intracellular concentrations of ADPR used to evoke the current ranged from 0.03 – 3mM. Each point on the curve represents the mean +/- SE of 6 – 11 recordings. Significant inhibition by GSH was observed for TRPM2 currents evoked by ADPR concentrations of 0.1, 0.3, and 1 mM ($p<0.001$), with no difference between groups at the highest (3 mM) and lowest (0.03 mM) ADPR concentration points ($p>0.05$). The EC50 value for ADPR was increased from 77 µM (control) to 269 µM (10 mM GSH) in the presence of 10 mM GSH, representing a ~3.5 fold change in sensitivity to ADPR. Concentration-response curves were fit using a sigmoidal concentration-response (variable slope), with a Hill slope of 2.2 in control, and 0.9 in the GSH data set.

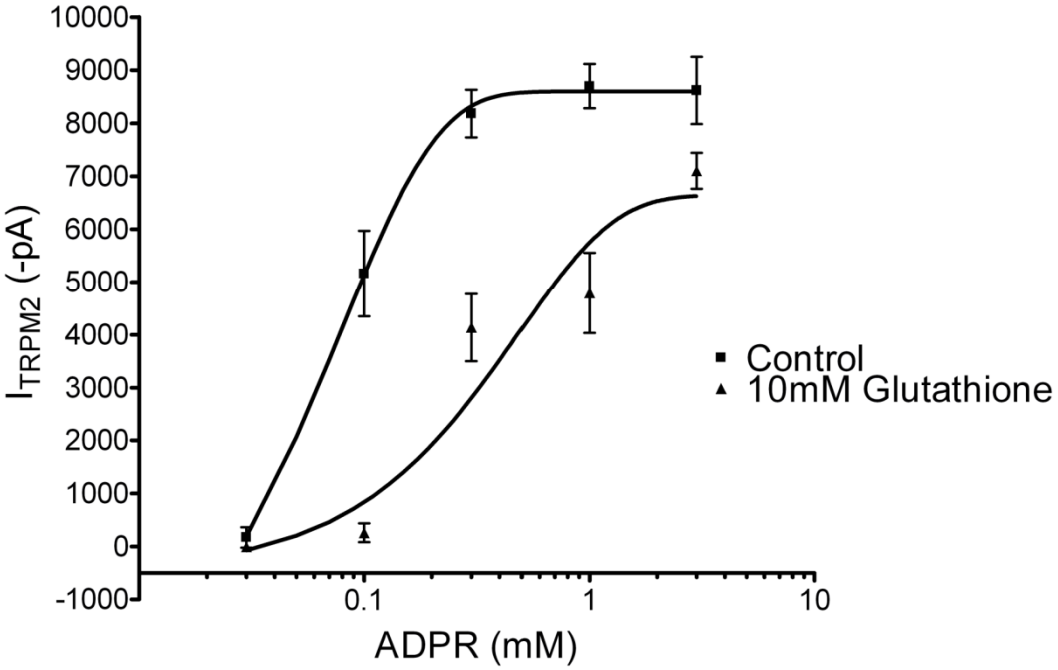
10000
9000
8000
7000
6000
5000
4000
3000
2000
1000
0
-1000
I_{TRPM2} (-pA)
0.1
1
10
ADPR (mM)
Control
10mM Glutathione

The concentration–response curves fit using a sigmoidal concentration–response (variable slope), results in a Hill slope of 2.2 in control, and 0.9 in the GSH data set. The rightward shift in the concentration-response relationship and decrease in the Hill coefficient confirm that GSH inhibits TRPM2 channels. The results with DTT and ophthalmic acid confirm that the effects of GSH are thiol independent. However, whether GSH functions as a channel blocker, competes for the ADPR binding site, or interferes with TRPM2 currents by binding to ADPR requires further investigation.

3.4 Discussion

In this study we demonstrate that TRPM2 function increases with time *in vitro* in cultured hippocampal pyramidal neurons. Moreover, we show that by altering the intracellular concentration of GSH TRPM2 current amplitude can be modulated in this system. Specifically, this was shown in experiments where GSH was supplied exogenously through the patch pipette, or alternatively, where we modulated endogenous GSH metabolism. We also demonstrate that ophthalmic acid, but not DTT, is able to recapitulate GSH mediated inhibition of TRPM2 currents, suggesting that GSH inhibits TRPM2 channels independently of its electron-donating capacity. Lastly, a 3.5-fold shift in the concentration-response curve and decrease in the Hill coefficient for ADPR generated TRPM2 currents suggest that GSH either disrupts the co-operative interaction between ADPR and TRPM2 or functions as a channel blocker. Further research is required to determine the precise nature of this interaction. The mechanism through which GSH inhibits TRPM2 and its relevance to the regulation of the channel in neurons is crucial to

understanding the pathways leading to neurotoxicity.

TRPM2 is a Ca^{2+} permeable non-selective ion channel implicated in oxidative stress-induced cell death (Fonfria et al., 2005; Jia et al., 2011; Takahashi et al., 2011). Several factors have been reported to modulate TRPM2 current response including Ca^{2+} concentration, temperature, pH, phosphorylation, the epilepsy related protein EFHC1, and CD38 (Katano et al., 2012; Numata et al., 2012; Takahashi et al., 2011). Recently, TRPM2 currents were shown to be inhibited by GSH in sensory neurons (Naziroglu et al., 2011) as well as in glial cells, where TRPM2 activation following chemically induced GSH depletion contributes to neuroinflammation (Lee et al., 2010; Naziroglu et al., 2011). Our own findings now demonstrate that intrinsic alterations in endogenous GSH content are associated with altered TRPM2 function in hippocampal pyramidal neurons. Collectively, these studies suggest that GSH is a physiologically relevant regulator of TRPM2 and that dynamic changes in GSH content are likely to be associated with parallel changes in TRPM2 function. Importantly, a reduction in GSH has been associated with normal aging in vivo (Chen et al., 1989; Liu, 2002; Rebrin et al., 2007; Robillard et al., 2011; Sasaki et al., 2001). Neurodegenerative disorders, including Parkinson's disease and progressive supranuclear palsy, are associated with enhanced depletion in intracellular GSH compared to age-matched controls (Martin & Teismann, 2009; Perry et al., 1982; Sian et al., 1994). GSH depletion is also observed following ischemia in animal models and in human subjects (M. F. Anderson & Sims, 2002; Bragin et al., 2010; Rehncrona & Siesjo, 1979; Salemi et al., 2009). Diminished levels of reduced GSH has also been linked to bipolar disorder, major depressive disorder, and schizophrenia (Do et al., 2000; Gawryluk et al., 2011). Importantly,

upregulation of glutathione with NAC treatment protects against neuronal cell death in vitro and in vivo (Andreassen et al., 2000; Clark et al., 2010; Henderson et al., 1996; Jayalakshmi et al., 2005; Mayer & Noble, 1994; Morshead & van der Kooy, 2000; Rothstein et al., 1994).

The findings in this manuscript raise the intriguing possibility that GSH depletion associated with aging, ischemia, and several psychiatric and neurodegenerative disorders, may be associated with enhanced TRPM2 channel function. Future experiments will be required to assess whether TRPM2 currents are also enhanced with age in vivo, and/or in models of neurological disease associated with GSH depletion. Furthermore, the contribution of TRPM2 to neurodegeneration and dysfunction associated with these conditions should be established. Interestingly, depletion of GSH in Parkinson's is one of the earliest biochemical markers of impending neuronal degeneration (Martin & Teismann, 2009). Moreover, TRPM2 is expressed and functional in dopaminergic neurons of the substantia nigra (Chung, Freestone, & Lipski, 2011). Accordingly, whether TRPM2 currents are enhanced in models of Parkinson's disease (or other neurodegenerative disease in which GSH is depleted) and whether knock-out of TRPM2 may attenuate neurodegeneration has yet to be investigated. Importantly, neurodegenerative diseases are well known to be associated with pronounced neuroinflammatory response. The demonstration that GSH depletion in glial cells promotes neuroinflammation through a mechanism involving TRPM2 (Lee et al., 2010), paired with our demonstration that GSH depletion facilitates TRPM2 function in vulnerable hippocampal pyramidal neurons, suggests that TRPM2 activation contributes to neuronal demise in neurodegenerative

disease through multiple mechanisms. By extension, TRPM2 may represent an important target for the development of novel therapeutic agents of benefit in the treatment of these debilitating neurological diseases.

References

Aksenova, M. V., Aksenov, M. Y., Markesbery, W. R., & Butterfield, D. A. , 1999. Aging in a dish: Age-dependent changes of neuronal survival, protein oxidation, and creatine kinase BB expression in long-term hippocampal cell culture.J.Neurosci.Res.58(2), 308-317.

Anderson, M. E. , 1998. Glutathione: An overview of biosynthesis and modulation.Chem.Biol.Interact.111-112, 1-14.

Anderson, M. F., & Sims, N. R. , 2002. The effects of focal ischemia and reperfusion on the glutathione content of mitochondria from rat brain subregions.J.Neurochem.81(3), 541-549.

Andreassen, O. A., Dedeoglu, A., Klivenyi, P., Beal, M. F., & Bush, A. I. , 2000. N-acetyl-L-cysteine improves survival and preserves motor performance in an animal model of familial amyotrophic lateral sclerosis.Neuroreport11(11), 2491-2493.

Aoyama, K., Watabe, M., & Nakaki, T. , 2008. Regulation of neuronal glutathione synthesis.J.Pharmacol.Sci.108(3), 227-238.

Aruoma, O. I., Halliwell, B., Hoey, B. M., & Butler, J. , 1989. The antioxidant action of N-acetylcysteine: Its reaction with hydrogen peroxide, hydroxyl radical, superoxide, and hypochlorous acid.Free Radic.Biol.Med.6(6), 593-597.

Bertrand, S. J., Aksenova, M. V., Aksenov, M. Y., Mactutus, C. F., & Booze, R. M. , 2011. Endogenous amyloidogenesis in long-term rat hippocampal cell cultures.BMC Neurosci.12, 38.

Bodhinathan, K., Kumar, A., & Foster, T. C. , 2010. Intracellular redox state alters NMDA receptor response during aging through Ca2+/calmodulin-dependent protein kinase II.J.Neurosci.30(5), 1914-1924.

Bragin, D. E., Zhou, B., Ramamoorthy, P., Muller, W. S., Connor, J. A., & Shi, H. , 2010. Differential changes of glutathione levels in astrocytes and neurons in ischemic brains by two-photon imaging.J.Cereb.Blood Flow Metab.30(4), 734-738.

Camandola, S., & Mattson, M. P. , 2011. Aberrant subcellular neuronal calcium regulation in aging and alzheimer's disease.Biochim.Biophys.Acta1813(5), 965-973.

Chen, T. S., Richie, J. P.,Jr, & Lang, C. A. , 1989. The effect of aging on glutathione and cysteine levels in different regions of the mouse brain.Proc.Soc.Exp.Biol.Med.190(4), 399-402.

Chung, K. K., Freestone, P. S., & Lipski, J. , 2011. Expression and functional properties of TRPM2 channels in dopaminergic neurons of the substantia nigra of the rat.J.Neurophysiol.106(6), 2865-2875.

Clark, J., Clore, E. L., Zheng, K., Adame, A., Masliah, E., & Simon, D. K. , 2010. Oral N-acetyl-cysteine attenuates loss of dopaminergic terminals in alpha-synuclein overexpressing mice.PLoS One5(8), e12333.

Cooper, A. J., & Kristal, B. S. , 1997. Multiple roles of glutathione in the central nervous system.Biol.Chem.378(8), 793-802.

de Bernardo, S., Canals, S., Casarejos, M. J., Solano, R. M., Menendez, J., & Mena, M. A. , 2004. Role of extracellular signal-regulated protein kinase in neuronal cell death induced by glutathione depletion in neuron/glia mesencephalic cultures.J.Neurochem.91(3), 667-682.

Do, K. Q., Trabesinger, A. H., Kirsten-Kruger, M., Lauer, C. J., Dydak, U., Hell, D., Holsboer, F., Boesiger, P., & Cuenod, M. , 2000. Schizophrenia: Glutathione deficit in cerebrospinal fluid and prefrontal cortex in vivo.Eur.J.Neurosci.12(10), 3721-3728.

Fonfria, E., Marshall, I. C., Boyfield, I., Skaper, S. D., Hughes, J. P., Owen, D. E., Zhang, W., Miller, B. A., Benham, C. D., & McNulty, S. , 2005. Amyloid beta-peptide(1-42) and hydrogen peroxide-induced toxicity are mediated by TRPM2 in rat primary striatal cultures.J.Neurochem.95(3), 715-723.

Fonfria, E., Murdock, P. R., Cusdin, F. S., Benham, C. D., Kelsell, R. E., & McNulty, S. , 2006. Tissue distribution profiles of the human TRPM cation channel family.J.Recept.Signal Transduct.Res.26(3), 159-178.

Gao, Y., Howard, A., Ban, K., & Chandra, J. , 2009. Oxidative stress promotes transcriptional up-regulation of fyn in BCR-ABL1-expressing cells.J.Biol.Chem.284(11), 7114-7125.

Gawryluk, J. W., Wang, J. F., Andreazza, A. C., Shao, L., & Young, L. T. , 2011. Decreased levels of glutathione, the major brain antioxidant, in post-mortem prefrontal cortex from patients with psychiatric disorders.Int.J.Neuropsychopharmacol.14(1), 123-130.

Henderson, J. T., Javaheri, M., Kopko, S., & Roder, J. C. , 1996. Reduction of lower motor neuron degeneration in wobbler mice by N-acetyl-L-cysteine.J.Neurosci.16(23), 7574-7582.

Herson, P. S., & Ashford, M. L. , 1999. Reduced glutathione inhibits beta-NAD+-activated non-selective cation currents in the CRI-G1 rat insulin-secreting cell line.J.Physiol.514 (Pt 1)(Pt 1), 47-57.

Jayalakshmi, K., Sairam, M., Singh, S. B., Sharma, S. K., Ilavazhagan, G., & Banerjee, P. K. , 2005. Neuroprotective effect of N-acetyl cysteine on hypoxia-induced oxidative stress in primary hippocampal culture.Brain Res.1046(1-2), 97-104.

Jia, J., Verma, S., Nakayama, S., Quillinan, N., Grafe, M. R., Hurn, P. D., & Herson, P. S. , 2011. Sex differences in neuroprotection provided by inhibition of TRPM2 channels following experimental stroke.J.Cereb.Blood Flow Metab.

Katano, M., Numata, T., Aguan, K., Hara, Y., Kiyonaka, S., Yamamoto, S., Miki, T., Sawamura, S., Suzuki, T., Yamakawa, K., & Mori, Y. , 2012. The juvenile myoclonic epilepsy-related protein EFHC1 interacts with the redox-sensitive TRPM2 channel linked to cell death.Cell Calcium

Keelan, J., Allen, N. J., Antcliffe, D., Pal, S., & Duchen, M. R. , 2001. Quantitative imaging of glutathione in hippocampal neurons and glia in culture using monochlorobimane.J.Neurosci.Res.66(5), 873-884.

Khanna, S., Roy, S., Ryu, H., Bahadduri, P., Swaan, P. W., Ratan, R. R., & Sen, C. K. , 2003. Molecular basis of vitamin E action: Tocotrienol modulates 12-lipoxygenase, a key mediator of glutamate-induced neurodegeneration.J.Biol.Chem.278(44), 43508-43515.

Kim, M. J., Oh, S. J., Park, S. H., Kang, H. J., Won, M. H., Kang, T. C., Park, J. B., Kim, J. I., Kim, J., & Lee, J. Y. , 2007. Neuronal loss in primary long-term cortical culture involves neurodegeneration-like cell death via calpain and p35 processing, but not developmental apoptosis or aging.Exp.Mol.Med.39(1), 14-26.

Kohr, G., Eckardt, S., Luddens, H., Monyer, H., & Seeburg, P. H. , 1994. NMDA receptor channels: Subunit-specific potentiation by reducing agents.Neuron12(5), 1031-1040.

Lee, M., Cho, T., Jantaratnotai, N., Wang, Y. T., McGeer, E., & McGeer, P. L. , 2010. Depletion of GSH in glial cells induces neurotoxicity: Relevance to aging and degenerative neurological diseases.FASEB J.24(7), 2533-2545.

Lesuisse, C., & Martin, L. J. , 2002. Long-term culture of mouse cortical neurons as a model for neuronal development, aging, and death.J.Neurobiol.51(1), 9-23.

Liu, R. M. , 2002. Down-regulation of gamma-glutamylcysteine synthetase regulatory subunit gene expression in rat brain tissue during aging.J.Neurosci.Res.68(3), 344-351.

MacDonald, J. F., Mody, I., & Salter, M. W. , 1989. Regulation of N-methyl-D-aspartate receptors revealed by intracellular dialysis of murine neurones in culture.J.Physiol.414, 17-34.

Martin, H. L., & Teismann, P. , 2009. Glutathione--a review on its role and significance in parkinson's disease.FASEB J.23(10), 3263-3272.

Mattson, M. P., Guthrie, P. B., & Kater, S. B. , 1989. Intrinsic factors in the selective vulnerability of hippocampal pyramidal neurons.Prog.Clin.Biol.Res.317, 333-351.

Mayer, M., & Noble, M. , 1994. N-acetyl-L-cysteine is a pluripotent protector against cell death and enhancer of trophic factor-mediated cell survival in vitro.Proc.Natl.Acad.Sci.U.S.A.91(16), 7496-7500.

McHugh, D., Flemming, R., Xu, S. Z., Perraud, A. L., & Beech, D. J. , 2003. Critical intracellular Ca2+ dependence of transient receptor potential melastatin 2 (TRPM2) cation channel activation.J.Biol.Chem.278(13), 11002-11006.

Morshead, C. M., & van der Kooy, D. , 2000. A cell-survival factor (N-acetyl-L-cysteine) alters the in vivo fate of constitutively proliferating subependymal cells in the adult forebrain.J.Neurobiol.42(3), 338-346.

Naziroglu, M., Ozgul, C., Cig, B., Dogan, S., & Uguz, A. C. , 2011. Glutathione modulates ca(2+) influx and oxidative toxicity through TRPM2 channel in rat dorsal root ganglion neurons.J.Membr.Biol.242(3), 109-118.

Numata, T., Sato, K., Christmann, J., Marx, R., Mori, Y., Okada, Y., & Wehner, F. , 2012. The {delta}C splice-variant of TRPM2 is the hypertonicity-induced cation channel (HICC) in HeLa cells, and the ecto-enzyme CD38 mediates its activation.J.Physiol.

Oja, S. S., Janaky, R., Varga, V., & Saransaari, P. , 2000. Modulation of glutamate receptor functions by glutathione.Neurochem.Int.37(2-3), 299-306.

Olah, M. E., Jackson, M. F., Li, H., Perez, Y., Sun, H. S., Kiyonaka, S., Mori, Y., Tymianski, M., & MacDonald, J. F. , 2009. Ca2+-dependent induction of TRPM2 currents in hippocampal neurons.J.Physiol.587(Pt 5), 965-979.

Parihar, M. S., Kunz, E. A., & Brewer, G. J. , 2008. Age-related decreases in NAD(P)H and glutathione cause redox declines before ATP loss during glutamate treatment of hippocampal neurons.J.Neurosci.Res.86(10), 2339-2352.

Perraud, A. L., Fleig, A., Dunn, C. A., Bagley, L. A., Launay, P., Schmitz, C., Stokes, A. J., Zhu, Q., Bessman, M. J., Penner, R., Kinet, J. P., & Scharenberg, A. M. ,

2001. ADP-ribose gating of the calcium-permeable LTRPC2 channel revealed by nudix motif homology.Nature411(6837), 595-599.

Perry, T. L., Godin, D. V., & Hansen, S. , 1982. Parkinson's disease: A disorder due to nigral glutathione deficiency?Neurosci.Lett.33(3), 305-310.

Rebrin, I., Forster, M. J., & Sohal, R. S. , 2007. Effects of age and caloric intake on glutathione redox state in different brain regions of C57BL/6 and DBA/2 mice.Brain Res.1127(1), 10-18.

Rehncrona, S., & Siesjo, B. K. , 1979. Cortical and cerebrospinal fluid concentrations of reduced and oxidized glutathione during and after cerebral ischemia.Adv.Neurol.26, 285-286.

Robillard, J. M., Gordon, G. R., Choi, H. B., Christie, B. R., & MacVicar, B. A. , 2011. Glutathione restores the mechanism of synaptic plasticity in aged mice to that of the adult.PLoS One6(5), e20676.

Rothstein, J. D., Bristol, L. A., Hosler, B., Brown, R. H.,Jr, & Kuncl, R. W. , 1994. Chronic inhibition of superoxide dismutase produces apoptotic death of spinal neurons.Proc.Natl.Acad.Sci.U.S.A.91(10), 4155-4159.

Sagara, J. I., Miura, K., & Bannai, S. , 1993. Maintenance of neuronal glutathione by glial cells.J.Neurochem.61(5), 1672-1676.

Salemi, G., Gueli, M. C., D'Amelio, M., Saia, V., Mangiapane, P., Aridon, P., Ragonese, P., & Lupo, I. , 2009. Blood levels of homocysteine, cysteine, glutathione, folic acid, and vitamin B(12) in the acute phase of atherothrombotic stroke.Neurol.Sci.

Sasaki, T., Senda, M., Kim, S., Kojima, S., & Kubodera, A. , 2001. Age-related changes of glutathione content, glucose transport and metabolism, and mitochondrial electron transfer function in mouse brain.Nucl.Med.Biol.28(1), 25-31.

Sebastia, J., Cristofol, R., Martin, M., Rodriguez-Farre, E., & Sanfeliu, C. , 2003. Evaluation of fluorescent dyes for measuring intracellular glutathione content in primary cultures of human neurons and neuroblastoma SH-SY5Y.Cytometry A.51(1), 16-25.

Sian, J., Dexter, D. T., Lees, A. J., Daniel, S., Agid, Y., Javoy-Agid, F., Jenner, P., & Marsden, C. D. , 1994. Alterations in glutathione levels in parkinson's disease and other neurodegenerative disorders affecting basal ganglia.Ann.Neurol.36(3), 348-355.

Sumoza-Toledo, A., & Penner, R. , 2011. TRPM2: A multifunctional ion channel for calcium signalling.J.Physiol.589(Pt 7), 1515-1525.

Takahashi, N., Kozai, D., Kobayashi, R., Ebert, M., & Mori, Y. , 2011. Roles of TRPM2 in oxidative stress.Cell Calcium

Thibault, O., Gant, J. C., & Landfield, P. W. , 2007. Expansion of the calcium hypothesis of brain aging and alzheimer's disease: Minding the store.Aging Cell.6(3), 307-317.

WALEY, S. G. , 1958. Acidic peptides of the lens. 3. the structure of ophthalmic acid.Biochem.J.68(1), 189-192.

Wang, W., Oliva, C., Li, G., Holmgren, A., Lillig, C. H., & Kirk, K. L. , 2005. Reversible silencing of CFTR chloride channels by glutathionylation.J.Gen.Physiol.125(2), 127-141.

Wang, X., & Michaelis, E. K. , 2010. Selective neuronal vulnerability to oxidative stress in the brain.Front.Aging Neurosci.2, 12.

Wullner, U., Seyfried, J., Groscurth, P., Beinroth, S., Winter, S., Gleichmann, M., Heneka, M., Loschmann, P., Schulz, J. B., Weller, M., & Klockgether, T. , 1999. Glutathione depletion and neuronal cell death: The role of reactive oxygen intermediates and mitochondrial function.Brain Res.826(1), 53-62.

Xie, Y. F., Belrose, J. C., Lei, G., Tymianski, M., Mori, Y., Macdonald, J. F., & Jackson, M. F. , 2011. Dependence of NMDA/GSK3beta mediated metaplasticity on TRPM2 channels at hippocampal CA3-CA1 synapses.Mol.Brain4(1), 44.

Yang, Y., Shi, W., Cui, N., Wu, Z., & Jiang, C. , 2010. Oxidative stress inhibits vascular K(ATP) channels by S-glutathionylation.J.Biol.Chem.285(49), 38641-38648.

CHAPTER 4

4. Fyn kinase, Aβ, and TRPM2: Potential implications to Alzheimer's Disease

4.1 Introduction

Alzheimer's disease (AD) is a progressive neurodegenerative disorder with a prevalence of approximately 500,000 individuals in Canada, representing 1.5% of our total population (Alzheimer Society of Canada, 2010). AD presents with degeneration of the basal forebrain cholinergic neurons, entorhinal cortex, hippocampus and cortex (Coyle, Price, & DeLong, 1983; Gomez-Isla et al., 1996). The degree of degeneration and synaptic loss in these areas correlate strongly with the severity of dementia (Scheff & Price, 2003).

Soluble oligomers of $A\beta_{42}$ are believed to initiate the primary insult leading to degeneration through modulation of a variety of pathways (Hardy & Selkoe, 2002). For example, $A\beta_{42}$ increases GSK-3β activity, which subsequently contributes to the pathological hyperphosphorylation of tau (Hernandez, Lucas, & Avila, 2012; Hooper, Killick, & Lovestone, 2008). Downregulation of endogenous tau attenuates neuronal cell death and behavioural deficits in a mouse model of AD, demonstrating that pathologically modified tau is critical for neurotoxicity in AD (Roberson et al., 2007). Although the mechanism through which tau contributes to neurotoxicity is still under investigation, recent evidence suggests that tau confers toxicity in AD, at least in part, by targeting the non-receptor tyrosine kinase Fyn to NMDA Receptors (NMDARs) (Ittner et al., 2010).

Exposure to a high concentration of Aβ induces a series of changes at the cellular level including reduced excitatory synaptic transmission in the hippocampus,

increased levels of intracellular Ca^{2+}, and increased neuronal death (Huang & Mucke, 2012). Several studies have suggested that aberrant activation of NMDARs in response to Aβ exposure could explain these phenomena (Alberdi et al., 2010; Hu et al., 2009; Molnar et al., 2004; Ronicke et al., 2010). Importantly, Aβ oligomer exposure exerts a dichotomous effect on excitatory synaptic transmission, enhancing transmission when concentrations are low, and decreasing transmission when concentrations are high (Puzzo, Privitera, & Palmeri, 2012). High concentrations of Aβ or prolonged exposure have also been shown to decrease NMDAR amplitude and promote internalization of NMDARs (Jacob et al., 2007; Kurup et al., 2010; Snyder et al., 2005). Furthermore, clinical trials with the NMDAR antagonist memantine only produces a modest improvement in moderate to severe AD, and marginal benefit in mild to moderate AD (McShane, Areosa Sastre, & Minakaran, 2006). It is therefore unlikely that the tau-Fyn-NMDAR complex can explain all of the toxicity observed in AD.

We propose that the Ca^{2+} permeable non-selective cation channel TRPM2 may participate in this toxic protein complex. TRPM2 channels are activated by oxidative stress, and have been shown to contribute to cell death in a variety of cell types (Takahashi et al., 2011). Furthermore, the decrease in NMDAR amplitude induced by Aβ requires the activation of another non-NMDAR inward current which, similar to TRPM2, displays a linear I-V relationship (Snyder et al., 2005). Indeed, one previous study demonstrated that knockdown of TRPM2 protected a striatal culture system from cell death induced by 20μM monomeric Aβ (Fonfria et al., 2005). Although the relevance to AD of striatal cultures and high concentrations of monomeric Aβ is questionable, this study did provide the first evidence that TRPM2 may participate in

AD. Furthermore, previous work in our lab has demonstrated that TRPM2 currents can be activated by strong stimulation of NMDARs (Olah et al., 2009). We have also demonstrated that TRPM2 interacts with the GluN1 subunit of NMDARs, and inhibition of GluN2B containing NMDAR significantly attenuates TRPM2 current development in cultured hippocampal neurons (M. Jackson & J. MacDonald, unpublished). This data suggests a unique physical and functional relationship between GluN2B containing NMDAR and TRPM2. We also previously demonstrated that TRPM2 contributes to maintaining GSK-3β activity, raising the possibility that TRPM2 may play a role in the pathological alterations to tau (Xie et al., 2011). Lastly, a recent study showed that TRPM2 is phosphorylated on tyrosine residues following exposure to oxidative stress (Zhang et al., 2007). The influx of Ca^{2+} observed after exposure to oxidative stress in TRPM2 expressing cells is reduced when cells are pretreated with PP2, an SFK inhibitor (Zhang et al., 2007).

In humans, the SFK family consists of 9 members including Src, Fyn, Yes, Fgr, Lck, Hck, Blk, Lyn, Frk. In this study, we focus on Fyn as a potential modulator of TRPM2 function. Fyn is expressed at the post-synaptic density in neurons, and modulates synaptic plasticity (Husi et al., 2000; Yang, Trepanier et al., 2011). Furthermore, Fyn demonstrates enhanced activity and/or expression in response to oxidative stress (Gao et al., 2009; Griendling et al., 2000; Sanguinetti, Cao, & Corley Mastick, 2003). Fyn has also been shown to promote neurotoxicity in models of Alzheimer's disease (Chin et al., 2004; Chin et al., 2005; Ho et al., 2005; Ittner et al., 2010; Lambert et al., 1998). Recently, our lab demonstrated that Fyn enhances GluN2B containing NMDAR currents and favours long-term depression (LTD) (Yang, Trepanier

et al., 2011). This finding is of particular importance because we have also shown that TRPM2 activity is required for NMDAR-dependent LTD (Xie et al., 2011).

In the present study we expand upon the initial finding that TRPM2 participates in Aβ mediated toxicity. We hypothesize that Aβ will enhance TRPM2 currents in cultured hippocampal neurons. We further investigate the hypothesis that TRPM2 is regulated by Fyn kinase by evaluating a potential physical and functional relationship between Fyn and TRPM2. These results provide a novel pathway through which TRPM2 activity is regulated, and also implicate TRPM2 in neurodegenerative processes, such as AD, associated with Fyn kinase.

4.2 Methods

Cell Culture

Mouse hippocampal primary neuronal cultures were prepared from embryonic day 17-18 mice. The hippocampus was dissected, enzymatically and mechanically dissociated with 0.05% Trypsin-EDTA, and plated at a density of $< 5 \times 10^5$ cells ml^{-1} on collagen coated Nunc™ 35 mm culture dishes (Fisher, Rochester, NY). Cells were maintained for 4 weeks in Neurobasal medium (Invitrogen, Burlington, Ontario, Canada), supplemented with B-27 (Invitrogen) and glucose (Sigma, Oakville, Ontario, Canada).

Aβ Oligomer Preparation

Amyloid (r-peptide, Bogart, GA, USA) was prepared according to a previously established protocol (Stine et al., 2003). Oligomerization of samples was confirmed by separation on a 16.5% Tris-Tricine gel (Biorad), transfer to a nitrocellulose membrane,

and detection of Aβ (Signet 6E10, 1:7000). Monomers, dimers, trimers, and tetramers were detectable using these oligomerization condtions (Figure 4.1).

MTT Assay

An MTT (3-(4,5-Dimethylthiazol-2-yl)-2,5-diphenyltetrazolium bromide) reduction assay was used to assess cell viability following Aβ oligomer exposure. The assay was conducted according to manufacturer's protocol with minor modifications. Briefly, MTT reagent (Sigma) was dissolved to 5mg/mL in PBS. The solution was then added to the cells at a concentration 50µg/mL for 1.5hours. Media was then removed, and 1mL DMSO was added to the cells. Absorbance was measured at 595nM and 650nM.

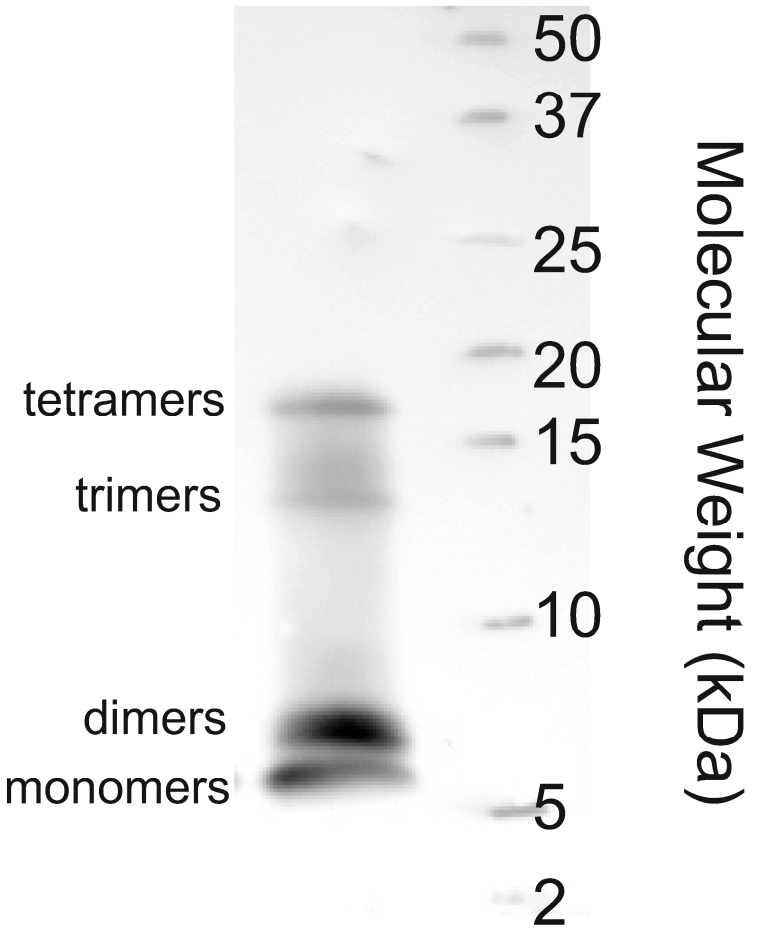

Figure 4.1 Amyloid Oligomers

Oligomerization of $A\beta_{1-42}$ (15µL of 10µM prepared Aβ, r-peptide) was confirmed by western blotting. Samples were separated on a 16.5% Tris-Tricine gel (Biorad), transferred to a nitrocellulose membrane, and probed for Aβ (Signet 6E10, 1:7000). Results indicate the presence of Aβ monomers, dimers, trimers, and tetramers.

Whole-Cell Recordings: Cultured Hippocampal Neurons

Whole-cell voltage-clamp recordings were performed as described previously (Olah et al., 2009). TRPM2 currents were generated with either repeated NMDAR activation or voltage ramps. Briefly, patch electrodes were filled with an intracellular solution (ICS) containing: 150mM cesium gluconate, 10mM Hepes, 2mM $MgCl_2$, with or without 0.3mM ADPR. Standard extracellular solution (ECS) contained 140mM NaCl, 5.4mM KCl, 25mM Hepes, 33mM glucose, 2mM $CaCl_2$.. Zero calcium ECS contained 2mM $BaCl_2$ in the place of $CaCl_2$. For voltage ramp recordings, ECS was also supplemented with 1mM $BaCl_2$ and 1mM $MgCl_2$. Voltage ramps (±100mV, 1/10sec) were applied in the presence of Ca^{2+} containing ECF.. For NMDA-evoked TRPM2 currents, NMDA currents were evoked for 5 seconds every minute with standard ECS supplemented with 100 μM NMDA and 3 μM d-serine, using a multibarrelled rapid perfusion system (SF-77B; Warner Instruments, Hamden, CT, USA). For both recording protocols, zero Ca^{2+} ECF was applied after the current was stable for at least 1 minute. Recordings were performed at a holding potential of -60mV at room temperature (20–22°C) using a Multiclamp 700A amplifier (Molecular Devices, Sunnyvale, CA). ECS was applied with a multibarrelled perfusion system (SF-77B; Warner Institute, Hamden, CT, USA). Data were filtered at 2 kHz, digitized, and acquired using pCLAMP and Axoscope software (Molecular Devices).

Whole-Cell Recordings: HEK293-TRPM2 Cells

HEK293 cells stably expressing an inducible flag-tagged human TRPM2 (HEK293-TRPM2) were generously provided by Dr. A.M. Sharenberg (University of Washington, Seattle, Washington). Cells were maintained in DMEM (Sigma)

supplemented with 10% fetal bovine serum (Invitrogen, Burlington, ON, Canada). Doxycycline (1µg/mL) was used to induce TRPM2 expression 24 hours prior to recording. ICS contained (in mM): 130 CsGluconate, 10 HEPES, 2 $MgCl_2$, 1 $CaCl_2$, 10 EGTA, and 4 Mg-ATP. ICS was adjusted to a pH of 7.3 and osmolality between 295-300 mOsm. Standard ECS as listed above omitting TTX and D-serine, and including 1 $MgCl_2$. Zero calcium ECS replaced the 2mM $CaCl_2$ with $BaCl_2$. Currents were evoked through intracellular application of ADPR at a concentration of 0.1mM. Calcium containing ECS was applied until a current of -1000 pA developed, followed by 2-3 minutes in zero calcium ECS. TRPM2 currents were then activated in the presence of Ca^{2+} ECS until the current began to inactive. A second peak was generated following 5 minutes in zero Ca^{2+} ECS. No difference in amplitude was observed between the first and second peak, so results presented in this report reflect data gathered from the first TRPM2 response generated.

Fyn Constructs

Wild-type Fyn Construct

Fyn kinase (accession number NM_00237.3) was amplified from a human cDNA library using KOD Hot Start DNA Polymerase (EMD Biosciences, San Diego, CA) using primers listed in table 1 and thermal profile: 95°C for 2 minutes followed by 10 cycles at 94°C for 15 seconds, 60°C (-1°C/cycle) for 15 seconds, and 72°C for 40 seconds, and 25 cycles at 94°C for 15 seconds, 50°C for 15 seconds, and 72°C for 40 seconds. The PCR product was then run on a 1% w/v agarose gel plus 0.5µg/mL of ethidium bromide (Sigma-Aldrich, Oakville, Canada). PCR product was extracted from the agarose gel using a GenElute gel extraction kit (Sigma). A double restriction

enzyme digest with NotI and AscI (NEB, Ipswich, MA) was carried out at 37°C for 2 hours, followed by purification with GenElute columns according to manufacturer's protocol (Sigma). The purified product was then ligated using T4 DNA ligase (NEB) at a 1:5 (vector:insert) molar ratio into NotI/AscI digested pcDNA3.1. Ligated product was transformed into JM109 competent cells (Promega, Madison, WI, USA) and grown up on LB + amplicillin plates overnight at 37°C. Colonies were then expanded in LB + amp selection medium overnight at 37°C, and pellets were subjected to miniprep using the GenElute Plasmid Miniprep kit (Sigma) according to manufactuer's protocol. Triple restriction digest (AscI/NotI/XhoI) was carried out to confirm incorporation of Fyn, and positive clones were confirmed by sequencing (London Regional Genomics Centre, Robarts Research Institute, London, Ontario).

Site Directed Mutagenesis

A constitutively active (Fyn Y531F) and dominant negative (Fyn K299M) form of Fyn kinase were created by site direct mutagenesis. Primers were designed to align with WT Fyn, replacing the lysine residue at amino acid 299 with a methionine (AAG → ATG) for FynK299M, and replacing tyrosine 531 with phenalalanine (TAC → TTC) for Fyn Y531F. Two separate PCR reactions were carried out to create fragment 1 and fragment 2 of FynK299M using primers listed in table 1 using the generated pcDNA3.1-hFyn as a template. The reaction was carried out with KOD polymerase (EMD Biosciences) using the following thermal profile: 95°C for 2 minutes followed by 10 cycles at 94°C for 15 seconds, 60°C (-1°C/cycle) for 15 seconds, and 72°C for 15 seconds, and 25 cycles at 94°C for 15 seconds, 50°C for 15 seconds, and 72°C for 15 seconds. Fragments 1 and 2 were then combined and the full length product was

generated with KOD polymerase at 95°C for 2 minutes followed by 5 cycles at 94°C for 15 seconds, 60°C (-1°C/cycle) for 15 seconds, and 72°C for 40 seconds. The reaction as paused to add WT Fyn forward and reverse primers, and the PCR reaction was resumed with 5 cycles at 94°C for 15 seconds, 55°C (-1°C/cycle) for 15 seconds, and 72°C for 40 seconds, and 25 cycles at 94°C for 15 seconds, 50°C for 15 seconds, and 72°C for 40 seconds. Y531F was generated with a single reaction using KOD polymerase, Y531F primers listed in table 4.1, and pcDNA3.1-hFyn as a template using the same thermal profile outlined for cloning WT Fyn.

PCR product from Fyn K299M and Y531F mutagenesis was run on a 1% w/v agarose gel plus 0.5µg/mL of ethidium bromide (Sigma) to confirm product size. The corresponding bands were cut out and extracted with the Sigma GenElute gel extraction kit according to protocol. A double restriction enzyme digest (NotI/AscI) followed by digest purification with genElute columns was completed prior to ligation of PCR product into pcDNA 3.1, transformation into JM109 competent cells, colony expansion and miniprep as described earlier. Fyn mutant incorporation was confirmed with triple restriction enzyme digest (AscI/NotI/XhoI), and positive clones were confirmed with sequencing (London Regional Genomics Centre).

Table 4.1. Primers used in site-directed mutagenesis

Construct	Forward Primer (5' → 3')	Reverse Primer (5' → 3')
WT Fyn	TAGGCGCGCCAACCATGGG CTGTGTGCAATGTAAGGA	TAGCGGCCGCTTACAGGTTT TCACCAGGTTGGTACT
Fyn K299M-1	TAGGCGCGCCAACCATGGG CTGTGTGCAATGTAAGGA	GGTTTAAGAGTCATTATGGC TACTTTTGTGTTTCC
Fyn K299M-2	GTAGCCATAATGACTCTTA AACCAGGCACAATG	TAGCGGCCGCTTACAGGTTT TCA
Fyn Y531F	ATGGCGCGCCAACCATGGG CTGTGTGCAATGTAAGGA	GAGCGGCCGCTTACAGGTTT TCACCAGGTTGGAACTGGG GCTC

Transfection

HEK-TRPM2 cells were maintained in DMEM + 10% fetal bovine serum (FBS) (Invitrogen). Prior to transfection, cells were plated on 100mm dishes at 30% confluency and induced to express TRPM2 with doxycycline (1µg/mL). The following day, cells were transfected with JetPRIME™ (Polyplus, Illkirch, France) according to the manufacturer's instructions, using 12.5µL instead of the recommended 20-30µL JetPRIME reagent. After 4 hours, media was replaced with DMEM + 10% FBS + 1µg/mL doxycycline. Cell lysates were collected 48 hours after transfection (lysis buffer: 150mM NaCl, 0.1% NP-40, 2mM $CaCl_2$, 50mM Tris-HCl (pH 7.5), supplemented with mini complete protease cocktail inhibitor tablet (Roche) and 1% Halt phosphatase inhibitor cocktail (Thermo, Rockford, IL, USA). Lysates were incubated on a nutating shaker for 20 minutes at 4ºC, followed by centrifugation for 30 minutes at 16000 x g at 4ºC. Protein was then quantified from the soluble fraction by BCA assay (Thermo).

Immunoprecipitation and Western Blot Analysis

Lysates (1mg protein) were brought up to a volume of 500µL with lysis buffer plus protease and phosphatase inhibitors and incubated overnight at 4ºC with 20µL packed monoclonal anti-Flag M2 agarose beads (Sigma). Immunoprecipitates were then rinsed 3x with 1mL lysis buffer, resuspended in 2x Laemmli sample buffer and heated for 30 minutes at 37ºC. Samples were subjected to SDS-PAGE on an 8% polyacrylamide gel and transferred onto a nitrocellulose membrane. Membranes were cut at 72kDa, and the top portion was probed with an anti-tyrosine antibody (4G10, 1:2000, mouse IgG; Millipore Corp, Billerica, MA) followed by anti-mouse-HRP secondary antibody (1:5000) and detection with ECL reagent (supersignal, Pierce). The top portion of the membrane was then stripped and re-probed for TRPM2 using anti-Flag-HRP (M2 clone, 1:1000; Sigma) and detected with ECL. The bottom portion of the gel was probed with an anti-Fyn antibody (H80, 1:500, rabbit igG; Santa Cruz Biotechnology, Santa Cruz, CA), followed by anti-rabbit-HRP secondary antibody (1:5000) and detection with ECL reagent. Blots were imaged with the VersaDoc™ imaging system (Biorad).

Statistical Analysis

Data are expressed as mean ± SEM. Statistical analysis was undertaken using GraphPad Prism® (GraphPad Software, San Diego, CA). An unpaired two-tailed t-test, one-way ANOVA followed by a Tukey's HSD post-hoc test, or two-way ANOVA followed by Bonferroni *post-hoc* test was used to analyze data. Results were considered significant when $p<0.05$.

4.3 Results

4.3.1 TRPM2 contributes to Aβ toxicity

Our first objective was to examine neuronal viability in response to Aβ treatment in cultured hippocampal neurons derived from wild type (WT) or TRPM2 knockout (KO) mice. MTT reduction was used to assess cell viability. Cultured hippocampal neurons at 3 weeks *in vitro* were treated for 24 hours with 1 μM oligomeric Aβ. Hippocampal neurons derived from WT cultures demonstrate a decrease in viability following treatment with Aβ ($p<0.05$, Figure 4.2). This reduction in viability is not observed in cultures derived from TRPM2 KO animals ($p> 0.05$). Importantly, a scrambled $A\beta_{42}$ peptide control did not decrease neuronal viability measured by MTT assay ($p>0.05$, data not shown). This demonstrate that the genetic deletion of TRPM2 protects hippocampal neurons from the loss of cell viability induced by Aβ oligomers.

4.3.2 Aβ indirectly potentiates TRPM2 currents

We reasoned that the decrease in cell viability occurs as a result of enhanced TRPM2 currents and increased intracellular Ca^{2+} levels. To examine this hypothesis, TRPM2 currents were evoked using in cultured hippocampal pyramidal neurons at 3-4 weeks *in vitro* following treatment for 24 hour with either 1μM $A\beta_{42}$ oligomers or vehicle control. TRPM2 current density was significantly enhanced following pre-treatment with Aβ (-17.01 ± 2.13 pA/pF, n=17) relative to vehicle control (-10.64 ± 1.03 pA/pF, n=15, p = 0.015, Figure 4.3A). Interestingly, the same effect is not observed with HEK293-TRPM2 cells pretreated with 1μM Aβ (-4447 ± 1680 pA, n=6) compared with vehicle treated controls (-5329 ± 1212 pA, n=7, p=0.67, FIGURE 4.3B), suggesting that Aβ does not act directly to augment TRPM2 function.

Figure 4.2. TRPM2 Knockout cultures are protected from Aβ toxicity.

Hippocampal cultures at 3 weeks *in vitro* were either left untreated, or treated for 24 hours with 1μM oligomerized $A\beta_{1\text{-}42}$. Relative to untreated WT (n=6), and KO (n=7) cultures, 1μM oligomerized $A\beta_{1\text{-}42}$ significantly reduced viability as measured by MTT assay in WT cultures, but not in KO cultures (n=8/group). *$p<0.05$, one-way ANOVA followed by *post-hoc* Tukey's test.

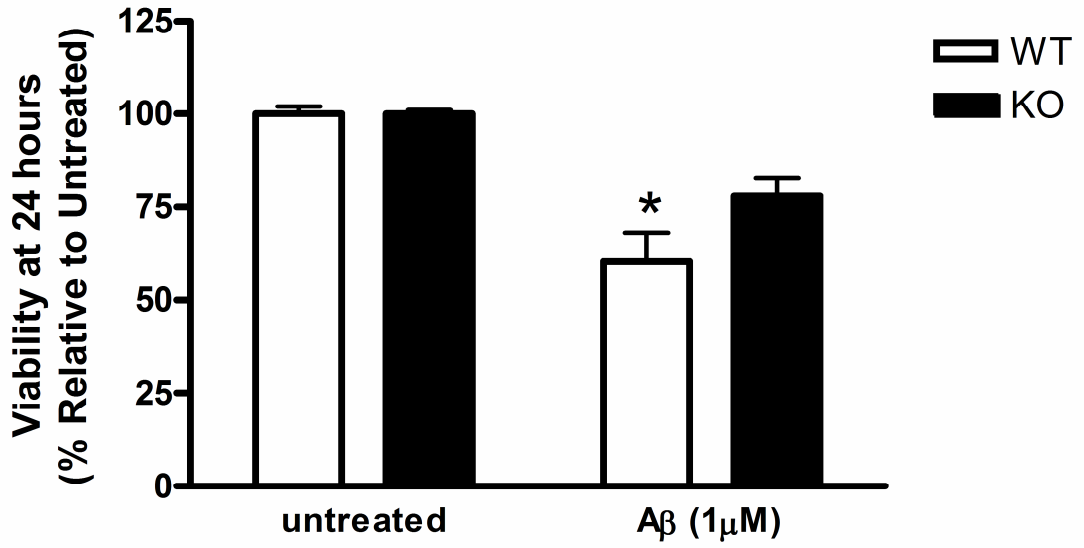
Viability at 24 hours
(% Relative to Untreated)
125
100
75
50
25
0
*
untreated
Aβ (1μM)
WT
KO

Figure 4.3. Aβ indirectly potentiates TRPM2 currents

(A) TRPM2 currents were generated in cultured hippocampal neurons at 3-4 weeks *in vitro*. Cells were treated for 24 hours with either 1μM oligomerized $A\beta_{1-42}$ (n = 17) or vehicle control (n = 15). Currents were normalized to capacitance to control for variation in cell size. Results demonstrate a current density of -10.64 ± 1.03 pA/pF (n=15) in control, and -17.01 ± 2.13 pA/pF (n=17) in the $A\beta_{1-42}$ treated group. (p=0.015); (B) HEK293-TRPM2 cells were similarly pretreated with either vehicle control (n=7) or 1μM $A\beta_{1-42}$ oligomers for 24 hours. Currents were induced with 0.1mM ADPR in the patch pipette. Treatment with $A\beta_{1-42}$ did not alter TRPM2 amplitude in these cells (p=0.67).

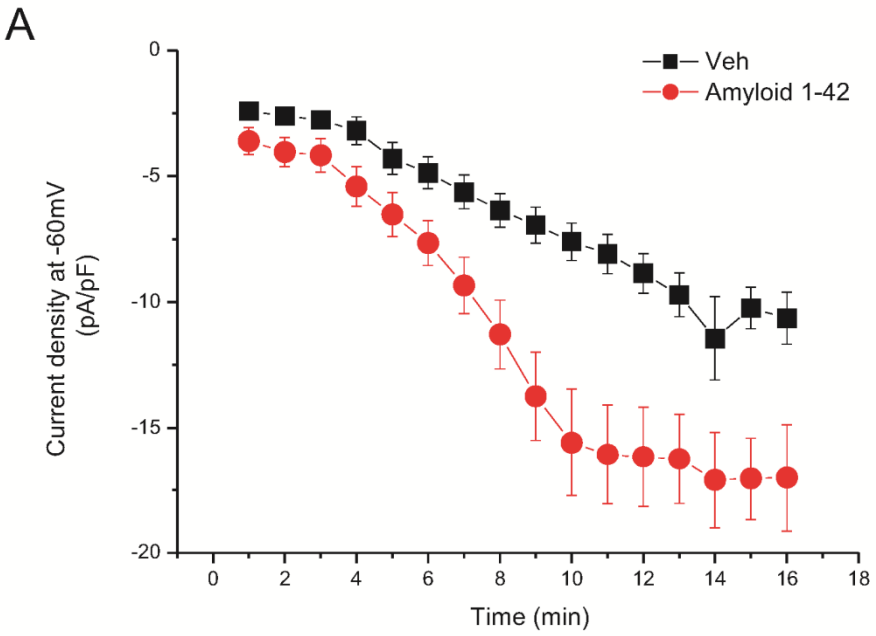
A
Veh
Amyloid 1-42
Current density at -60mV
(pA/pF)
0
-5
-10
-15
-20
0
2
4
6
8
10
12
14
16
18
Time (min)

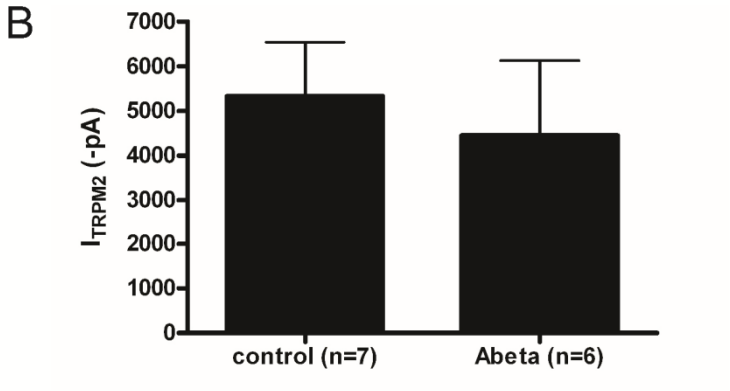
B
I_{TRPM2} (-pA)
7000
6000
5000
4000
3000
2000
1000
0
control (n=7)
Abeta (n=6)

4.3.1 Fyn Potentiates TRPM2 Currents

A growing body of literature implicates Fyn as a critical player in synaptic deficits and neurotoxicity associated with Alzheimer's disease (Yang et al., 2011). Therefore, we examined whether Fyn could regulate TRPM2 function. Cultured hippocampal neurons at 3-4 weeks *in vitro* were used to examine whether currents elicited from endogenously expressed TRPM2 are enhanced by recombinant Fyn . Several studies have demonstrated that Fyn regulates NMDARs, enhancing phosphorylation and activity of the receptor (Salter & Kalia, 2004; Yang, Trepanier et al., 2011); therefore, in order to exclude any effect of Fyn on the NMDAR, a voltage-ramp protocol was used to elicit a TRPM2 response. Currents were generated with 0.3 mM ADPR, with or without 1 U/mL Fyn, in the patch pipette. Ramps were applied either immediately after breakthrough (n=5/group), or after 10 minutes to allow Fyn to diffuse into the cell (n=3/group). Results from both protocols were combined. As shown in Figure 4.4A-C, a significant increase in TRPM2 current is observed when Fyn is delivered via patch pipette in comparison to controls (Fyn, -1087 ± 134.2, N=10; control, -607.4 ± 121.1, N=9; $p<0.05$).

HEK 293 cells stably expressing inducible flag-tagged TRPM2 (HEK293-TRPM2) used to examine whether inclusion of Fyn (1U/mL) in the patch pipette directly enhances TRPM2 currents. As shown in figure 4.4D, when compared with control (-3743 ± 477.8, N=8) recombinant Fyn significantly increased TRPM2 currents (-5470 ± 425.4, N=8).

Figure 4.4. Fyn potentiates TRPM2 currents

TRPM2 currents were generated using a voltage ramp protocol in cultured hippocampal pyramidal neurons with 0.3mM ADPR in the patch pipette. Dashed line indicates application of 0 Ca^{2+} ECF. (A) Representative control recording; (B) Representative Fyn (1U/mL) recording; (C) Compared with controls (-607.4 ± 121.1, N=9), Fyn (1 U/mL, -1087 ± 134.2, N=10) significantly augmented TRPM2 currents; (D) TRPM2 currents were generated in HEK293-TRPM2 cells with 0.1 mM ADPR in the patch pipette. When compared with controls (-3743 ± 477.8, N=8), Fyn (1 U/mL, -5470 ± 425.4, N=8) significantly potentiates TRPM2 amplitude.

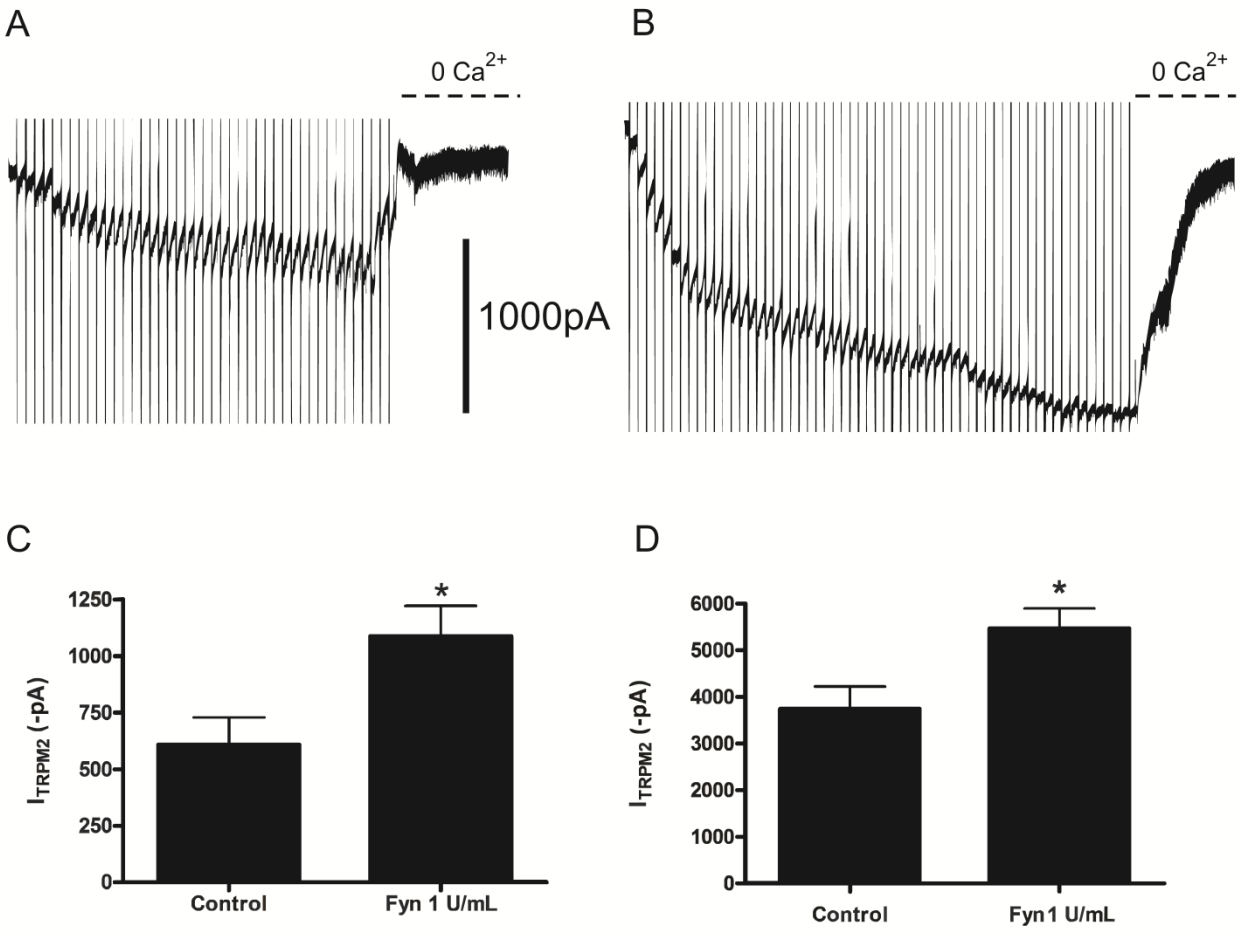
A
0 Ca2+
1000pA
B
0 Ca2+
C
I TRPM2 (-pA)
1250
1000
750
500
250
0
*
Control
Fyn 1 U/mL
D
I TRPM2 (-pA)
6000
5000
4000
3000
2000
1000
0
*
Control
Fyn 1 U/mL

4.3.2 Fyn Phosphorylates TRPM2

We next examined whether Fyn promotes TRPM2 tyrosine phosphorylation in HEK293-TRPM2 cells transfected with various Fyn constructs. Fyn kinase was cloned into a pcDNA3.1 vector and site directed mutagenesis was used to produce a consitutively active form of Fyn kinase (Fyn Y531F) as well as an inactive Fyn kinase (Fyn K299M). These forms of Fyn have been previously described and characterized (Maulon et al., 2001; Twamley et al., 1992). HEK293-TRPM2 cells were transfected with these constructs or empty vector control, and induced to express TRPM2. TRPM2 was immunoprecipitated, run by SDS-PAGE, and probed for tyrosine phosphorylation (Figure 4.5). Results demonstrate that there is a significant difference between groups (p= 0.0124), with constitutively active Fyn enhancing TRPM2 tyrosine phosphorylation by approximately 6-fold over WT Fyn (p <0.05, one-way ANOVA followed by *post-hoc* Tukey's test).

4.3.3 Fyn Co-Immunoprecipitates with TRPM2

To examine whether Fyn interacts with TRPM2, TRPM2 pull-downs from HEK293-TRPM2 cells transfected with the various Fyn constructs were run by SDS-PAGE and probed for Fyn. Indeed, Fyn interacts with TRPM2. Interestingly, a significant difference between groups was observed (p = 0.009), with an enhanced interaction observed with the Fyn Y531F constitutively active mutant relative to WT (Figure 4.6A,B, p < 0.05). No significant difference between Y531F and WT Fyn input was observed (data not shown), suggesting that the interaction between Fyn and TRPM2 is enhanced when Fyn kinase is active.

Figure 4.5. TRPM2 tyrosine phosphorylation by Fyn.

HEK293-TRPM2 cells were transfected with empty vector (EV), wildtype Fyn (WT), constitutively active Fyn (Y531F), or inactive Fyn (K299M). Flag-tagged TRPM2 channels were immunoprecipitated from protein lysates and probed for tyrosine phosphorylation, and were subsequently striped and re-probed for TRPM2. Normalized values (pY TRPM2 / total TRPM2) were compared between groups (n=4 per treatment). (**A**) Representative blot. (**B**) A significant increase in tyrosine phosphorylation of TRPM2 is observed when co-transfected with constitutively active Fyn. Results are analyzed by one-way ANOVA followed by post-hoc Tukey's test. Identical letters at top of bars indicate no significant difference between groups ($p>0.05$).

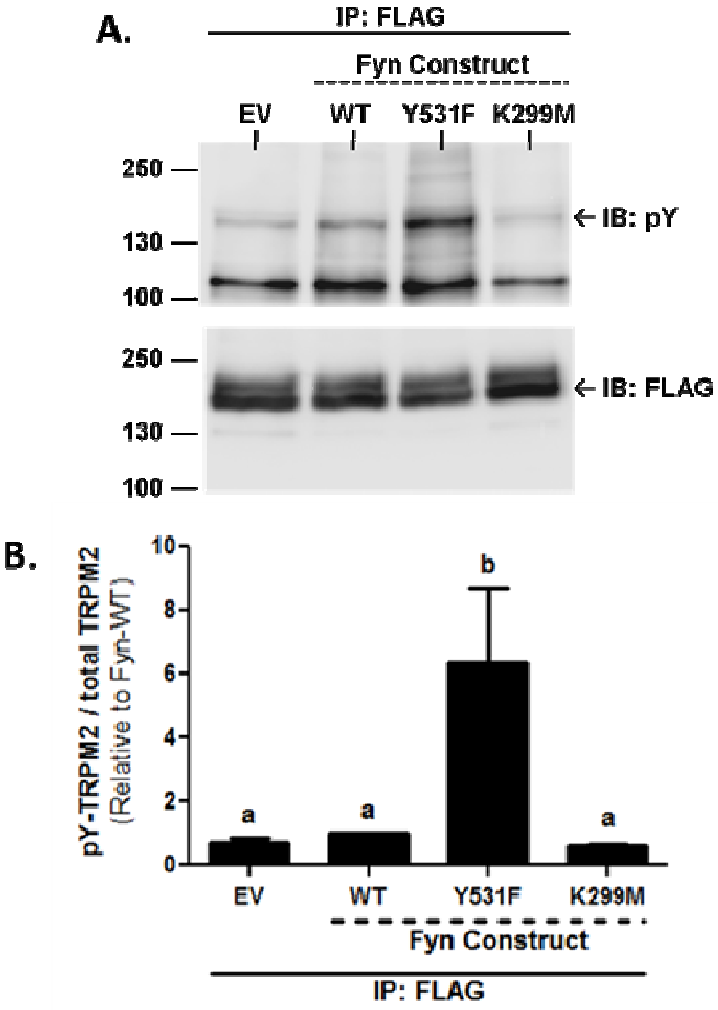
A.
IP: FLAG
Fyn Construct
EV
WT
Y531F
K299M
250
130
100
← IB: pY
250
130
100
← IB: FLAG
B.
pY-TRPM2 / total TRPM2
(Relative to Fyn-WT)
10
8
6
4
2
0
a
a
b
a
EV
WT
Y531F
K299M
Fyn Construct
IP: FLAG

Figure 4.6. TRPM2 Interacts with Fyn

In 4 separate experiments, HEK293-TRPM2 cells were transfected with empty vector (EV), wildtype Fyn (WT), constitutively active Fyn (Y531F), or inactive Fyn (K299M). Flag-tagged TRPM2 channels were immunoprecipitated from protein lysates, and immunoprecipitates were then run by SDS-PAGE, transferred to a nitrocellulose membrane, and probed for Fyn. To control for variations in TRPM2 expression and pull-down, the Fyn signal was normalized to flag-TRPM2 (**A**) Representative blot. (**B**) Fyn was co-immunoprecipitated with TRPM2 irrespective of the Fyn variant used. A significant increase in pull-down was observed with constitutively active Fyn (Y531F) relative to all other groups. Results are analyzed by one-way ANOVA followed by post-hoc Tukey's test. Identical letters at top of bars indicate no significant difference between groups ($p>0.05$).

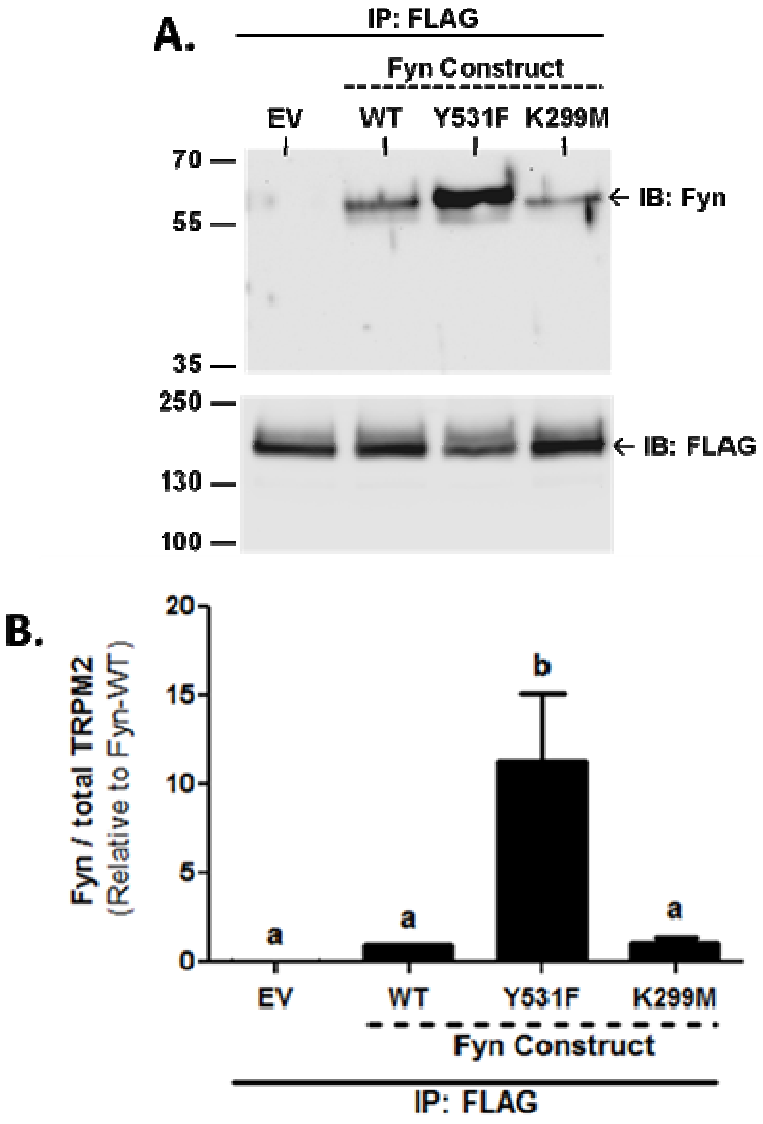
A.
IP: FLAG
Fyn Construct
EV
WT
Y531F
K299M
70
55
35
250
130
100
← IB: Fyn
← IB: FLAG
B.
Fyn / total TRPM2
(Relative to Fyn-WT)
20
15
10
5
0
a
a
b
a
EV
WT
Y531F
K299M
Fyn Construct
IP: FLAG

4.3.4 Fyn(39-57) Peptide Attenuates TRPM2 Currents

Our current results suggest that Fyn is an important regulator of TRPM2. We therefore wanted to examine whether a peptide developed against the unique domain of Fyn could inhibit TRPM2 currents. This peptide corresponds to Fyn amino acids 39-57, and is proposed to disrupt interactions between Fyn and target or scaffolding proteins ((Yang, Trepanier et al., 2011). As shown in Figure 4.7, TRPM2 currents of -692.0166 +/- 88.57842 pA in amplitude are elicited in control conditions in cultured hippocampal neurons (n=12) after 25 minutes of recording; however, inclusion of the Fyn(39-57) peptide (25 ng/mL in the patch pipette) significantly diminished the TRPM2 response (-224.2 +/- 24.2 pA, n=9).

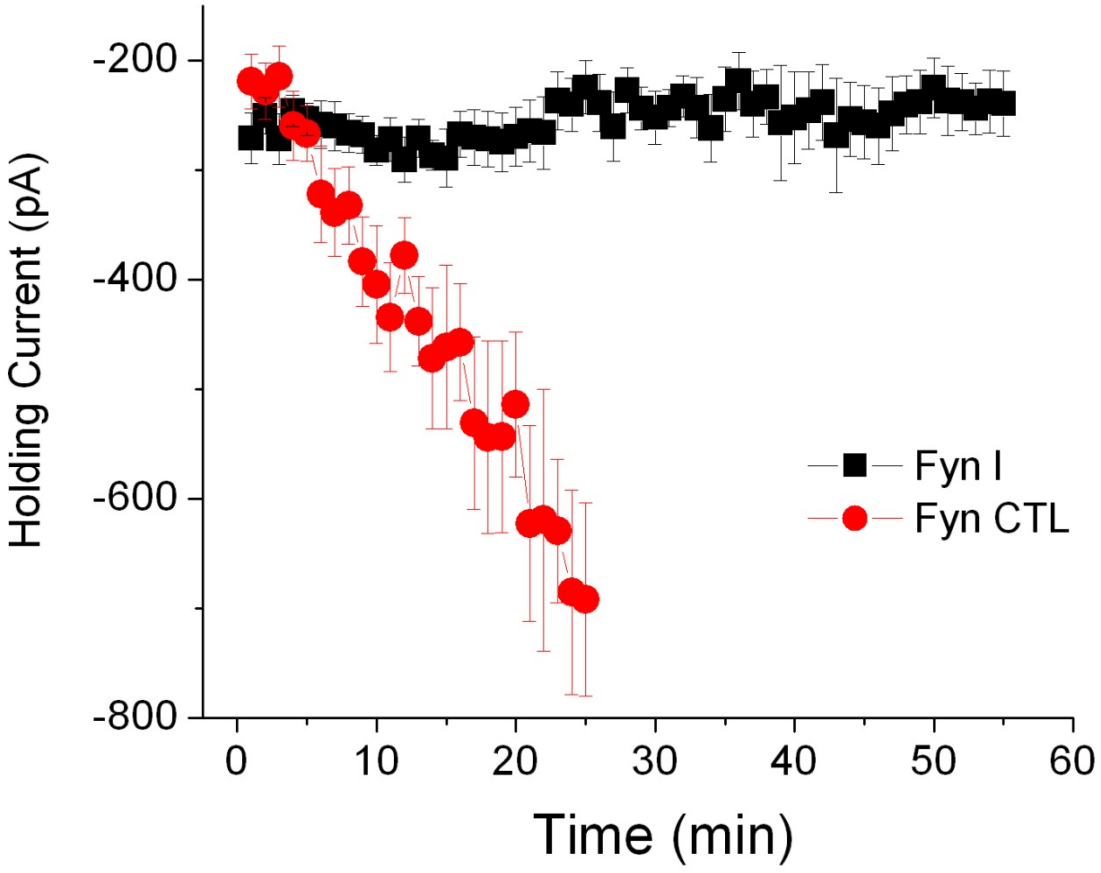

Figure 4.7. Fyn(39-57) peptide attenuates TRPM2 in hippocampal neurons

Cultured hippocampal neurons at 3-4 weeks *in vitro* were used to assess the effect of a the Fyn(39-57) mimetic peptide. In the absence of ADPR, repeated applications of NMDA activates TRPM2 and enhances the holding current to -692.0166 +/- 88.57842 pA after 25 minutes (Fyn CTL, n=12). Inclusion of the Fyn(39-57) peptide (25 ng/mL) in the patch pipette significantly attenuates the TRPM2 response, resulting in a current of -224.2 +/- 24.2 pA after 25 minutes (Fyn I, n=9).

4.4 Discussion

In this study, we demonstrate a role for TRPM2 in Aβ mediated cell death, and also examined the physical and functional link between Fyn kinase and TRPM2 channels. We employed cultured hippocampal neurons to demonstrate that the genetic deletion of TRPM2 attenuates the decrease in cell viability induced by a 24 hour treatment with 1μM oligomeric Aβ. One study had previously concluded that a dominant negative form of TRPM2 and knock-down of TRPM2 can protect against Aβ-mediated cell death (Fonfria et al., 2005). Importantly, this preliminary finding was investigated using 20 μM Aβ in striatal cultures; however, degeneration in Alzheimer's disease occurs within the basal forebrain cholinergic neurons, entorhinal cortex, hippocampus, and cortex (Coyle et al., 1983; Gomez-Isla et al., 1996)(Coyle et al., 1983; Gomez-Isla et al., 1996), and it is the oligomeric, not monomeric, form of Aβ that has been shown to induce an influx of intracellular calcium, significantly increase oxidative stress, and be particularly toxic to neurons (De Felice et al., 2007; Demuro et al., 2005; Lambert et al., 1998). The use of hippocampal cultures, along with use of oligomeric Aβ used in this study more accurately reflects the pathological conditions associated with Alzheimer's disease, and implicates the channel in the disease process. Subsequent studies should be designed to assess whether genetic deletion of TRPM2 can modify morbidity or mortality in transgenic models of Alzheimer's disease.

Following exposure to Aβ oligomers, TRPM2 currents are enhanced in cultured hippocapal neurons. This increase in current cannot be recapitulated in HEK cells expressing the TRPM2 channel. This suggests that Aβ enhances TRPM2 currents through an indirect mechanism. We hypothesize that the pathway will include Fyn

kinase. Therefore, we examined whether Fyn kinase could regulate the TRPM2 channel. In cultured hippocampal pyramidal neurons, we demonstrate that inclusion of Fyn kinase in the patch pipette increases TRPM2 current density when compared with controls. In addition, we used HEK293-TRPM2 cells transfected with empty vector or various forms of Fyn to demonstrate that TRPM2 is tyrosine phosphorylated by Fyn kinase, and this phosphorylation is significantly enhanced with constitutively active Fyn relative to WT Fyn. Furthermore, we demonstrate that Fyn interacts with TRPM2, and this interaction may be increased when Fyn is active. A peptide which mimics the unique domain of Fyn disrupts TRPM2 activation in cultured hippocampal pyramidal neurons.

Further experiments are required to assess whether Fyn is involved in the potentiation of TRPM2 currents by Aβ. Furthermore, it is unclear whether the interaction between Fyn and TRPM2 is direct or through a separate scaffolding protein. Analysis of the structure of TRPM2 reveals several proline rich motifs (PxxP), which could be involved in binding to the SH3-domain of Fyn kinase. These motifs are located in both the N- and C- terminal portions of TRPM2 at amino acids 544-547, 551-554, 575-578, 1078-1081, 1248-1251, and 1324-1327. Deletion of one of both of the N-terminal PxxP motif at 544-547 and 551-554 does not alter activation of TRPM2 by ADPR or H_2O_2 (Kuhn et al., 2009). Whether any PxxP motifs in TRPM2 participate in the interaction between Fyn and TRPM2 has not been investigated. Further research is also required to identify tyrosine phosphorylation sites on TRPM2 targeted by Fyn. The predictive software programs GPS 2.1 and PhosphoNet online application identify 10 putative sites on TRPM2 which may be phosphorylated by Fyn. These sites are Y74,

Y142, Y523, Y682, Y1127, Y1132, Y1271, Y1301, Y1349 and Y1503. Studies are currently in progress to identify the site(s) on TRPM2 which are phosphorylated by Fyn.

Our current results show the importance of continuing studies to determine the pathway through which TRPM2 currents are augmented by Aβ. Whether Fyn participates in this effect remains to be elucidated. A more complete understanding of this pathway may help to identify whether TRPM2 or the interaction between Fyn and TRPM2 could represent a potential target for development of novel therapeutics in AD.

References

Alberdi, E., Sanchez-Gomez, M. V., Cavaliere, F., Perez-Samartin, A., Zugaza, J. L., Trullas, R., Domercq, M., & Matute, C. , 2010. Amyloid beta oligomers induce Ca2+ dysregulation and neuronal death through activation of ionotropic glutamate receptors.Cell Calcium47(3), 264-272.

Alzheimer Society of Canada. (2010). *Rising tide: The impact of dementia on canadian society*from http://www.alzheimer.ca/english/rising_tide/rising_tide_report.htm

Chin, J., Palop, J. J., Puolivali, J., Massaro, C., Bien-Ly, N., Gerstein, H., Scearce-Levie, K., Masliah, E., & Mucke, L. , 2005. Fyn kinase induces synaptic and cognitive impairments in a transgenic mouse model of alzheimer's disease.J.Neurosci.25(42), 9694-9703.

Chin, J., Palop, J. J., Yu, G. Q., Kojima, N., Masliah, E., & Mucke, L. , 2004. Fyn kinase modulates synaptotoxicity, but not aberrant sprouting, in human amyloid precursor protein transgenic mice.J.Neurosci.24(19), 4692-4697.

Coyle, J. T., Price, D. L., & DeLong, M. R. , 1983. Alzheimer's disease: A disorder of cortical cholinergic innervation.Science219(4589), 1184-1190.

De Felice, F. G., Velasco, P. T., Lambert, M. P., Viola, K., Fernandez, S. J., Ferreira, S. T., & Klein, W. L. , 2007. Abeta oligomers induce neuronal oxidative stress through an N-methyl-D-aspartate receptor-dependent mechanism that is blocked by the alzheimer drug memantine.J.Biol.Chem.282(15), 11590-11601.

Demuro, A., Mina, E., Kayed, R., Milton, S. C., Parker, I., & Glabe, C. G. , 2005. Calcium dysregulation and membrane disruption as a ubiquitous neurotoxic mechanism of soluble amyloid oligomers.J.Biol.Chem.280(17), 17294-17300.

Fonfria, E., Marshall, I. C., Boyfield, I., Skaper, S. D., Hughes, J. P., Owen, D. E., Zhang, W., Miller, B. A., Benham, C. D., & McNulty, S. , 2005. Amyloid beta-peptide(1-42) and hydrogen peroxide-induced toxicity are mediated by TRPM2 in rat primary striatal cultures.J.Neurochem.95(3), 715-723.

Gao, Y., Howard, A., Ban, K., & Chandra, J. , 2009. Oxidative stress promotes transcriptional up-regulation of fyn in BCR-ABL1-expressing cells.J.Biol.Chem.284(11), 7114-7125.

Gomez-Isla, T., Price, J. L., McKeel, D. W.,Jr, Morris, J. C., Growdon, J. H., & Hyman, B. T. , 1996. Profound loss of layer II entorhinal cortex neurons occurs in very mild alzheimer's disease.J.Neurosci.16(14), 4491-4500.

Griendling, K. K., Sorescu, D., Lassegue, B., & Ushio-Fukai, M. , 2000. Modulation of protein kinase activity and gene expression by reactive oxygen species and their role in vascular physiology and pathophysiology.Arterioscler.Thromb.Vasc.Biol.20(10), 2175-2183.

Hardy, J., & Selkoe, D. J. , 2002. The amyloid hypothesis of alzheimer's disease: Progress and problems on the road to therapeutics.Science297(5580), 353-356.

Hernandez, F., Lucas, J. J., & Avila, J. , 2012. GSK3 and tau: Two convergence points in alzheimer's disease.J.Alzheimers Dis.

Ho, G. J., Hashimoto, M., Adame, A., Izu, M., Alford, M. F., Thal, L. J., Hansen, L. A., & Masliah, E. , 2005. Altered p59Fyn kinase expression accompanies disease progression in alzheimer's disease: Implications for its functional role.Neurobiol.Aging26(5), 625-635.

Hooper, C., Killick, R., & Lovestone, S. , 2008. The GSK3 hypothesis of alzheimer's disease.J.Neurochem.104(6), 1433-1439.

Hu, N. W., Klyubin, I., Anwy, R., & Rowan, M. J. , 2009. GluN2B subunit-containing NMDA receptor antagonists prevent abeta-mediated synaptic plasticity disruption in vivo.Proc.Natl.Acad.Sci.U.S.A.106(48), 20504-20509.

Huang, Y., & Mucke, L. , 2012. Alzheimer mechanisms and therapeutic strategies.Cell148(6), 1204-1222.

Husi, H., Ward, M. A., Choudhary, J. S., Blackstock, W. P., & Grant, S. G. , 2000. Proteomic analysis of NMDA receptor-adhesion protein signaling complexes.Nat.Neurosci.3(7), 661-669.

Ittner, L. M., Ke, Y. D., Delerue, F., Bi, M., Gladbach, A., van Eersel, J., Wolfing, H., Chieng, B. C., Christie, M. J., Napier, I. A., Eckert, A., Staufenbiel, M., Hardeman, E., & Gotz, J. , 2010. Dendritic function of tau mediates amyloid-beta toxicity in alzheimer's disease mouse models.Cell

Jacob, C. P., Koutsilieri, E., Bartl, J., Neuen-Jacob, E., Arzberger, T., Zander, N., Ravid, R., Roggendorf, W., Riederer, P., & Grunblatt, E. , 2007. Alterations in expression of glutamatergic transporters and receptors in sporadic alzheimer's disease.J.Alzheimers Dis.11(1), 97-116.

Kuhn, F. J., Kuhn, C., Naziroglu, M., & Luckhoff, A. , 2009. Role of an N-terminal splice segment in the activation of the cation channel TRPM2 by ADP-ribose and hydrogen peroxide.Neurochem.Res.34(2), 227-233.

Kurup, P., Zhang, Y., Xu, J., Venkitaramani, D. V., Haroutunian, V., Greengard, P., Nairn, A. C., & Lombroso, P. J. , 2010. Abeta-mediated NMDA receptor endocytosis in alzheimer's disease involves ubiquitination of the tyrosine phosphatase STEP61.J.Neurosci.30(17), 5948-5957.

Lambert, M. P., Barlow, A. K., Chromy, B. A., Edwards, C., Freed, R., Liosatos, M., Morgan, T. E., Rozovsky, I., Trommer, B., Viola, K. L., Wals, P., Zhang, C., Finch, C. E., Krafft, G. A., & Klein, W. L. , 1998. Diffusible, nonfibrillar ligands derived from Abeta1-42 are potent central nervous system neurotoxins.Proc.Natl.Acad.Sci.U.S.A.95(11), 6448-6453.

Maulon, L., Mari, B., Bertolotto, C., Ricci, J. E., Luciano, F., Belhacene, N., Deckert, M., Baier, G., & Auberger, P. , 2001. Differential requirements for ERK1/2 and P38 MAPK activation by thrombin in T cells. role of P59Fyn and PKCepsilon.Oncogene20(16), 1964-1972.

McShane, R., Areosa Sastre, A., & Minakaran, N. , 2006. Memantine for dementia.Cochrane Database Syst.Rev.(2)(2), CD003154.

Molnar, Z., Soos, K., Lengyel, I., Penke, B., Szegedi, V., & Budai, D. , 2004. Enhancement of NMDA responses by beta-amyloid peptides in the hippocampus in vivo.Neuroreport15(10), 1649-1652.

Olah, M. E., Jackson, M. F., Li, H., Perez, Y., Sun, H. S., Kiyonaka, S., Mori, Y., Tymianski, M., & MacDonald, J. F. , 2009. Ca2+-dependent induction of TRPM2 currents in hippocampal neurons.J.Physiol.587(Pt 5), 965-979.

Puzzo, D., Privitera, L., & Palmeri, A. , 2012. Hormetic effect of amyloid-beta peptide in synaptic plasticity and memory.Neurobiol.Aging33(7), 1484.e15-1484.e24.

Roberson, E. D., Scearce-Levie, K., Palop, J. J., Yan, F., Cheng, I. H., Wu, T., Gerstein, H., Yu, G. Q., & Mucke, L. , 2007. Reducing endogenous tau ameliorates amyloid beta-induced deficits in an alzheimer's disease mouse model.Science316(5825), 750-754.

Ronicke, R., Mikhaylova, M., Ronicke, S., Meinhardt, J., Schroder, U. H., Fandrich, M., Reiser, G., Kreutz, M. R., & Reymann, K. G. , 2010. Early neuronal dysfunction by amyloid beta oligomers depends on activation of NR2B-containing NMDA receptors.Neurobiol.Aging

Salter, M. W., & Kalia, L. V. , 2004. Src kinases: A hub for NMDA receptor regulation.Nat.Rev.Neurosci.5(4), 317-328.

Sanguinetti, A. R., Cao, H., & Corley Mastick, C. , 2003. Fyn is required for oxidative- and hyperosmotic-stress-induced tyrosine phosphorylation of caveolin-1.Biochem.J.376(Pt 1), 159-168.

Scheff, S. W., & Price, D. A. , 2003. Synaptic pathology in alzheimer's disease: A review of ultrastructural studies.Neurobiol.Aging24(8), 1029-1046.

Snyder, E. M., Nong, Y., Almeida, C. G., Paul, S., Moran, T., Choi, E. Y., Nairn, A. C., Salter, M. W., Lombroso, P. J., Gouras, G. K., & Greengard, P. , 2005. Regulation of NMDA receptor trafficking by amyloid-beta.Nat.Neurosci.8(8), 1051-1058.

Stine, W. B.,Jr, Dahlgren, K. N., Krafft, G. A., & LaDu, M. J. , 2003. In vitro characterization of conditions for amyloid-beta peptide oligomerization and fibrillogenesis.J.Biol.Chem.278(13), 11612-11622.

Takahashi, N., Kozai, D., Kobayashi, R., Ebert, M., & Mori, Y. , 2011. Roles of TRPM2 in oxidative stress.Cell Calcium

Twamley, G. M., Kypta, R. M., Hall, B., & Courtneidge, S. A. , 1992. Association of fyn with the activated platelet-derived growth factor receptor: Requirements for binding and phosphorylation.Oncogene7(10), 1893-1901.

Xie, Y. F., Belrose, J. C., Lei, G., Tymianski, M., Mori, Y., Macdonald, J. F., & Jackson, M. F. , 2011. Dependence of NMDA/GSK3beta mediated metaplasticity on TRPM2 channels at hippocampal CA3-CA1 synapses.Mol.Brain4(1), 44.

Yang, K., Belrose, J., Trepanier, C. H., Lei, G., Jackson, M. F., & MacDonald, J. F. , 2011. Fyn, a potential target for alzheimer's disease.J.Alzheimers Dis.27(2), 243-252.

Yang, K., Trepanier, C., Sidhu, B., Xie, Y. F., Li, H., Lei, G., Salter, M. W., Orser, B. A., Nakazawa, T., Yamamoto, T., Jackson, M. F., & Macdonald, J. F. , 2011. Metaplasticity gated through differential regulation of GluN2A versus GluN2B receptors by src family kinases.EMBO J.31(4), 805-816.

Zhang, W., Tong, Q., Conrad, K., Wozney, J., Cheung, J. Y., & Miller, B. A. , 2007. Regulation of TRP channel TRPM2 by the tyrosine phosphatase PTPL1.Am.J.Physiol.Cell.Physiol.292(5), C1746-58.

CHAPTER 5

5. Discussion

TRPM2 is a Ca^{2+} permeable channel activated by oxidative stress which has also been tightly linked to cell death (Takahashi et al., 2011). The highest level of TRPM2 expression is observed in the brain, where TRPM2 is expressed in several cell types including pyramidal neurons of the hippocampus (Fonfria et al., 2006; Olah et al., 2009). The purpose of this PhD thesis was to determine the physiological role of TRPM2 in these neurons, and elucidate novel pathways which regulate channel expression or function. A combination of electrophysiology and molecular biology approaches in cultured cell lines, primary hippocampal cultures, and hippocampal slice preparations were employed. Results presented in this thesis demonstrate that: (1) TRPM2 participates in NMDAR-dependent LTD by regulating GSK-3β activity, as well as expression of AMPAR and PSD-95 (Xie et al., 2011); (2) TRPM2 activity is enhanced in cultured hippocampal neurons over time *in vitro* due to the loss of tonic inhibition by GSH (Belrose et al., 2012); (3) TRPM2 plays a role in Aβ toxicity, potentially through a pathway involving Fyn, a tyrosine kinase which regulates TRPM2 in an activity dependent manner. This section will address the significance and implications of these findings.

5.1 TRPM2 Participates in Synaptic Plasticity

This thesis was the first to characterize the physiological role for TRPM2 in hippocampal pyramidal neurons. Employing TRPM2 knockout (KO) mice allowed us to validate the functional expression of TRPM2 in hippocampal pyramidal neurons. We determined that TRPM2 contributes to NMDAR-dependent LTD at hippocampal CA3-

CA1 synapses. The absence of TRPM2 does not alter NMDAR currents or NMDAR subunit composition. Similarly, no change in VDCC currents is observed in cultured hippocampal pyramidal neurons from KO animals relative to WT control. Instead, the loss of NMDAR-dependent LTD in KO hippocampal slices results from increased inactivation of GSK-3β, and a reduction in the expression of PSD-95 and AMPARs. The loss of NMDAR-LTD could be recapitulated with the TRPM2 antagonist clotrimazole, demonstrating that the observed changes in synaptic plasticity were not due to developmental changes induced by genetic deletion of TRPM2. Furthermore, increasing the activity of GSK-3β by treatment with quinpirole, a D2 receptor agonist, rescued LTD induction.

The signaling pathway through which TRPM2 regulates GSK-3β activity is likely to involve Ca^{2+}. The increase in Ser9 phosphorylation in KO animals could suggest a decrease in activity of a Ca^{2+}-dependent phosphatase. Calcineurin (also known as PP2B), a phosphatase regulated by Ca^{2+}, dephosphorylates GSK-3β at Ser9, and could mediate the change in GSK-3β activation downstream of TRPM2 (Y. Kim et al., 2009). Whether calcineurin activity is decreased in KO hippocampal tissue has not yet been assessed.

The decrease in AMPAR and PSD-95 expression in KO hippocampal slices also requires further exploration. This result, combined with a reduced AMPA/NMDA ratio, and a diminished mEPSC amplitude in KO slices, suggests that the contribution of AMPAR to excitatory synaptic transmission is reduced when TRPM2 is absent. The current study used total hippocampal lysates to assess AMPAR and PSD-95 expression. Whether the reduction in AMPAR is synapse specific, extrasynaptic, or was uniform

across the cell was not assessed. We demonstrated that clotrimazole could inhibit NMDAR-dependent LTD. Whether this treatment also produced a reduction in PSD-95 and AMPAR, or whether the loss of expression is due to a prolonged loss of TRPM2 or development changes due to genetic deletion of TRPM2 was not investigated. Lastly, the mechanism responsible for reduced AMPAR and PSD-95 expression was not explored. Whether a change in AMPAR and PSD-95 is due to a reduced transcription, translation, trafficking to the cell membrane, or enhanced degradation, should be explored to identify potential pathways through which TRPM2 may be regulating AMPAR and PSD-95 expression.

The behavioural consequences resulting from the genetic deletion of TRPM2 is still under investigation. Preliminary results in our lab have shown that TRPM2 KO mice perform the same as their WT controls on tests of locomotion, anxiety, and spatial learning. Specifically, no differences are observed between WT and KO animals at 9 months of age on the open field, elevated plus maze, Barnes maze, or object recognition tasks (M. Chen et al., unpublished). The absence of NMDAR-dependent LTD provides some insight into which behavioural tasks should be examined next in TRPM2 KO animals relative to controls. Specifically, the absence of LTD has been shown to impair behavioural flexibility, which can be evaluated by reversal learning in the Morris water maze and by the delayed non-match to place T-maze task (J. I. Kim et al., 2011).

Identification of the physiological role of TRPM2 in hippocampal pyramidal neurons not only contributes to the characterization of the TRPM2 channel, but it also furthers our understanding of the cellular mechanisms underlying learning and memory.

Furthermore, it allows us to identify potential consequences of directly inhibiting TRPM2 in a clinical setting.

5.2 TRPM2 Activity and Aging

TRPM2 currents are enhanced in cultured hippocampal neurons over time *in vitro.* The functional increase in TRPM2 currents is attributed to depletion of GSH with age, and the loss of tonic inhibition of the channel by GSH. Contrary to the previously proposed mechanisms of TRPM2 inhibition by GSH, inhibition is not due to the reducing effects of GSH. Inhibition by GSH is also independent of protein interactions with the cysteine residue in GSH since the effects of GSH can be recapitulated with ophthalmic acid, an analogue with an aminobutyrate group replacing the cysteine residue. The interaction between GSH and TRPM2 may play an important role in aging and neurological diseases associated with depletion of GSH.

A shift in the concentration-response curve shows that GSH produces a 3.5fold inhibition of the TRPM2 response to the intracellular agonist, ADPR. Interestingly, preliminary evidence suggests that ADPR may enhance the interaction between GSH and TRPM2 (J. Belrose, unpublished). Rather than GSH competing for the ADPR binding site on TRPM2, this result raises the possibility that GSH may function by binding to ADPR and disrupting proper channel activation. In support of this idea, a previous publication demonstrated that GSH covalently binds to ribose through an interaction between the glutamyl group of GSH and the aldehyde group of ribose (Januel et al., 2003). Whether this reaction also occurs between GSH and ADPR has not yet been assessed.

To determine whether TRPM2 currents are also elevated with age *in vivo*, TRPM2 currents can be recorded from aged WT hippocampal slices. As mentioned previously, no TRPM2 KO phenotype has been identified out to 9 months of age on the open field, elevated plus maze, object recognition, or Barnes Maze (M. Chen, unpublished). The results presented in this thesis suggest that a behavioural phenotype may be more apparent in aged mice.

In addition to normal aging, GSH is also reduced in Parkinson's disease (Martin & Teismann, 2009). TRPM2 is expressed and functional in dopaminergic neurons of the substantia nigra affected by Parkinson's disease (Chung, Freestone, & Lipski, 2011). Most Parkinson's disease cases are sporadic, with familial Parkinson's accounting for less than 15% of cases. Transgenic mouse models targeting the various genes implicated in familial Parkinson's disease have not yet produced a model that displays nigrostriatal neuronal degeneration (Blandini & Armentero, 2012). The 1-methyl 4-phenyltetrahydropyridine (MPTP) systemic neurotoxin model of Parkinson's disease, however, is selectively toxic to the dopaminergic neurons in the nigrostriatal pathway within one week following injection (Blandini & Armentero, 2012). To examine whether TRPM2 is implicated in Parkinson's disease, TRPM2 WT and KO animals could be assessed for performance on a grid-walking test and treadmill activity immediately prior to and two weeks following injection of vehicle control or MPTP.

In addition to GSH depletion in Parkinson's disease, GSH is also reduced in progressive supranuclear palsy, bipolar disorder, major depressive disorder, and schizophrenia (Martin & Teismann, 2009; Perry, Godin, & Hansen, 1982; Sian et al., 1994)(Anderson & Sims, 2002; Bragin et al., 2010; Rehncrona & Siesjo, 1979; Salemi

et al., 2009)(Do et al., 2000; Gawryluk et al., 2011). Several studies have linked SNPs in TRPM2 to bipolar disorder (Kostyrko et al., 2006; McQuillin et al., 2006; Xu et al., 2006; Xu et al., 2009). Whether the other neurodegenerative and neuropsychiatric disorders associated with GSH depletion demonstrate SNPs in TRPM2 has not yet been investigated.

5.3 Potential Implications to Alzheimer's disease

Alzheimer's disease (AD) is a progressive neurodegenerative disorder affecting memory, orientation, and reasoning. In Canada, the disease is estimated to affect 1.5% of our total population (Alzheimer Society of Canada, 2010).

Soluble oligomers of Aβ initiates a toxic cascade, resulting in the pathological modification of tau, and subsequent targeting of Fyn kinase to NMDARs (Ittner et al., 2010). The interaction between Fyn and tau is disrupted in tau -/-and tau74 mice (transgenic mice which express only the N-terminal projection domain of tau), decreasing the targeting of Fyn to the synapse. A reduction in mortality and cognitive deficits in an AD mouse model (APP23) are observed when these mice are crossed with tau -/- or tau74 mice. The Tat-NR2B9c peptide, a peptide which disrupts the interaction between NMDAR subunit 2B (GluN2B) and PSD-95, similarly rescued the memory deficits and lethality in APP23 mice (Ittner et al., 2010).

In agreement with the finding that Fyn is instrumental in AD, behavioural deficits and neurotoxicity in an AD mouse model can be enhanced with overexpression of Fyn (Chin et al., 2004; Chin et al., 2005). Similarly, hippocampal slices from Fyn knockout mice are protected from cell death induced by soluble oligomeric Aβ

(Lambert et al., 1998). In contrast, in the triple transgenic (3xTg) model of Alzheimer's disease, 3xTg(+/-) mice exhibit augmented spatial learning deficits and Aβ accumulation when Fyn is knocked down (Fyn+/-) relative to controls (Fyn(+/+)3xTg(+/-)) (Minami et al., 2012). This last result is not surprising when one considers the role for Fyn in LTP induction (Grant et al., 1992; Kojima et al., 1997). Furthermore, Fyn plays a critical role in oligodendrocyte production and subsequent neuronal myelination (Kramer-Albers & White, 2011; Osterhout et al., 1999). A conditional knockout of Fyn kinase in an AD mouse model would help to clarify whether the enhanced deficits in the 3xTg(+/-) mice are a result of developmental changes, or whether the effect can also be recapitulated when Fyn is knocked out after disease onset. Until this phenomenon has been explored further, the study by Minami and colleagues (2012) raises the possibility that global inhibition of Fyn may not provide therapeutic benefit to individuals diagnosed with AD. Further research into pathways altered by Fyn may uncover a more targeted approach for pharmacological intervention in AD.

As discussed previously, the toxic triad of tau, Fyn, and NMDARs are unlikely to explain all of the neurotoxicity and synaptic deficits observed in AD. Here, we propose that TRPM2 may participate in this protein complex. First, we demonstrate that TRPM2 plays a role in decreasing synaptic strength, a hallmark of AD (Xie et al., 2011). We further demonstrate that currents are enhanced by glutathione depletion over time *in vitro*, raising the possibility that glutathione depletion with age *in vivo* may produce an age-dependent increase in TRPM2 currents (Belrose et al., 2012). In chapter 4, we demonstrated that genetic deletion of TRPM2 protects against the reduction in

cell viability associated with oligomeric Aβ treatment. Furthermore, we demonstrated that TRPM2 currents are indirectly enhanced by Aβ, and that the channel is regulated by Fyn, an important player in AD (Belrose, Johnson, Li, Caetano, MacDonald & Jackson, unpublished).

A future direction of this project will examine the hypothesis that knockout of TRPM2 will protect against memory deficits and mortality in a mouse model of Alzheimer's disease. To examine whether knockout of TRPM2 also protects against mortality and cognitive deficits in an Alzheimer's disease mouse model, we have crossed TRPM2+/- mice with APPswePS1dE9 transgenic mice. This model of Alzheimer's disease co-expresses the swedish mutation of APP with a presinilin (PS1) lacking exon 9 (Jankowsky et al., 2004; Malm, Koistinaho, & Kanninen, 2011; Xiong et al., 2011) Four genotypes ($TRPM2^{+}AD^{-}$, $TRPM2^{-}AD^{-}$, $TRPM2^{+}AD^{+}$, AND $TRPM2^{-}AD^{+}$) will be tested on the open field, elevated plus maze, object recognition, Barnes maze, and Morris Water Maze to assess for changes in locomotion, anxiety, and memory. In APPswePS1dE9 mice, memory deficits on the Morris water maze appear at 12 months of age (Xiong et al., 2011). We propose that the deficits observed in the $TRPM2^{+}AD^{+}$ will be attenuated in the $TRPM2^{-}AD^{+}$.

We also hypothesize that the enhancement of TRPM2 currents by Aβ oligomers involves Fyn kinase. To examine this hypothesis, shRNA targeting Fyn will be used to knock-down expression of Fyn. A lentiviral system will be used to infect cultured hippocampal neurons with Fyn shRNA or scrambled shRNA control. In addition to allowing expression of shRNA driven by a U6 promoter, the transfer vector (pLB) used also allows expression of GFP with expression driven by a CMV promoter. Infection

rates in excess of 80% have routinely been achieved in our cultured hippocampal neurons. If Fyn is involved in potentiation of TRPM2 current by Aβ, we anticipate that knockdown of Fyn kinase would attenuate Aβ-mediated enhancement of TRPM2 currents in cultured neurons relative to scrambled shRNA infected controls.

5.4 Regulation of TRPM2 by Fyn

Fyn interacts with and phosphorylates TRPM2, and enhances TRPM2 currents. This is the first study to identify a kinase which acts upon TRPM2, and represents a novel regulatory mechanism which may play an important role in oxidative stress and Alzheimer's disease. It is unclear whether the interaction between Fyn and TRPM2 is direct or through a separate scaffolding protein. Analysis of the structure of TRPM2 reveals several proline rich motifs (PxxP), which could be involved in binding to the SH3-domain of Fyn kinase. Whether any PxxP motifs in TRPM2 participate in the interaction between Fyn and TRPM2 has not been investigated. Alternatively, Fyn may interact with TRPM2 through an intermediate protein such as a scaffolding protein. The precise nature of the interaction between TRPM2 and Fyn requires further exploration, and may lead to the development of a more specific inhibitory peptide.

The current study used intracellular applications of recombinant Fyn kinase to assess the effect on TRPM2 currents. We demonstrated that acute Fyn kinase enhanced TRPM2 current amplitude; however, it is unclear whether a more chronic exposure to activated Fyn would produce the same effect. Results from western blotting experiments raise the possibility that Fyn exerts a dichotomous effect on TRPM2: acutely enhancing currents, and reducing TRPM2 expression in more chronic

conditions. Total cell lysate from HEK293-TRPM2 cells transfected with the various Fyn constructs were separated by SDS-PAGE to assess TRPM2 and Fyn expression. To our surprise, we consistently observed a decrease in TRPM2 expression normalized to β-actin when constitutively active Fyn was transfected (Figure 5.1). Importantly, no change in β-actin levels was observed between groups ($p>0.05$). This decline in TRPM2 expression may represent a difference in protein production, trafficking, endocytosis and degradation, or cell proliferation and viability. If cells expressing TRPM2 have diminished proliferation, or undergo apoptosis or necrosis in response to overexpression of constitutively active Fyn, we would expect a decrease in total protein levels in lysates collected from these cells. Analysis of protein concentration reveals that there is no difference in protein levels between the groups (one way ANOVA, $p = 0.68$, data not shown). Further research is needed to first assess whether surface expression of TRPM2 is altered, and subsequently to assess whether a change in protein production, trafficking, endocytosis, or degradation underlies the reduction of TRPM2 in response to constitutively active Fyn. This result also raises the intriguing possibility that, although acute Fyn enhances TRPM2 currents, chronically active Fyn may decrease TRPM2 activity through a reduction in TRPM2 expression.

Figure 5.1. Constitutively active Fyn decreases TRPM2 expression.

Total protein from HEK-TRPM2 cells transfected with EV, WT, constitutively active (Y531F), or inactive (K299M) Fyn were separated by SDS-PAGE and analyzed for flag-TRPM2 and Fyn input, normalized to β-actin expression. (A) Representative blots; (B) TRPM2 input normalized to β-actin demonstrates a significant reduction in TRPM2 expression relative to empty vector (n=4/treatment) (C) Fyn input normalized to β-actin demonstrates expression of Fyn with transfection of each construct. A significant reduction in Fyn expression is observed with K299M relative to Y531F; however, neither construct exhibit a significant change in expression relative to WT Fyn (n=4). Results are analyzed by one-way ANOVA followed by post-hoc Tukey's test. Identical letters at top of bars indicate no significant difference between groups ($p>0.05$).

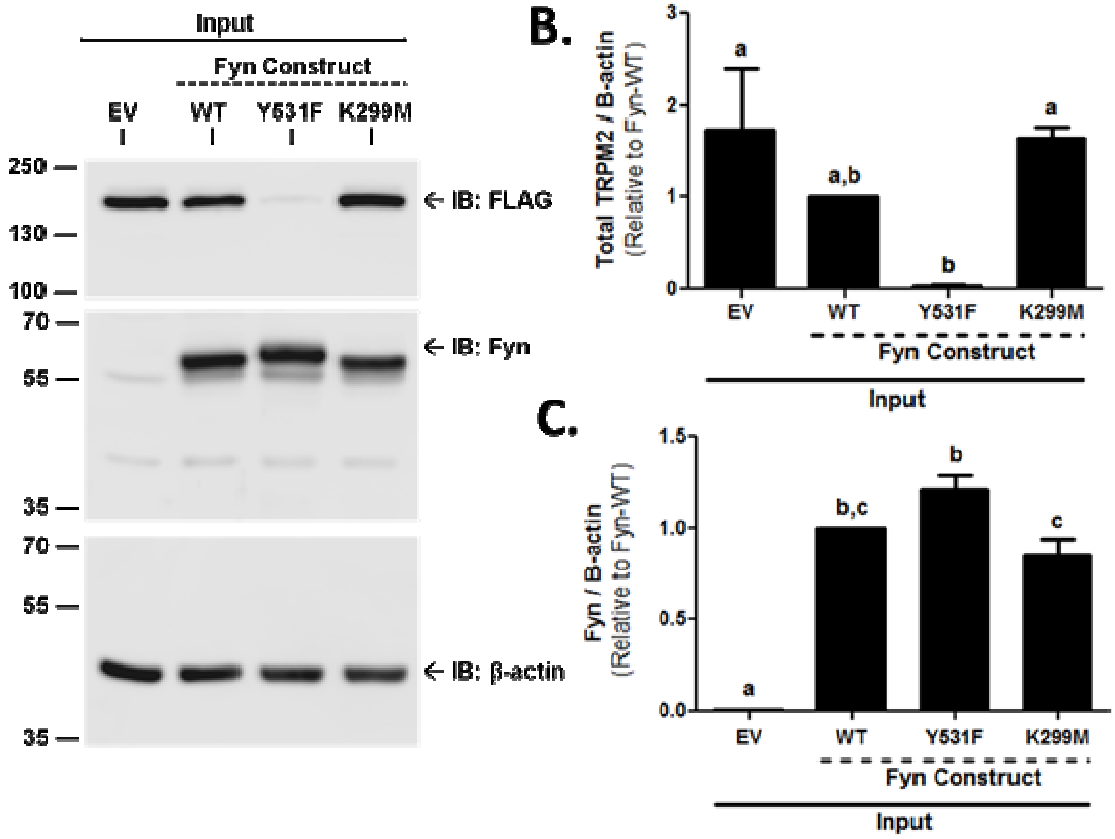
Input
Fyn Construct
EV
WT
Y531F
K299M
250
130
100
70
55
35
70
55
35
← IB: FLAG
← IB: Fyn
← IB: β-actin
B.
Total TRPM2 / B-actin
(Relative to Fyn-WT)
3
2
1
0
a
a,b
b
a
EV
WT
Y531F
K299M
Fyn Construct
Input
C.
Fyn / B-actin
(Relative to Fyn-WT)
1.5
1.0
0.5
0.0
a
b,c
b
c
EV
WT
Y531F
K299M
Fyn Construct
Input

Interestingly, TRPM7, another member of the TRPM subfamily of cation channels, may be regulated by Src kinase, a related kinase with significant homology to Fyn (Jiang, Newell, & Schlichter, 2003). Similar to the inhibition of TRPM2 by Fyn(39-57), TRPM7 currents are inhibited with Src(40-58) in microglia (Jiang et al., 2003). Considering the similarity between TRPM2 and TRPM7, as well as the homology between Fyn and Src kinase, we wondered whether Src kinase may also regulate TRPM2 channels. In HEK293-TRPM2 cells, we demonstrate that recombinant Src (1U/mL) in the patch pipette significantly potentiates TRPM2 currents (-6193 ± 505.1, N=10) relative to controls (-4831 ± 213.9, N=7) as shown in Figure 5.2.

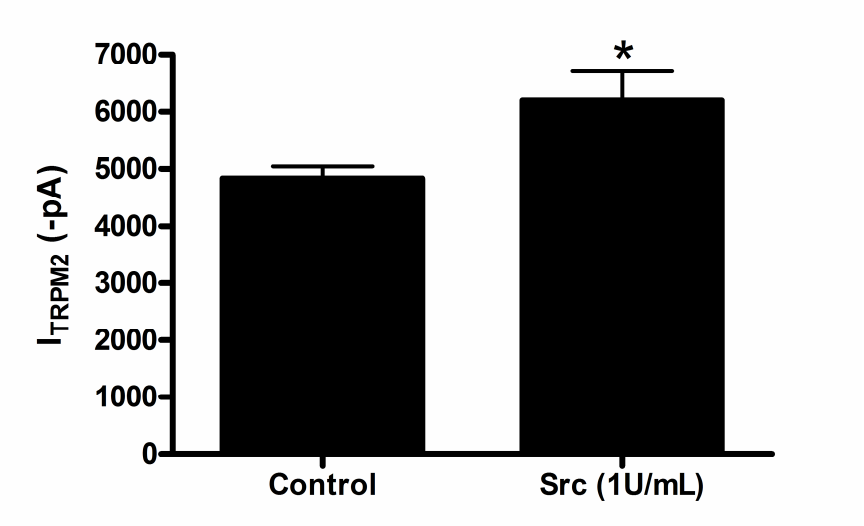

Figure 5.2. Src potentiates TRPM2 currents

TRPM2 currents were generated in HEK293-TRPM2 cells with 0.1 mM ADPR in the patch pipette. When compared with controls (-4831 ± 213.9, N=7), Src (1 U/mL, -6193 ± 505.1 N=10) significantly potentiates TRPM2 amplitude

5.5 Conclusion

Our lab previously demonstrated that TRPM2 is expressed and functional in hippocampal pyramidal neurons; however, the physiological role and various pathways regulating TRPM2 had not yet been established (Olah et al., 2009). Substantial evidence demonstrates that TRPM2 plays an important role in cell death (Takahashi et al., 2011). Here, we identified that TRPM2 is required for NMDAR-dependent LTD through the regulation of GSK-3β activity (Xie et al., 2011). We examined TRPM2 currents over time *in vitro* and provide evidence that TRPM2 currents are enhanced with GSH depletion (Belrose et al., 2012). This raises the possibility that TRPM2 currents may be enhanced with normal aging and in the various neurodegenerative and psychiatric disorders associated with GSH depletion. Furthermore, we demonstrate that cultured hippocampal neurons derived from TRPM2 KO mice show an attenuated loss of cell viability following treatment with Aβ oligomers when compared with WT cultures. We also demonstrate that Fyn kinase is capable of interacting with, and phosphorylating TRPM2. Delivery of recombinant Fyn through the patch pipette potentiates TRPM2 currents. Combined, this data raises the possibility that TRPM2 may play a role in Alzheimer's disease pathology (Figure 5.3)

Elucidating the properties and physiological role(s) of TRPM2 is still in the early stages; however, these findings open the door to several subsequent studies on the significance of TRPM2 to normal function and potential contribution to various neurological diseases.

Figure 5.3 Summary

In addition to a role for TRPM2 in cell death, the channel also participates in decreasing synaptic strength via regulation of GSK-3β activity. TRPM2 is tonically inhibited by GSH which can be depleted with age. Furthermore, the channel is activated by Fyn, a Src-family kinase implicated in Alzheimer's disease. Treatment with Aβ, the initiating factor of Alzheimer's pathogenesis, enhances TRPM2 currents through an unknown mechanism. This may involve Fyn kinase since treatment with Aβ results in the downstream hyperphosphorylation of tau via several kinases including GSK-3β, and the mislocalization of Fyn in response to pathologically modified tau.

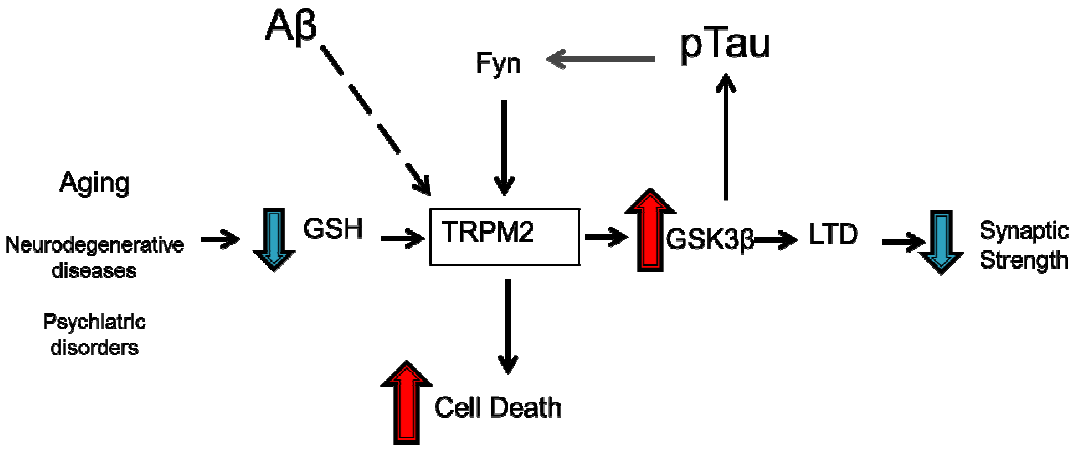
Aβ
Fyn
pTau
Aging
Neurodegenerative diseases
Psychiatric disorders
GSH
TRPM2
GSK3β
LTD
Synaptic Strength
Cell Death

References

Alzheimer Society of Canada. (2010). *Rising tide: The impact of dementia on canadian society*from http://www.alzheimer.ca/english/rising_tide/rising_tide_report.htm

Anderson, M. F., & Sims, N. R. , 2002. The effects of focal ischemia and reperfusion on the glutathione content of mitochondria from rat brain subregions.J.Neurochem.81(3), 541-549.

Belrose, J. C., Xie, Y. F., Gierszewski, L. J., Macdonald, J. F., & Jackson, M. F. , 2012. Loss of glutathione homeostasis associated with neuronal senescence facilitates TRPM2 channel activation in cultured hippocampal pyramidal neurons.Mol.Brain5(1), 11.

Blandini, F., & Armentero, M. T. , 2012. Animal models of parkinson's disease.FEBS J.279(7), 1156-1166.

Bragin, D. E., Zhou, B., Ramamoorthy, P., Muller, W. S., Connor, J. A., & Shi, H. , 2010. Differential changes of glutathione levels in astrocytes and neurons in ischemic brains by two-photon imaging.J.Cereb.Blood Flow Metab.30(4), 734-738.

Chin, J., Palop, J. J., Puolivali, J., Massaro, C., Bien-Ly, N., Gerstein, H., Scearce-Levie, K., Masliah, E., & Mucke, L. , 2005. Fyn kinase induces synaptic and cognitive impairments in a transgenic mouse model of alzheimer's disease.J.Neurosci.25(42), 9694-9703.

Chin, J., Palop, J. J., Yu, G. Q., Kojima, N., Masliah, E., & Mucke, L. , 2004. Fyn kinase modulates synaptotoxicity, but not aberrant sprouting, in human amyloid precursor protein transgenic mice.J.Neurosci.24(19), 4692-4697.

Chung, K. K., Freestone, P. S., & Lipski, J. , 2011. Expression and functional properties of TRPM2 channels in dopaminergic neurons of the substantia nigra of the rat.J.Neurophysiol.106(6), 2865-2875.

Do, K. Q., Trabesinger, A. H., Kirsten-Kruger, M., Lauer, C. J., Dydak, U., Hell, D., Holsboer, F., Boesiger, P., & Cuenod, M. , 2000. Schizophrenia: Glutathione deficit in cerebrospinal fluid and prefrontal cortex in vivo.Eur.J.Neurosci.12(10), 3721-3728.

Fonfria, E., Murdock, P. R., Cusdin, F. S., Benham, C. D., Kelsell, R. E., & McNulty, S. , 2006. Tissue distribution profiles of the human TRPM cation channel family.J.Recept.Signal Transduct.Res.26(3), 159-178.

Gawryluk, J. W., Wang, J. F., Andreazza, A. C., Shao, L., & Young, L. T. , 2011. Decreased levels of glutathione, the major brain antioxidant, in post-mortem prefrontal cortex from patients with psychiatric disorders.Int.J.Neuropsychopharmacol.14(1), 123-130.

Grant, S. G., O'Dell, T. J., Karl, K. A., Stein, P. L., Soriano, P., & Kandel, E. R. , 1992. Impaired long-term potentiation, spatial learning, and hippocampal development in fyn mutant mice.Science258(5090), 1903-1910.

Ittner, L. M., Ke, Y. D., Delerue, F., Bi, M., Gladbach, A., van Eersel, J., Wolfing, H., Chieng, B. C., Christie, M. J., Napier, I. A., Eckert, A., Staufenbiel, M., Hardeman, E., & Gotz, J. , 2010. Dendritic function of tau mediates amyloid-beta toxicity in alzheimer's disease mouse models.Cell

Jankowsky, J. L., Fadale, D. J., Anderson, J., Xu, G. M., Gonzales, V., Jenkins, N. A., Copeland, N. G., Lee, M. K., Younkin, L. H., Wagner, S. L., Younkin, S. G., & Borchelt, D. R. , 2004. Mutant presenilins specifically elevate the levels of the 42 residue beta-amyloid peptide in vivo: Evidence for augmentation of a 42-specific gamma secretase.Hum.Mol.Genet.13(2), 159-170.

Januel, C., Fay, L. B., Ruggiero, D., Lagarde, M., & Vericel, E. , 2003. Covalent coupling of reduced glutathione with ribose: Loss of cosubstrate ability to glutathione peroxidase.Biochim.Biophys.Acta1620(1-3), 125-132.

Jiang, X., Newell, E. W., & Schlichter, L. C. , 2003. Regulation of a TRPM7-like current in rat brain microglia.J.Biol.Chem.278(44), 42867-42876.

Kim, J. I., Lee, H. R., Sim, S. E., Baek, J., Yu, N. K., Choi, J. H., Ko, H. G., Lee, Y. S., Park, S. W., Kwak, C., Ahn, S. J., Choi, S. Y., Kim, H., Kim, K. H., Backx, P. H., Bradley, C. A., Kim, E., Jang, D. J., Lee, K., Kim, S. J., Zhuo, M., Collingridge, G. L., & Kaang, B. K. , 2011. PI3Kgamma is required for NMDA receptor-dependent long-term depression and behavioral flexibility.Nat.Neurosci.14(11), 1447-1454.

Kim, Y., Lee, Y. I., Seo, M., Kim, S. Y., Lee, J. E., Youn, H. D., Kim, Y. S., & Juhnn, Y. S. , 2009. Calcineurin dephosphorylates glycogen synthase kinase-3 beta at serine-9 in neuroblast-derived cells.J.Neurochem.111(2), 344-354.

Kojima, N., Wang, J., Mansuy, I. M., Grant, S. G., Mayford, M., & Kandel, E. R. , 1997. Rescuing impairment of long-term potentiation in fyn-deficient mice by introducing fyn transgene.Proc.Natl.Acad.Sci.U.S.A.94(9), 4761-4765.

Kostyrko, A., Hauser, J., Rybakowski, J. K., & Trzeciak, W. H. , 2006. Screening of chromosomal region 21q22.3 for mutations in genes associated with neuronal Ca2+ signalling in bipolar affective disorder.Acta Biochim.Pol.53(2), 317-320.

Kramer-Albers, E. M., & White, R. , 2011. From axon-glial signalling to myelination: The integrating role of oligodendroglial fyn kinase.Cell Mol.Life Sci.68(12), 2003-2012.

Lambert, M. P., Barlow, A. K., Chromy, B. A., Edwards, C., Freed, R., Liosatos, M., Morgan, T. E., Rozovsky, I., Trommer, B., Viola, K. L., Wals, P., Zhang, C., Finch, C. E., Krafft, G. A., & Klein, W. L. , 1998. Diffusible, nonfibrillar ligands derived from Abeta1-42 are potent central nervous system neurotoxins.Proc.Natl.Acad.Sci.U.S.A.95(11), 6448-6453.

Malm, T., Koistinaho, J., & Kanninen, K. , 2011. Utilization of APPswe/PS1dE9 transgenic mice in research of alzheimer's disease: Focus on gene therapy and cell-based therapy applications.Int.J.Alzheimers Dis.2011, 517160.

Martin, H. L., & Teismann, P. , 2009. Glutathione--a review on its role and significance in parkinson's disease.FASEB J.23(10), 3263-3272.

McQuillin, A., Bass, N. J., Kalsi, G., Lawrence, J., Puri, V., Choudhury, K., Detera-Wadleigh, S. D., Curtis, D., & Gurling, H. M. , 2006. Fine mapping of a susceptibility locus for bipolar and genetically related unipolar affective disorders, to a region containing the C21ORF29 and TRPM2 genes on chromosome 21q22.3.Mol.Psychiatry11(2), 134-142.

Minami, S. S., Clifford, T. G., Hoe, H. S., Matsuoka, Y., & Rebeck, G. W. , 2012. Fyn knock-down increases abeta, decreases phospho-tau, and worsens spatial learning in 3xTg-AD mice.Neurobiol.Aging33(4), 825.e15-825.e24.

Olah, M. E., Jackson, M. F., Li, H., Perez, Y., Sun, H. S., Kiyonaka, S., Mori, Y., Tymianski, M., & MacDonald, J. F. , 2009. Ca2+-dependent induction of TRPM2 currents in hippocampal neurons.J.Physiol.587(Pt 5), 965-979.

Osterhout, D. J., Wolven, A., Wolf, R. M., Resh, M. D., & Chao, M. V. , 1999. Morphological differentiation of oligodendrocytes requires activation of fyn tyrosine kinase.J.Cell Biol.145(6), 1209-1218.

Perry, T. L., Godin, D. V., & Hansen, S. , 1982. Parkinson's disease: A disorder due to nigral glutathione deficiency?Neurosci.Lett.33(3), 305-310.

Rehncrona, S., & Siesjo, B. K. , 1979. Cortical and cerebrospinal fluid concentrations of reduced and oxidized glutathione during and after cerebral ischemia.Adv.Neurol.26, 285-286.

Salemi, G., Gueli, M. C., D'Amelio, M., Saia, V., Mangiapane, P., Aridon, P., Ragonese, P., & Lupo, I. , 2009. Blood levels of homocysteine, cysteine,

glutathione, folic acid, and vitamin B(12) in the acute phase of atherothrombotic stroke.Neurol.Sci.

Sian, J., Dexter, D. T., Lees, A. J., Daniel, S., Agid, Y., Javoy-Agid, F., Jenner, P., & Marsden, C. D. , 1994. Alterations in glutathione levels in parkinson's disease and other neurodegenerative disorders affecting basal ganglia.Ann.Neurol.36(3), 348-355.

Takahashi, N., Kozai, D., Kobayashi, R., Ebert, M., & Mori, Y. , 2011. Roles of TRPM2 in oxidative stress.Cell Calcium

Xie, Y. F., Belrose, J. C., Lei, G., Tymianski, M., Mori, Y., Macdonald, J. F., & Jackson, M. F. , 2011. Dependence of NMDA/GSK3beta mediated metaplasticity on TRPM2 channels at hippocampal CA3-CA1 synapses.Mol.Brain4(1), 44.

Xiong, H., Callaghan, D., Wodzinska, J., Xu, J., Premyslova, M., Liu, Q. Y., Connelly, J., & Zhang, W. , 2011. Biochemical and behavioral characterization of the double transgenic mouse model (APPswe/PS1dE9) of alzheimer's disease.Neurosci.Bull.27(4), 221-232.

Xu, C., Li, P. P., Cooke, R. G., Parikh, S. V., Wang, K., Kennedy, J. L., & Warsh, J. J. , 2009. TRPM2 variants and bipolar disorder risk: Confirmation in a family-based association study.Bipolar Disord.11(1), 1-10.

Xu, C., Macciardi, F., Li, P. P., Yoon, I. S., Cooke, R. G., Hughes, B., Parikh, S. V., McIntyre, R. S., Kennedy, J. L., & Warsh, J. J. , 2006. Association of the putative susceptibility gene, transient receptor potential protein melastatin type 2, with bipolar disorder.Am.J.Med.Genet.B.Neuropsychiatr.Genet.141B(1), 36-43.

APPENDICES

IOS Press – Publisher of Journal of Alzheimer's Disease
Author Copyright Agreement: License to Publish
In order to publish your article we need your agreement. Please take a moment to read the terms of this license. By submitting your article to one of our books or journals (henceforth 'publications'), you and all co-authors of your submission agree to the terms of this license. You do not need to fill out a copyright form for confirmation.

By submitting your article to one of our publications you grant us (the publisher) the exclusive right to both reproduce and/or distribute your article (including the abstract) throughout the world in electronic, printed or any other medium, and to authorize others (including Reproduction Rights Organizations such as the Copyright Licensing Agency and the Copyright Clearance Center, and other document distributors) to do the same. You agree that we may publish your article, and that we may sell or distribute it, on its own, or with other related material.

By submitting your article for publication to one of our publications, you promise that the article is your original work, has not previously been published, and is not currently under consideration by another publication. You also promise that the article does not, to the best of your knowledge, contain anything that is libellous, illegal or infringes anyone's copyright or other rights. If the article contains material that is someone else's copyright, you promise that you have obtained the unrestricted permission of the copyright owner to use the material and that the material is clearly identified and acknowledged in the text.

We promise that we will respect your rights as the author(s). That is, we will make sure that your name(s) is/are always clearly associated with the article and, while you do allow us to make necessary editorial changes, we will not make any substantial alterations to your article without consulting you.

Copyright remains yours, and we will acknowledge this in the copyright line that appears on your article. You also retain the right to use your own article (provided you acknowledge the published original in standard bibliographic citation form) in the following ways, as long as you do not sell it in ways that would conflict directly with our efforts to disseminate it.

1. **You are free to use the manuscript version of your article for internal, educational or other purposes of your own institution or company;**
2. **You may use the article, in whole or in part, as the basis for your own further publications or spoken presentations;**
3. For a fee of €100, you will have the right to mount the final version of your article as published by IOS Press on your own, your institution's, company's or funding agency's website. You can order this right together with the final published version of your article with the form sent to the corresponding author along with the proofs of your paper.

BioMed Central copyright and license agreement

In submitting a research article ('article') to any of the journals published by BioMed Central Ltd ('BioMed Central') I certify that:

1. I am authorized by my co-authors to enter into these arrangements.
2. I warrant, on behalf of myself and my co-authors, that:

a. the article is original, has not been formally published in any other peer-reviewed journal, is not under consideration by any other journal and does not infringe any existing copyright or any other third party rights;

b. I am/we are the sole author(s) of the article and have full authority to enter into this agreement and in granting rights to BioMed Central are not in breach of any other obligation. If the law requires that the article be published in the public domain, I/we will notify BioMed Central at the time of submission upon which clauses 3 through 6 inclusive do not apply;

c. the article contains nothing that is unlawful, libellous, or which would, if published, constitute a breach of contract or of confidence or of commitment given to secrecy;

d. I/we have taken due care to ensure the integrity of the article. To my/our - and currently accepted scientific - knowledge all statements contained in it purporting to be facts are true and any formula or instruction contained in the article will not, if followed accurately, cause any injury, illness or damage to the user.

And I agree to the following license agreement:

BioMed Central Open Access license agreement

Brief summary of the agreement

Anyone is free:

- to copy, distribute, and display the work;
- to make derivative works;
- to make commercial use of the work;

Under the following conditions: Attribution

- the original author must be given credit;
- for any reuse or distribution, it must be made clear to others what the license terms of this work are;
- any of these conditions can be waived if the authors gives permission.

Statutory fair use and other rights are in no way affected by the above.

Full BioMed Central Open Access license agreement

(Identical to the 'Creative Commons Attribution License')

ANIMAL USE PROTOCOL

January 29, 2009

This is the Original Approval for this protocol
A Full Protocol submission will be required in 2013

Dear Dr. Macdonald and Dr. Jackson:
Your Animal Use Protocol form entitled: Non-Selective Cation Channels in Stroke
Funding Agency CHR -Grant #MOP-15514
has been approved by the University Council on Animal Care. This approval is valid from **January 29, 2009 to January 31, 2010.** The protocol number for this project is **2009-002**.

1. This number must be indicated when ordering animals for this project.
2. Animals for other projects may not be ordered under this number.
3. If no number appears please contact this office when grant approval is received. If the application for funding is not successful and you wish to proceed with the project, request that an internal scientific peer review be performed by the Animal Use Subcommittee office.
4. Purchases of animals other than through this system must be cleared through the ACVS office. Health certificates will be required.

ANIMALS APPROVED FOR 4 Years

Species	Strain	Other Detail	Pain Level	Animal # Total for 4 Years
Mouse	Swiss	Pregnant females	C	800
Rat	Wistar	2 week -adults	C	5200
Mouse	NR2A KO	2 week -adults	C	600
Mouse	NR2A KO	adult breeders M/F	C	40
Mouse	TRPM2 KO	2 week -adults	C	1600
Mouse	TRPM2 KO	adult breeders M/F	C	40

REQUIREMENTS/COMMENTS
Please ensure that individual(s) performing procedures on live animals, as described in this protocol, are familiar with the contents of this document

c.c. Approved Protocol - J. MacDonald, M. Jackson, W. Lagerwerf, M. Pickering
Approval Letter - J. MacDonald, M. Jackson, W. Lagerwerf, M. Pickering

***The* University *of* Western Ontario**
Animal Use Subcommittee / University Council on Animal Care
Health Sciences Centre, ● London, Ontario ● CANADA – N6A 5C1
PH: 519-661-2111 ext. 86770 ● FL 519-661-2028 ● www.uwo.ca / animal

Curriculum Vitae

EDUCATION

In Progress	MD/PhD candidate – University of Western Ontario Anatomy & Cell Biology Supervisor: Dr. John MacDonald Thesis topic: *TRPM2 in the CNS: Physiological role and critical regulatory pathways*
2009	MSc – McMaster University Medical Sciences Supervisor: Dr. Margaret Fahnestock Thesis topic: *Mechanism of brain derived neurotrophic factor (BDNF) dysregulation in Alzheimer's disease and related tauopathies*
2007	BHSc (honours) – McMaster University Bachelor of Health Sciences Supervisor: Dr. Laurie Doering Thesis topic: *Fragile-X Mental Retardation Protein (FMRP) Expression in Astrocytes*

AWARDS & HONOURS

2012	Canadian Society for Clinical Investigation (CSCI) Young Investigators Forum Poster Award (*neuroscience*) Value: $100
2012	Suzanne M. Bernier Publication Award Publication Award – Department of Anatomy & Cell Biology Value: $150
2012	London Health Research Day Poster Award – Neuroscience and Mental Health Value: $500

2011	A.C. Camargo Global Meeting of Translational Science Travel Award One of 50 international candidates selected to attend the course "Molecular Medicine: From Bench to Bedside" in Sao Paulo, Brazil Value: Full coverage of travel costs (hotel, transportation, meals)
2010	Canadian Society for Clinical Investigation (CSCI) Young Investigators Forum Poster Award (*neuroscience*) Value: $75 + one year associate membership with CSCI
2009 - 2015	CIHR – MD/PhD Program Grant Awarded to the top ranked incoming MD/PhD student Value: $132,000
2009	NSERC – PGS (D3) - **declined** Value: $63,000
2009 - 2012	University of Western Ontario – Schulich Graduate Scholarship Value: ~ $7000/year (tuition stipend)
2009	NSERC – Michael Smith Foreign Study Supplement (MFSS) - **declined** Value: $4,360
2008	NSERC – CGS (M) Alexander Graham Bell Scholarship Value: $17,500
2008	McMaster Medical Sciences Scholarship Value: $5,000
2007	Ontario Graduate Scholarship (OGS) Value: $15,000

PUBLICATIONS/PRESENTATIONS

PUBLICATIONS

Appleton, T.*, **Belrose, J.C.*,** Ward, M., & Young, F. (submitted, *Clinical and Investigative Medicine*). Strength in numbers: Growth of Canadian clinician investigator training in the 21st century. **these authors contributed equally to this work*

Jamshidi, F., Schmidt, A., & **Belrose, J.C.** (submitted, *Clinical and Investigative Medicine*). Scientific overview: CSCI-CITAC annual general meeting and young investigators forum 2011.

MacDonald, J.F., **Belrose, J.C.,** Xie, Y.F., & Jackson, M.F. (2013). Nonselective ion channels and links to hippocampal ischemia, aging, and dementia. *Adv. Exp. Med. Biol. 961*: 433-447.

Belrose, J.C., Xie, Y.F., Gierszewski, L.J., MacDonald, J.F., & Jackson, M.F. (2012). Loss of glutathione homeostasis associated with neuronal senescence facilitates TRPM2 channel activation in cultured hippocampal pyramidal neurons. *Molecular Brain, 5*:11.

Belrose, J.C., Caetano, F., Yang, K., Lockhart, B.M.W., Jackson, M.F., & MacDonald, J.F. (2012). Mechanisms of calcium influx following stroke. In Li, Y.V. & Zhang, J.H (Eds), *Metal Ion in Stroke*. New York, NY: Springer. (ISBN 978-1-4419-9662-6)

Xie, Y.F.*, **Belrose, J.C.*,** Tymianski, M., Mori, Y., MacDonald, J.F., Jackson, M.F. (2011). Dependence of NMDA/GSK3β mediated metaplasticity on TRPM2 channels at hippocampal CA3-CA1 synapses. *Molecular Brain, 4*:44. **these authors contributed equally to this work*

Yang, K.*, **Belrose, J.***, Trepanier, C.H., Lei, G., Jackson, M.F., & MacDonald, J.F. (2011). Fyn, a potential target for Alzheimer's disease. REVIEW. *Journal of Alzheimer's Disease, 27*(2): 243-252. **these authors contributed equally to this work*

ABSTRACTS/POSTERS

Belrose, J.C., Johnson, M., Li, H., Jackson, M.F. MacDonald, J.F. Regulation of TRPM2 function by glutathione and fyn kinase: Implications for neurotoxicity following stroke. Poster presented at the Canadian Stroke Congress, Calgary, Alberta, Canada (September 2012).

Belrose, J.C., Johnston, M., Chen, M., Li, H., Martyn, A.C, Prado, M.A., Prado, V.F., Jackson, M.F., MacDonald, J.F. TRPM2 is implicated in cellular senescence and Aβ-mediated toxicity in hippocampal neurons. Poster presented at the Canadian Association for Neuroscience conference, Vancouver, British Columbia, Canada (May 2012)

Belrose, J.C., Caetano, F., Li, H., Chen, M., Jackson, M.F., MacDonald, J.F. (March 2012). TRPM2 is implicated in cellular senescence and Aβ-mediated cell death of hippocampal neurons. Poster presented at the London Health Research Day, London, Ontario.

Belrose, J.C., MacDonald, J.F., Jackson, M.F. (September 2011). Reduced glutathione inhibits TRPM2 currents. Poster presented at the Canadian Society for Clinical Investigation Young Investigator Forum, Ottawa, Ontario.

Belrose, J.C., MacDonald, J.F., Jackson, M. (July 2011). TRPM2 current potentiation with age *in vitro* is dependent on oxidative stress. Poster presented at the 8th IBRO World Congress of Neuroscience, Florence, Italy

Caetano, F., Leon, N., **Belrose, J.C.,** Jackson, M.F., MacDonald, J.F. (May 2011). TRPM2 channel regulation by the Fyn kinase. Poster presented at the 31st Annual Meeting of the Southern Ontario Neuroscience Association, Guelph, Ontario.

Belrose, J.C., Jackson, M., MacDonald, J.F. (March 2011). TRPM2 currents are augmented by chronic oxidative stress. Poster presented at the 2011 Margaret Moffat Research Day, London, Ontario.

Belrose, J.C., Masoudi, R., Fahnestock, M. (November 2010). Increased proNGF and decreased BDNF in non-Alzheimer's disease tauopathies. Poster presented at the Society for Neuroscience, San Diego, California

Belrose, J.C., Jackson, M., & MacDonald, J. (September 2010). TRPM2 currents increase with age *in vitro*. Poster presented at the Canadian Society for Clinical Investigation Young Investigator Forum, Ottawa, Ontario.

Belrose, J.C., Jackson, M., & MacDonald, J. (March 2010). TRPM2 currents increase with age *in vitro*, and may be functionally linked to NMDA Receptors. Poster presented at Margaret Moffat Day, London, Ontario.

INVITED PRESENTATIONS

Belrose, J.C.*, Appleton, T.*, Ward, M., Young, F. (2011, September) Strength in numbers: Growth of Canadian clinician investigator training. Paper presented at the 2011 Canadian Society of Clinical Investigation / Clinician Investigator Trainee Conference, Ottawa, Ontario. **these authors contributed equally to this work*

Belrose, J.C., Li, H., Jackson, M.F., MacDonald, J.F. (2010, November). A potential role for TRPM2 in Alzheimer's disease. Presented at the 2010 Anatomy and Cell Biology Research Day, London, Ontario

TEACHING EXPERIENCE

Mentored 4th year Undergraduate Honors Thesis Projects
Toby Yip – 2009 - 2010
Nilien Leon – 2010-2011
Lynn Gierszewski – 2011-2012

Sept '08 – April '09 Teaching Assistant – School of Nursing

- Courses: Health Science 1CC7/2CC7 – Integrated Biological Bases of Nursing I & II
- Facilitated a tutorial of 15 RPN to BScN (diploma to degree) nursing students

VOLUNTEER HISTORY

2011 – present *MD/PhD student representative – University of Western Ontario*

- Student representative at recruitment events, Schulich Grad Studies Student Representative Council, MD/PhD committee, & MD/PhD admissions committee

2011 – present *MD/PhD Program – Seminar Series*

- Organize bi-monthly seminar series to increase mentorship between established clinician scientists and current trainees at the University of Western Ontario

2009 – 2012 *Clinician Investigator Trainee Association of Canada (CITAC)*
Positions: VP External/VP External-elect (2010 – 2012)
Policy Director (2009-2010)

- Represent CITAC in forming partnerships with external groups & develop memoranda of understandings with collaborating agencies
- Develop policies of interest to membership (i.e., funding advocacy for trainees)
- Coordinate special interest projects